

THERMAL ANALYSIS AND CONTROL
OF SMALL SATELLITES IN LOW EARTH ORBIT

by

KATELYN ELIZABETH BOUSHON

A THESIS

Presented to the Faculty of the Graduate School of the
MISSOURI UNIVERSITY OF SCIENCE AND TECHNOLOGY

In Partial Fulfillment of the Requirements for the Degree

MASTER OF SCIENCE IN AEROSPACE ENGINEERING

2018

Approved by

Henry Pernicka, Advisor
Derek Hengeveld
Edward Kinzel

ProQuest Number: 10793247

All rights reserved

INFORMATION TO ALL USERS

The quality of this reproduction is dependent upon the quality of the copy submitted.

In the unlikely event that the author did not send a complete manuscript and there are missing pages, these will be noted. Also, if material had to be removed, a note will indicate the deletion.



ProQuest 10793247

Published by ProQuest LLC (2018). Copyright of the Dissertation is held by the Author.

All rights reserved.

This work is protected against unauthorized copying under Title 17, United States Code
Microform Edition © ProQuest LLC.

ProQuest LLC.
789 East Eisenhower Parkway
P.O. Box 1346
Ann Arbor, MI 48106 – 1346

© 2018

Katelyn Elizabeth Boushon

All Rights Reserved

ABSTRACT

Small satellites are becoming more popular in the space sector, primarily due to their lower cost and shorter development time. Much of the information available about satellite thermal analysis and control refers to larger spacecraft. Sorting through this information to find the practices specifically applicable for small satellites can be a daunting task, particularly for inexperienced engineers. This thesis study is intended to inform the reader about basic thermal control and analysis methods that relate specifically to small satellites in low Earth orbit. A case study involving a satellite designed by the Missouri University of Science and Technology Satellite Research Team is presented to demonstrate the use of computer software for thermal analysis and the thermal control methods used to ensure that the satellite electrical component temperatures remain in the necessary range for proper operation.

The process presented in the case study involves the construction of multiple revisions of the potential satellite thermal model. The analysis results presented demonstrate how increasing model complexity and nodal resolution affect resulting satellite temperatures. The passive thermal control method of manipulating satellite surface optical properties is used to raise the satellite component temperatures to the necessary range.

ACKNOWLEDGMENTS

First, I would like to thank my advisor, Dr. Hank Pernicka, for his constant encouragement and support throughout my time as a student. When I was an undergraduate student on the Missouri S&T Satellite Research Team, Dr. Pernicka encouraged me to become more involved and take on leadership positions. He supported my endeavor to attend graduate school, and took me on as a research assistant to work on thermal analysis and control for the satellite research team. I am very grateful to Dr. Pernicka for all his help and for his dedication to his work and his students. Additionally, I would like to thank the other members of my committee, Dr. Hengeveld and Dr. Kinzel. Dr. Hengeveld's guidance and instruction on spacecraft thermal analysis and control methods were essential to the success of my research.

I would also like to thank my parents for their unending love and support. They have always encouraged me to work hard and never stop pursuing my dreams. Through setbacks and challenging times my parents have been encouraging and supportive, and for that I am very grateful. Without their help, reassurance, and support I would never have been able to get to where I am today.

Furthermore, I would like to thank C&R Technologies for providing the Missouri S&T satellite research team with their Thermal Desktop software free of charge. Specifically, I would like to thank Cindy Beer at CRTech for all her help with the software installation and for answering my many questions.

Finally, I would like to thank the members of the Missouri S&T Satellite Research Team for their hard work and dedication. In particular, I would like to thank Yezad Anklesaria and Jill Davis for their help and technical advice with my work on the satellite research team.

TABLE OF CONTENTS

	Page
ABSTRACT	iii
ACKNOWLEDGMENTS	iv
LIST OF ILLUSTRATIONS	x
LIST OF TABLES	xii
NOMENCLATURE	xiii
SECTION	
1. INTRODUCTION	1
1.1. MOTIVATION	1
1.2. HISTORY OF SMALL SATELLITES AND THERMAL ANALYSIS	3
1.3. THESIS STUDY GOALS AND OVERVIEW	5
2. HEAT TRANSFER CONCEPTS	7
2.1. MODES OF HEAT TRANSFER	7
2.1.1. Radiation	7
2.1.2. Conduction	9
2.1.3. Convection.....	10
2.1.4. Combined Modes of Heat Transfer	11
2.2. HEATING FLUXES.....	11
2.2.1. Ground Environment.....	11
2.2.2. Ascent Heating	12
2.2.3. Low Earth Orbit Environment.....	12
2.2.3.1 Direct solar radiation.....	13
2.2.3.2 Albedo radiation.....	14
2.2.3.3 Earth IR.....	15
2.2.3.4 Spacecraft heat generation	15
2.2.3.5 Spacecraft heat emission.....	16
2.3. THERMAL ENERGY BALANCE	16
3. SATELLITE THERMAL ANALYSIS	18
3.1. THERMAL EXTREMA ANALYSIS CASES.....	18

3.1.1. Hot Case	19
3.1.2. Cold Case	19
3.2. NUMERICAL APPROXIMATION METHODS	20
3.2.1. Finite Difference Approximation	21
3.2.2. Finite Element Approximation.....	21
3.2.3. Steady State	21
3.2.4. Transient.....	22
3.3. COMPUTER THERMAL MODELING	22
3.3.1. Modeling Software	22
3.3.2. Modeling Iterations	23
3.3.3. Spatially Averaged Properties	24
3.4. VERIFICATION OF RESULTS	25
3.4.1. Simplified Thermal Analysis.....	25
3.4.2. Thermal Balance Test.....	26
4. SATELLITE THERMAL CONTROL.....	29
4.1. THERMAL CONTROL HARDWARE	29
4.1.1. Passive Thermal Control	29
4.1.1.1 Insulation.....	30
4.1.1.2 Surface coatings and finishes.....	32
4.1.1.2.1 Common surface treatments	33
4.1.1.2.2 Surface degradation and contamination.....	35
4.1.1.2.3 Electrical grounding.....	36
4.1.1.3 Tapes	36
4.1.1.4 Sunshields	37
4.1.1.5 Radiators	37
4.1.1.6 Heat pipes.....	38
4.1.1.7 Phase change materials	40
4.1.1.8 Heat switches	40
4.1.2. Active Thermal Control.....	41
4.1.2.1 Heaters	41
4.1.2.1.1 Heater types	41

4.1.2.1.2 Heater control.....	42
4.1.2.1.3 Heater system failure modes.....	43
4.1.2.2 Thermoelectric coolers.....	43
4.1.2.3 Louvers	44
4.1.3. Emerging Technologies for Small Satellite Use	46
4.1.3.1 Thermal straps.....	46
4.1.3.2 Deployable radiators	46
4.1.3.3 Fluid loops	46
4.2. MOUNTINGS AND INTERFACES.....	47
4.2.1. Thermal Contact Conductance	47
4.2.2. Bolted-Joint Conductance	48
4.2.3. Interface Filler Conductance	48
5. THERMAL DESIGN PROCESS.....	51
6. CASE STUDY: MR SAT AND MRS SAT.....	55
6.1. SATELLITE TEAM HISTORY.....	55
6.2. MR AND MRS SAT OVERVIEW	56
6.2.1. Mission Overview	56
6.2.2. Overview of Subsystems	56
6.3. THERMAL SUBSYSTEM OVERVIEW	59
6.3.1. Satellite Temperature Specifications.....	60
6.3.2. Thermal Environment and Heating Fluxes	61
6.3.2.1 Hot case.....	62
6.3.2.2 Cold case.....	63
6.4. THERMAL ANALYSIS USING THERMAL DESKTOP.....	63
6.4.1. Extrema Case Construction	66
6.4.2. Single Node Analysis – Model Revision A.....	66
6.4.2.1 Model construction	66
6.4.2.2 Analysis results	67
6.4.2.3 Discussion	71
6.4.3. Eight Node Analysis – Model Revision B	71
6.4.3.1 Model construction	71

6.4.3.2 Analysis results	71
6.4.3.3 Discussion	71
6.4.4. Multi-Node Analysis	72
6.4.4.1 Explicit panel modeling – model revision C.....	72
6.4.4.1.1 Model construction	72
6.4.4.1.2 Analysis results	74
6.4.4.1.3 Discussion	74
6.4.4.2 External surface and internal components – model revision D. 75	
6.4.4.2.1 Model construction	78
6.4.4.2.2 Analysis results	79
6.4.4.2.3 Discussion	79
6.4.4.3 Model revision E – potential thermal control system design.....	80
6.4.4.3.1 Surface properties and design changes	81
6.4.4.3.2 Analysis results	88
6.4.4.3.3 Discussion	88
6.4.5. Future Work	89
6.4.6. Lessons Learned	95
7. CONCLUSION	100
7.1. THESIS SUMMARY	100
7.2. CONTRIBUTIONS TO THE SMALL SATELLITE COMMUNITY	102
APPENDICES	
A. THERMAL MODELING, ANALYSIS, AND DESIGN PROCESS.....	103
B. PROPERTIES OF COMMON SURFACE COATINGS AND FINISHES.....	110
C. GEOMETRIES, MATERIAL PROPERTIES OF PANELS, BOXES, AND COMPONENTS, AND CONDUCTANCE USED IN THERMAL MODEL CONSTRUCTION	112
D. SINGLE NODE ANALYSIS – MODEL REVISION A AND EIGHT NODE ANALYSIS – MODEL REVISION B INPUT PARAMETERS	117
E. MULTI NODE ANALYSIS – MODEL REVISION C AND D EXPLICITLY MODELED PANELS INPUT PARAMETERS	119
F. MULTI NODE ANALYSIS – HEAT LOADS FOR MODEL REVISIONS C AND D	121

G. MULTI NODE ANALYSIS – MODEL REVISION D STEADY STATE ANALYSIS RESULTS	123
H. MODEL REVISION E INPUT INFORMATION	127
BIBLIOGRAPHY.....	130
VITA	134

LIST OF ILLUSTRATIONS

Figure	Page
2.1. Orbit Beta Angle [14]	13
3.1. Simple Thermal Balance Test Profile [14]	27
4.1. Typical MLI Blanket Composition [14]	30
4.2. Surface Coating Combination Patterns [1]	32
4.3. Optical Properties of Common Surface Treatments [14]	33
4.4. Heat Pipe Schematic [14].....	38
4.5. Variable Conductance Heat Pipe Schematic [1].....	39
4.6. Liquid Trap Diode Schematic [1]	39
4.7. Custom Shaped Patch Heaters [14].....	42
4.8. Peltier Thermoelectric Couple [14]	44
4.9. Venetian Blind Louvers [1]	45
4.10. Bolted-Joint Interface [14].....	48
5.1. Thermal Analysis and Design Process [18].....	51
6.1. Satellite Pair in Mated Configuration	57
6.2. MR SAT Panel Numbering.....	61
6.3. ISS Beta Angle Versus Day	62
6.4. MR SAT Hot Case Orbit – Beta Angle of 60°	67
6.5. MR SAT Cold Case Orbit – Beta Angle of 0°	68
6.6. MR SAT Side Lumped Model Panel Components.....	68
6.7. Wireframe Single Node Thermal Model Before Merging Nodes	69
6.8. Wireframe Single Node Thermal Model with Merged Nodes.....	69
6.9. Model Revision A – Hot Case Transient Analysis	70
6.10. Model Revision A – Cold Case Transient Analysis	70
6.11. MR SAT Model Revision B – Edge Contactors.....	75
6.12. Model Revision B – Hot Case Transient Analysis	76
6.13. Model Revision B – Cold Case Transient Analysis.....	76
6.14. MR SAT Internal Component Layout	77
6.15. MR SAT Side Panel Brackets.....	77

6.16. MR SAT Model Revision C – Conduction and Heat Load Locations	78
6.17. Model Revision C Hot Case Transient – Isogrid Panels.....	80
6.18. Model Revision C Hot Case Transient – Solar Panel PCB	82
6.19. Model Revision C Hot Case Transient – Honeycomb Panels	83
6.20. Model Revision C Cold Case Transient – Isogrid Panels.....	83
6.21. Model Revision C Cold Case Transient – Solar Panel PCB.....	84
6.22. Model Revision C Cold Case Transient – Honeycomb Panels.....	84
6.23. MR SAT Internal Electrical Component Mounting Locations.....	85
6.24. MR SAT Model Revision D – Conduction and Heat Load Locations	85
6.25. Model Revision D Hot Case Transient – Isogrid Panels	90
6.26. Model Revision D Hot Case Transient – Solar Panel PCB	90
6.27. Model Revision D Hot Case Transient – Honeycomb Panels	91
6.28. Model Revision D Cold Case Transient – Isogrid Panels.....	91
6.29. Model Revision D Cold Case Transient – Solar Panel PCB	92
6.30. Model Revision D Cold Case Transient – Honeycomb Panels	92
6.31. MR SAT Thermal Model Revision E	93
6.32. Model Revision E Hot Case Transient – Isogrid Panels.....	96
6.33. Model Revision E Hot Case Transient – Solar Panel PCB.....	96
6.34. Model Revision E Hot Case Transient – Aluminum Panels.....	97
6.35. Model Revision E Cold Case Transient – Isogrid Panels	97
6.36. Model Revision E Cold Case Transient – Solar Panel PCB.....	98
6.37. Model Revision E Cold Case Transient – Aluminum Panels.....	98

LIST OF TABLES

Table	Page
1.1. Small Satellite Classifications.....	2
4.1. Screw Thermal Conductance Design Guideline	49
6.1. MR SAT Critical Component Operational Temperatures	60
6.2. Orbit Parameters for Extrema Environment Cases	64
6.3. MR SAT Electrical Components Total Heat Loads for Extrema Cases	64
6.4 Model Revision Information.....	65
6.5. Model Revision B – Steady State Analysis	75
6.6. Model Revision C – Hot Case Steady State.....	78
6.7. Model Revision C – Cold Case Steady State.....	80
6.8. Model Revision D – Transient Analysis Results for Electrical Components	86
6.9. Model Revision D – Transient Analysis Results for Batteries	87
6.10. Model Revision E – Transient Results for Batteries.....	93
6.11. Model Revision E – Transient Results for Components.....	94

NOMENCLATURE

Symbol	Description
NASA	National Aeronautics and Space Administration
kg	Kilograms
cm	Centimeters
LOHARP	Lockheed Heat Rate Program
TRASYS	Thermal Radiation Analysis System
SSPTA	Simplified Space Payload Thermal Analyzer
CINDA	Chrysler Improved Numerical Differencing Analyzer
TSS	Thermal Synthesizer System
VBA	Visual Basic for Applications
W	Watts
m	Meters
ε	Emissivity
A	Surface Area
σ	Stefan-Boltzmann Constant
T	Temperature
K	Kelvin
e	Emission
q	Heat Flux
\dot{Q}	Heat Transfer Rate
α	Absorptivity
a	Absorption
i	Incident
F	View Factor
k	Thermal Conductivity
s	Surface
∞	Fluid
h	Heat Transfer Coefficient
km	Kilometers

°	Degrees
C	Celsius
IR	Infrared
LEO	Low Earth Orbit
β	Beta Angle
S	Solar Constant
θ	Incident Angle
A_f	Albedo Factor
E	Earth
c_p	Specific Heat
ρ	Density
t	Time
∇	Vector of Partial Derivatives
q^*	Volumetric Heat Generation
FDM	Finite Difference Method
FEM	Finite Element Method
SINDA	Systems Improved Numerical Differencing Analyzer
n	Number of Surfaces
M	Mass
MLI	Multilayer Insulation
ε^*	Effective Emissivity of MLI
g	Grams
L	Liters
PCM	Phase Change Material
TEC	Thermoelectric Cooler
C	Thermal Contact Conductance
h	Heat Transfer Coefficient
RTV	Room Temperature Vulcanized
MR SAT	Missouri-Rolla Satellite
MRS SAT	Missouri-Rolla Second Satellite
RSO	Resident Space Object

UNP	University Nanosatellite Program
AFRL	Air Force Research Laboratory
ISS	International Space Station
GNC	Guidance, Navigation, and Control
ERM	Ejector Release Mechanism
PCB	Printed Circuit Board
GPS	Global Positioning System
IMU	Inertial Measurement Unit
UART	Universal Asynchronous Receiver-Transmitter
I ² C	Inter-Integrated Circuit
CM	Computer Module
MCU	Multipoint Control Unit

1. INTRODUCTION

Spacecraft thermal control is integral to mission success. The process of thermal control for a spacecraft involves managing the energy entering and leaving the spacecraft to ensure that the components of the spacecraft remain within an acceptable temperature range. Spacecraft perform optimally and have longer working lives when the temperature of their components remains within these boundaries, often near the temperature at which they were fabricated [1]. Thus, the first step in the thermal control process is to establish the temperature specifications in which the spacecraft will be operated during its lifetime. The thermal design ensures that these specified values are not exceeded, particularly those in orbit. This is substantiated during the development process by analysis, similarity studies, and testing.

1.1. MOTIVATION

Small satellites have been a “disruptive force” and are offering many new opportunities in the space sector [2], [3]. While larger systems require enormous investments, small satellites are enabling low cost missions and are revolutionizing a portion of the space sector [4]. They allow for new technologies to be tested without a high financial risk, for faster development times, and for space to be accessible to new entrants. Start-up companies, universities, and countries with aspirations of developing space programs can build spacecraft and reach space with modest budgets, and government funding can go farther for research and science projects when smaller budgets are allotted that allow for a higher total number of missions.

It should be noted that the classification of small satellites varies for different organizations [2]. The most commonly used definitions of small satellite classifications in the United States are defined by NASA on their webpage [5]. Small satellites are defined as spacecraft with a mass less than 180 kg, though there are many subcategories within the realm of small satellites, as shown in Table 1.1.

Table 1.1. Small Satellite Classifications [5]

Classification	Mass [kg]
Minisatellite	100-180
Microsatellite	10-100
Nanosatellite	1-10
Picosatellite	0.01-1
Femtosatellite	0.001-0.01

The rapid development of spacecraft is critical for educational as well as military applications. University satellite engineering programs typically only last a few years, and small missions with short durations can allow students the opportunity to work on a satellite from the design phase through testing and even launch and data collection. The military requires technology demonstrations to be completed quickly so that the technology can be implemented and responses to new threats can be promptly addressed.

With the need for rapid development comes the need for streamlined and improved fidelity of thermal analysis and control for small satellites. There are many thermal control technologies with a great deal of flight heritage on traditionally larger spacecraft, but these approaches often cannot adapt to the needs of small satellites [6]. The performance of these technologies on small satellites may be compromised, and their effectiveness decreased. At this point in time, there are only a few technologies that are commonly used for thermal control on small satellites. Emerging forms of thermal control are being developed specifically for small satellites, but they are still at lower technology readiness levels.

It can often be challenging to find resources that focus on thermal control pertaining to small satellites specifically. The process of researching and selecting possible thermal control techniques and hardware can be time consuming, and is coupled with the potentially lengthy process of creating a computer model and performing a thermal analysis. It is likely very beneficial for those working on a small satellite to have access to a document that describes in detail the process of designing a thermal control system, possible thermal control technologies to use, and the process of how to perform a

thermal analysis. This thesis study considers the design process and proven methods of thermal analysis and control specifically focused on small satellites, thus providing a resource for future reference.

1.2. HISTORY OF SMALL SATELLITES AND THERMAL ANALYSIS

While small satellites are being seen as an emerging class in the space sector, they are not exactly new. The first artificial Earth orbiting satellite in space was the Russian Sputnik 1, launched in 1957 and weighing only 83.6 kg [6]. The following year saw the United States satellite Explorer 1 launched into space, weighing just 14 kg [4]. And while the technological progress of the Space Race saw American and Soviet space activity focused on ever larger rockets and spacecraft, numerous small satellites were launched as well. During the Apollo period of the 1960s, the first weather satellite, Tiros, weighing 122 kg, and the first geosynchronous communications satellite, Syncom, weighing 35 kg were launched. The average weight of spacecraft being launched into space increased through the 1960s and 1970s [6].

Many space applications trace their roots to smaller spacecraft including weather, communications, and robotic and human exploration. But each of these applications grew into larger systems with superior capabilities. The level of performance and impressive results obtained from these applications seemed the logical future of space missions, with accomplishments seemingly impossible to obtain from smaller platforms. Spacecraft applications in the 1960s were that of communications, remote sensing, and exploration. The 1970s brought about the application of navigation, and the 1980s finally saw the first educational application from the University of Surrey [6]. The CubeSat, developed at the California Polytechnic State University and Stanford University in the late 1990s [2], popularized the use of small satellites for education. CubeSats use a standard size and form factor, where one unit measures 10 cm x 10 cm x 10 cm [5].

The increased popularity of small satellite use in recent years has helped to bring about the newest application of satellites: technology research and development. NASA, the Department of Defense, and the United States Air Force have invested heavily in small satellite technology development in recent years [7]. Many commercial companies are also leveraging the use of small satellites including Pumpkin Space Systems, AAC

Microtec, Adcole Maryland Aerospace, Blue Canyon Technologies, Clyde Space, Millennium Space Systems, and Tyvak International [8].

With satellites becoming smaller, radical changes in design considerations have resulted as compared to designs for larger satellites. Small satellites face the limitations of reduced volume, mass, and power leading to a reduction in capability when compared with larger satellites [9]. Small satellite design also involves an acceptance of more risk than traditional satellites. More traditional methods of spacecraft thermal control require additional testing and development for small satellite applications [10]. Surface coatings and insulation can still be easily applied to small satellites and allow for a reduced parts count and decreased complexity for the thermal control system. Small satellite designs generally have reduced part counts overall, due to the smaller scale of the satellite [6]. This results in the satellite not requiring nearly as complex finite element structural and thermal modeling schemes as their larger and more intricate counterparts.

Early spacecraft thermal models were typically based on correlation with extensive test data collected during thermal vacuum testing [11]. Numerical modeling was verified and updated using scale and full-size modeling experimental data [12]. General purpose heat transfer programs were developed in the 1960s to calculate radiation view factors, conductors, and heating rates. These programs included the Lockheed Heat Rate Program (LOHARP), the NASA Thermal Radiation Analysis System (TRASYS), the Simplified Space Payload Thermal Analyzer (SSPTA), the Chrysler Improved Numerical Differencing Analyzer (CINDA), and more [11], [13], [14].

In more recent history, thermal modeling and analysis has been conducted using specialized computer software packages including the Thermal Synthesizer System (TSS) by SPACEDESIGN, THERMICA by Network Analysis Inc., FEMAP/SINDAG Modeling System by Network Analysis Inc., I-DEAS TMG Thermal Modeling System, ITAS by Analytix Corporation, and Thermal Desktop by Cullimore and Ring Technologies [14]. Advances in software have led to thermal programs that have the versatility to handle almost any situation. Their speed and numerical accuracy have greatly improved, along with simplified utility and improved graphics [1].

There have also been a few attempts by universities at creating simplified thermal analysis modeling tools using MATLAB scripts and VBA Excel Macros [15], [16]. While these tools appear desirable, utilizing more affordable and readily available software, they rely on assumptions which oversimplify physical structures and heat transfer concepts. They often frequently do not publish the entirety of their codes, which makes it challenging, if not impossible, for others to utilize their tools.

1.3. THESIS STUDY GOALS AND OVERVIEW

Thermal control system design and thermal analysis can be a daunting task, especially for inexperienced engineers. An overwhelming amount of information is available pertaining to the subject, but much of it refers to larger spacecraft and can be distracting from the practices that should be followed for small satellites. Thermal control in particular has many technologies available that must be sorted through to select those which are most appropriate for small platforms.

The goal of this thesis study is to provide an organized and comprehensive resource to guide the small satellite thermal control system design and analysis process. A practical summary of the thermal model construction, analysis, and design process is shown in Appendix A. This thesis identifies pitfalls that can be avoided by future engineers during the process and help them to work more efficiently and effectively. Section 2 introduces heat transfer concepts and discusses how they pertain to a satellite system in space. The types of heating that a satellite will experience throughout its lifetime are also discussed in this section, as well as the energy balance approach for analyzing satellite thermal levels. Section 3 offers information about methods of thermal analysis, and walks the reader through how to approach performing a small satellite thermal analysis using modern computer software. This section also discusses the importance of computer model results verification through testing.

Section 4 discusses the necessary functions of a small satellite thermal control system, and provides information about available thermal control technologies. Both passive and active thermal control methods and all possible thermal control hardware for satellites are described, but the emphasis of the section is on technologies that are most

suitable for small satellites. This section also provides information about mountings and interfaces and how they can affect temperature distributions in satellites.

Section 5 describes the thermal control design process, which involves collecting information, performing analyses, and making design decisions. Section 6 describes a case study that presents the Missouri S&T Satellite Research Team's MR and MRS SAT small satellites. The detailed thermal analysis performed for the larger of the satellites is presented showing the reader each step of the process using thermal modeling software. Information about the thermal control techniques chosen for the satellites is also presented, along with justification for why certain technologies were selected.

2. HEAT TRANSFER CONCEPTS

It is important to have a knowledge base in heat transfer concepts before delving into the complexities of thermal analysis and control. A satellite will encounter different heating fluxes caused by different heat transfer modes throughout its lifetime. This flow of heat, or thermal energy, into, out of, and within a satellite can be described by using the energy balance approach. This approach can provide a better understanding of the interaction between a satellite and the thermal environment to which it is exposed during individual mission phases.

2.1. MODES OF HEAT TRANSFER

There are three modes of heat transfer including radiation, conduction, and convection. A satellite will typically transfer heat through radiation and conduction, which account for the heat exchange between the components inside the satellite in a vacuum. Heat rejection from the satellite to space and heat transfer to the satellite by celestial bodies is limited to radiation. The satellite will encounter convection on the ground, during ascent, and potentially from heat transfer from fluids in sealed containers [1].

2.1.1. Radiation. Radiation is the energy emitted by matter in the form of electromagnetic waves as the result of the changes in the atoms or molecules [17]. This can also be described as the heat exchange between a surface and its surroundings by electromagnetic energy. Any surface at a temperature greater than absolute zero will emit radiation. Radiation emission in units W/m^2 of a perfect emitter, or black body, is governed by the Stefan-Boltzmann law, given by Equation 1. Heat flux, which is the flow of energy per unit area per unit time, is denoted by q . The rate of emission in watts from a real, or nonideal, surface is given by Equation 2, where \dot{Q} denotes the rate of heat flux. Q represents the total amount of heat transferred. The radiation emission depends on the emissivity ε , the surface area A in m^2 , the Stefan-Boltzmann constant σ , and the temperature T in K. The subscript “e” denotes radiation emission. The Stefan-Boltzmann constant is $5.67 \times 10^{-8} W/m^2 \cdot K^4$.

$$q_e = \sigma T^4 \quad (1)$$

$$\dot{Q}_e = \varepsilon A \sigma T^4 \quad (2)$$

The emissivity of a surface is the measure of how closely a surface approximates the radiation emission of an ideal perfect radiator, defined in the range $0 \leq \varepsilon \leq 1$. An ideal surface with perfect radiation would have an emissivity of 1. The absorptivity α of a surface is the fraction of radiation energy incident on a surface that is absorbed by that surface. Its value is also in the range $0 \leq \alpha \leq 1$. An ideal perfect absorber would have an absorptivity of 1. The rate at which a surface absorbs radiation is given by Equation 3. The subscript “a” denotes radiation absorption, and the subscript “i” denotes incident radiation.

$$\dot{Q}_a = \alpha \dot{Q}_i \quad (3)$$

Generally, the emissivity and absorptivity of a surface depend on the temperature and wavelength of radiation. This dependence is sometimes ignored in practical applications [17]. The emissivity and absorptivity optical property values for different materials can be found in various books and in charts online [14]. They are also often provided in specification sheets for materials and components.

Radiation exchange among surfaces depends on temperature and geometric aspects as well as the surface material, smoothness, and curvature [1]. It can also be a function of the radiation wavelength and direction. Accounting for all effects is extremely complicated, so the heat exchange is generally approximated by introducing a “view factor.” This view factor, or shape or configuration factor, is the fraction of radiation leaving one surface which is intercepted by another and is denoted by F . The rate of

radiation exchange between two surfaces is given by Equation 4 [18]. The subscripts “1” and “2” denote some surface 1 and some surface 2.

$$\dot{Q}_{1,2} = \varepsilon_1 A_1 * \varepsilon_2 A_2 * F_{1,2} \sigma (T_1^4 - T_2^4) \quad (4)$$

There are many different sources that cite different methods of determining the view factor from one surface to another. The view factor also depends on the shapes of the surfaces, so there are many different combinations of shapes to consider as well. Many heat transfer textbooks list view factor calculations for simple situations including aligned parallel surfaces, perpendicular rectangles with a common edge, and surfaces within an enclosure [1], [17], [19]. These common geometries can be useful for representing surfaces inside a satellite. Another relevant view factor case for a small satellite may include the view factor between a small planar surface tilted to or facing a sphere, which could represent the side panel of a satellite facing the Earth or a celestial body. The resources [20] and [21] were found that catalog many different view factor calculations and may be very useful for engineers wishing to perform a first order approximation of the radiation incident upon their spacecraft.

2.1.2. Conduction. Conduction is the transfer of energy from more energetic particles of a material to the adjacent less energetic ones with no apparent displacement of matter [1], [17]. Fourier’s law of heat conduction shows that conduction is caused by the temperature gradient through a solid material, given by Equation 5 [19]. The rate of heat conduction in watts through a material depends on the material’s geometry and thickness as well as the temperature difference across the material.

The temperature gradient across the material thickness is denoted by dT/dx , and the thermal conductivity in W/m-K of the material is k . The negative sign indicates that the heat flows from the higher temperature to the lower temperature. Conductivity depends on material temperature, but it generally remains constant in the range of temperatures that satellites encounter [1]. Material thermal conductivity values can be

found in material specification sheets, in heat transfer textbooks, online, and in other resources including [14].

$$\dot{Q}_{cond} = -kA \frac{dT}{dx} \quad (5)$$

In general, heat conduction is three-dimensional and time dependent [17]. Approximations can sometimes be made to simplify the conduction problem down to be steady rather than transient, and one-dimensional or two-dimensional rather than three-dimensional. Heat conduction is said to be steady rather than transient when temperature does not vary with time. Heat conduction is one-dimensional when conduction is negligible in all but one of the dimensions, and two-dimensional when it is only negligible in the third dimension. In practice, most heat conduction problems can be approximated to be one-dimensional, and Equation 5 will be sufficient. Steady-state and transient heat transfer is discussed in more detail in Section 3.

2.1.3. Convection. Convection is heat transfer between a solid surface and a fluid flowing over it results either from a pressure difference, termed forced convection, or from variations in gravity and density, termed natural or free convection [1]. Newton's law of cooling states that the rate of heat transfer between a surface and a fluid is proportional to the difference between the surface temperature T_s and the fluid temperature T_∞ , given in watts by Equation 6. The constant of proportionality h is called the heat transfer coefficient, and is an experimentally or analytically determined parameter which depends on surface geometry and flow conditions [17]. The heat transfer coefficient is provided in W/m^2-K , and can be found in heat transfer textbooks such as [17] and [19].

$$\dot{Q}_{conv} = hA(T_s - T_\infty) \quad (6)$$

In satellite thermal analysis, convection will take place during ground operations, ascent, and through the use of thermal control measures such as heat pipes and pumped fluid loops. During ground operations, the satellite will be exposed to free convection from the ambient atmosphere. The free molecular heating effect caused by friction in the upper atmosphere may be encountered by satellites during ascent and in orbits that are below 180 km [14]. Heat pipes and pumped fluid loops utilize convection effects to transfer heat and improve heat sharing in a satellite on orbit [1], [10].

2.1.4. Combined Modes of Heat Transfer. All three modes of heat transfer cannot exist in a medium simultaneously [17]. In opaque solids only conduction can occur, but in semitransparent solids both radiation and conduction can occur. As an example, a solid may be experiencing conduction and radiation but not convection. Although, while an outer surface may be experiencing convection and radiation, the inner portion of the material may experience conduction as heat is transferred from the outer surface to the inner material.

2.2. HEATING FLUXES

Different heating fluxes are present during different stages of a satellite's life, including ground, ascent, and orbit. Heating on the ground is a combination of satellite heat generation and the conditions of the surrounding air. During ascent aerodynamic heating and free molecular heating of the launch vehicle fairing that the satellite is housed in are caused by friction in the upper atmosphere [14]. Heating in space is due mainly to satellite internal heat generation and radiation from the Sun and other celestial bodies. The time a satellite will spend in orbit is far longer than any other stage, so most of the focus of the thermal engineering effort is spent on ensuring the temperature stability of the satellite in space [1].

2.2.1. Ground Environment. While on the ground the heating fluxes experienced by the satellite will be from equipment heat dissipation and from the surrounding air conditions [1]. The temperature, humidity, and flow rate of the air surrounding the satellite may be adjusted to maintain desired temperatures using proven air-conditioning equipment. It may also be necessary to establish constraints on how long

the satellite may be powered up during testing and storage in room temperature conditions to prevent satellite components from exceeding their temperature limits [14].

2.2.2. Ascent Heating. Satellite heating during ascent is determined by the temperature reached by the launch vehicle fairing which protects the payloads being sent to space [19]. Heating of the fairing is caused by air friction, occurring for about two to five minutes after liftoff. While the fairing may rise to temperatures as high as 180°C for about a minute, the temperature effect inside the fairing is usually minor because of its interior insulation and low-emissivity surfaces [1]. The temperature rise inside the fairing is due to radiation and conduction between the fairing and the payloads.

Once the launch vehicle reaches an altitude of about 116 km, the fairing is jettisoned to save weight. The payloads then experience heating directly resulting from frictional forces, or free molecular heating, but the low density of the atmosphere at this altitude causes minor heat fluxes [22]. From this point onward, the payloads also experience heating from solar, albedo, and Earth IR loads. The ascent phase of a payload's life usually lasts 30 to 45 minutes, which for a small satellite in low Earth orbit will result in insertion into the final mission orbit [14].

2.2.3. Low Earth Orbit Environment. The altitude of a satellite in low Earth orbit (LEO) is between 150 km and 1000 km. This altitude lies above the outer limits of the atmosphere and below the Van Allen radiation belts [23]. This means that the only external sources of heat that a satellite will be subjected to are direct solar radiation, Earth albedo radiation, and Earth infrared radiation. Effects from other celestial bodies, from elementary particle bombardment, and from space background are assumed to be negligible [1].

Before analyzing environmental heating in LEO, it is important to define the orbit beta angle β . The beta angle is the minimum angle between the orbit plane and the solar vector and can vary from -90 to +90 degrees, as shown in Figure 2.1 [14]. An orbit with a beta angle of zero will appear edgewise when viewed from the Sun. In an orbit like this a satellite will pass over Earth's subsolar point where the amount of radiation from the Sun reflected off the Earth will be highest, but this orbit also has the longest eclipse time. As the beta angle increases, the amount of radiation reflected off the Earth from the Sun decreases, but the eclipse time decreases as well. Eclipse time drops to zero for a circular

orbit with a beta angle equal to 90 degrees, but there is also no radiation reflection off the Earth from the Sun in this type of orbit. Beta angles can be expressed as positive or negative. The beta angle is positive if the satellite is progressing in a counterclockwise direction around the orbit as seen from the Sun, and negative if clockwise.



Figure 2.1. Orbit Beta Angle [14]

2.2.3.1 Direct solar radiation. The radiant energy from the Sun is the most significant heat source in LEO. The radiation is nearly constant, and is equal along all directions [14], [18]. The lengthy distance of the Earth from the Sun allows for the assumption that the radiation propagates along parallel rays, leading to the term “solar vector,” which is a vector with direction along the solar rays and a magnitude of the solar constant S [1]. The solar constant is the “rate at which solar energy is incident on a surface normal to the Sun’s rays at the outer edge of the atmosphere” in W/m^2 [17]. Due to the Earth’s elliptical orbit, the solar constant will vary based on the time of year. The Earth is farthest from the Sun during the northern hemisphere’s summer, and the minimum value of the solar constant is about $1322 \text{ W}/\text{m}^2$. When the Earth is closest to the Sun, during the northern hemisphere’s winter, the solar constant is about $1414 \text{ W}/\text{m}^2$ [14].

The amount of radiation from the Sun impinging on a surface is characterized by the solar constant and the orientation of the object with respect to the Sun. The heat flux in W/m^2 , as a result of direct solar radiation, absorbed by a surface depends upon the solar absorptivity α of the surface, the solar constant S , and the incident angle θ from the surface normal to the solar vector, as shown in Equation 7 [1]. Solar infrared radiation has much shorter wavelengths than those emitted by a body at room temperature, which

is the typical satellite temperature. This allows for selection of surface finishes which have a low absorptivity in the short-wavelength part of the infrared spectrum, and a high emissivity in the long-wavelength part of the spectrum [14].

$$q_{solar} = \alpha S \cos\theta \quad (7)$$

2.2.3.2 Albedo radiation. The solar energy reflected off the Earth is referred to as “albedo radiation.” The amount of albedo radiation incident upon a spacecraft is a function of spacecraft orientation and orbit and can be a significant source of radiation when the spacecraft is near the Earth [16]. Albedo is considered to be in the same spectrum as solar radiation, and is calculated as a fraction of the solar constant. The heat flux due to albedo that is incident on a surface depends on the surface absorptivity α , the solar constant S , the albedo factor A_f , and the view factor F between the surface and the Earth, given by Equation 8 [15]. The view factor can be calculated using the methods mentioned previously, in resources [20] and [21]. Surfaces facing away from the Earth will receive no heat flux due to albedo.

$$q_{albedo} = \alpha S A_f F \quad (8)$$

The albedo factor is dependent upon the surface properties of the Earth. The amount of incident solar radiation reflected by the Earth varies between 25% and 55%, depending on those surface properties [14]. Clouds, water, ice, land, and forests have different reflectance values and will result in different albedo factors. The albedo factor for clouds is typically about 0.8, and the factor for forests and fields can vary from 0.03 to 0.3 [22].

2.2.3.3 Earth IR. Any solar radiation incident on the Earth that is not reflected as albedo is absorbed by the Earth and reemitted as long-wave infrared radiation [14]. The IR energy emitted by the Earth can vary with season, latitude, the local temperature of the Earth's surface, and the amount of cloud cover. These localized variations can be significant, but they are far less severe than variations in albedo. The Earth IR intensities of interest for satellites are the long-term averages, so the variations are not of great concern [22].

The Earth IR energy absorbed by a surface is a function of the Earth's temperature and the orientation of the surface with respect to Earth [15]. The heat flux, in W/m^2 , absorbed by the surface of a satellite depends on the Stefan-Boltzmann constant σ , the surface emissivity ε , the view factor between the Earth and the surface F , and the effective ideal radiator, or black body, temperature of the Earth T_E , as shown in Equation 9 [1], [16]. The effective black body temperature of the Earth is on average 255 K [16].

$$q_{IR} = \sigma \varepsilon F T_E \quad (9)$$

Earth emitted radiation is long-wave infrared radiation, which is the same band of radiation normally emitted by satellites. This explains why the fraction of Earth IR radiation absorbed by a satellite is determined by its emissivity ε . This also means that a surface finish chosen in order to reflect Earth IR radiation will also reduce the surface's radiation emission ability [1].

2.2.3.4 Spacecraft heat generation. Along with external heat fluxes, the heat generated inside the satellite must be considered. This internal heat generation results from energy dissipation by components that are necessary for the satellite functions [24]. Component heat dissipation may vary around the orbit and at different times during the mission due to the requirements of different mission phases. For satellites without moving parts, the electrical-power draw for components will be converted entirely to heat [14]. The total amount of heat produced by a satellite will then depend only on the power consumption of the components.

2.2.3.5 Spacecraft heat emission. Another heat flux that must be considered is the heat radiating from the satellite itself. A satellite will radiate heat into space as a black body, at 0 K for practical purposes, with a certain emissivity [22]. This heat transfer will take place at the satellite boundaries from the total surface area of the satellite. The amount of radiation emission is limited by the available surface area and optical properties [24].

2.3. THERMAL ENERGY BALANCE

Thermal control of a satellite on orbit is typically accomplished by balancing the energy absorbed from the environment and generated internally to the energy stored and emitted by the satellite as IR radiation, which follows the law of conservation of energy [14]. This thermal energy balance is shown by Equation 10. The heat entering the satellite comes from the external heating fluxes experienced in LEO. The heat flux in W/m^2 entering the satellite is a combination of all the external heat fluxes incident on the satellite in the LEO environment, as shown in Equation 11 [24]. The total heat flux incident on each of the satellite's external surfaces should be considered when using this approach to determine the total absorbed heat flux.

The heat generated is the total heat dissipated by the satellite components. Stored heat is a function of satellite mass and thermophysical properties including density and specific heat [1], [24]. The energy stored is also called the heat capacity, thermal mass, or thermal capacitance [17], [24]. The heat storage capability of a material is represented by both the heat capacity and the specific heat c_p , where the heat capacity expresses it "per unit volume" and the specific heat expresses it "per unit mass." The heat stored in a volumetric element of a material in watts, which depends on the material density ρ and specific heat, is given by in Equation 12 [1]. Heat rejected from the satellite occurs through radiation from the satellite external surfaces. It should be noted that this energy balance does not take into account effects due to conduction.

$$\dot{Q}_{in} + \dot{Q}_{generated} = \dot{Q}_{stored} + \dot{Q}_{out} \quad (10)$$

$$q_{in} = q_{solar} + q_{albedo} + q_{IR} \quad (11)$$

$$\dot{Q}_{stored} = \left(\rho c_p \frac{\delta T}{\delta t} \right) \Delta x \Delta y \Delta z \quad (12)$$

3. SATELLITE THERMAL ANALYSIS

The purpose of satellite thermal analysis is to predict the temperatures of the satellite under known or assumed environmental conditions [1]. The analysis starts with the identification of component temperature limits and heat dissipation. Thermal boundary conditions for each mission phase must also be identified, including spacecraft altitude and orientation relative to the Sun and Earth. Modern design techniques utilize analytical processes assisted by computer modelling programs that use the identified inputs [22]. Surface radiation and view factors are established using radiation or ray-tracing techniques employed by software, which defines the interaction between all the spacecraft surfaces by radiation. A practical approach to thermal model construction, analysis, and control is presented in Appendix A.

3.1. THERMAL EXTREMA ANALYSIS CASES

In order to define upper and lower bounds on temperature predictions, and to account for errors and uncertainties, thermal engineers use hot and cold cases in their analyses [1]. This analysis approach of designing to meet specified temperatures even under accumulated biases builds confidence in the model. The parameters used for these cases are chosen such that the resulting thermal loads are as extreme as the satellite will realistically experience during its lifetime. The temperatures reached during normal on-orbit operating conditions will lie between the temperatures reached during the hot and cold case operating conditions [14].

Hot and cold case input parameters can include the solar vector, albedo factors, component dissipation, beta angle, and altitude. Many small satellites are launched as secondary payloads, and their resulting orbit and altitude may depend upon that of the main payload being launched. For academic missions in particular, it may be easier to find a launch if the mission can be performed over a wide range of orbit options. In instances such as this, the hot and cold cases may need to encompass a wide range of beta angles and altitudes as input parameters.

Any parameters that are not direct measurements from the satellite material and structure may also be manipulated for a hot or cold case. Input parameters including

conductivity k , specific heat c_p , density ρ , and beginning and end-of-life optical properties can be changed for a hot case versus a cold case [1]. It may make sense to use an average value for the analysis instead of a separate hot and cold case value, in order to reduce the number of variables in the analysis.

It is important to choose parameters and make assumptions that remain realistic within the scope of the satellite mission. It would be excessive to assume that the heat flux values in the LEO environment cause solar impingement on surfaces that are not actually facing the Sun. It would also be detrimental not to take advantage of possible available electrical power that can be used for heaters during orbits with low electronics dissipation, which could be overlooked if the chosen parameters are unrealistic. It should also be noted that unexpected occurrences such as power loss, hardware malfunctions, and radiator misalignment are considered failure modes, and do not set the basis for performance requirements or the thermal design [1].

3.1.1. Hot Case. For a hot case analysis, input data will be chosen such that the resulting temperatures are as high as the satellite may experience during its mission. Such input data for the hot case will include the highest values for many parameters that are addressed here. The solar vector S may be chosen as the average value, but a more extreme and potential hot case for a satellite may occur when the Earth is closest to the Sun, with a solar constant of about 1419 W/m^2 . Albedo factors may be chosen in a similar way, with those occurring during the warmest time of year chosen for this case, with the highest reasonable albedo factor measuring 0.55 [25]. Any other properties that are approximated in the analysis should also be chosen to result in higher temperatures. The power profile for components in a hot case analysis will correspond to the mission mode resulting in the greatest component heat dissipation [1].

3.1.2. Cold Case. Parameters chosen for a cold case should be selected to result in temperatures as low as the satellite may realistically experience during its mission. This will include the lowest solar vector S of about 1317 W/m^2 and the lowest albedo factors A_f of 0.18 [25]. Any other approximations made in the analysis should also be chosen to result in low temperatures. The power profile for components in a cold case analysis should not be assumed zero, but should correspond to the mission mode resulting in the least amount of heat dissipation, likely a safety mode.

3.2. NUMERICAL APPROXIMATION METHODS

Predicting the temperature of a satellite is accomplished by applying the conservation of energy principle. This is typically written as a second-order partial differential equation, as shown in standard notation by Equation 13. It depends upon the vector of partial derivatives along each axis ∇ , the thermal conductivity k , the temperature T in K, the volumetric heat generation q^* , the density ρ , the specific heat c_p , and time t . This equation is then solved using initial and boundary conditions that define the heat exchange at a location. Finding exact analytical expressions for temperature from this equation is generally not possible because of the interface conductivities on temperature [1].

$$\nabla * (k * \nabla T) + q^* = \rho c_p \left(\frac{\delta T}{\delta t} \right) \quad (13)$$

Actual satellites also include jumps in material properties and other nonuniformities that would require an unmanageable number of equations and boundary conditions. The more practical approach to solving the problem of predicting satellite temperatures is to use simplifications and numerical approximation methods applied to a thermal model of a satellite [1]. The approximation methods of thermal modeling subdivide the satellite into nodes or elements that are connected by conduction and radiation. Convection can be included as well if necessary. In order to create a thermal model, engineers must first configure nodes or elements to realistically represent the actual system. The total number of nodes or elements for a model will depend on the satellite size, complexity, and nodal resolution required [18]. Engineers must also define heat flow paths between nodes or elements using conductors, and include heating or cooling rates at necessary locations in the model. Once the thermal model has been constructed, the numerical approximation methods are applied, usually using computer software, to calculate the temperatures [1].

3.2.1. Finite Difference Approximation. The finite difference approximation method (FDM) determines the solution to a finite difference model that approximates the actual satellite using nodes. Each node represents a concentration of parameters at a single point in the thermal system. The nodes are connected using conduction and/or radiation heat transfer principles. This method uses Taylor series approximation to construct a system of finite difference equations. The finite difference equations are then converted to a set of algebraic equations that can be solved to find the temperatures using iterative techniques, matrix inversion schemes, or decomposition methods. This approach of using finite difference node meshes to make up the thermal model is also referred to as “lumped-parameter representation” [14].

3.2.2. Finite Element Approximation. The finite element approximation method (FEM) utilizes elements to create the thermal model. Different element types that can be used have different shapes and a different number of nodes. Some examples of element types are one-dimensional bar elements, two-dimensional triangular, rectangular, and quadrilateral elements, and three-dimensional hexahedral, pentahedral, and tetrahedral elements. Each element has nodes at its corners, where parameter values such as temperatures are calculated. The parameters can vary across the element, and can be found using interpolation functions [14].

The FEM determines an explicit expression for the satellite temperatures in terms of known functions. These expressions for temperatures are a finite element approximation for the actual temperature. The expression depends on the degrees of freedom specified by the engineer, and the shape, or interpolation functions. The ultimate purpose of this method is to create a set of algebraic equations for the temperatures of the elements and nodes, which can be done using the Galerkin method of weighted residuals. The accuracy of this method can be improved by using a mesh with more elements [14].

3.2.3. Steady State. In steady state analysis calculations, the heat flux entering the spacecraft and the heat flux leaving the spacecraft is constant [22]. Steady state, by definition, means that the temperature and heat flux at a point in a body will not change with time [18]. However, the temperature may vary from one point to another.

3.2.4. Transient. A realistic practical thermal design for a satellite is generally based on transient considerations [1]. However, the starting point for a transient analysis calculation is the temperature distribution found from the steady state calculation [22]. The transient calculation will result in the satellite temperature history at successive time intervals. Smaller time intervals will result in more accurate temperature calculations. A standard technique employed to verify a transient analysis is to repeat the calculations at smaller and smaller time steps and to observe the trend of convergence to an asymptote [1]. For a transient model, the temperature will typically vary with time as well as location [17].

3.3. COMPUTER THERMAL MODELING

3.3.1. Modeling Software. Computer thermal modeling involves constructing a thermal model of the satellite and then calculating temperatures at nodes in the model by applying a numerical approximation method. Most thermal software used in the satellite industry employs the finite difference approximation method, although, FDM tends to have mesh-generation issues. Many software packages overcome these issues by using FEM mesh generators to construct the mesh and then convert it to a finite difference mesh for FDM software codes. The temperatures calculated by the codes are then returned to the FEM mesh generation code for display [14].

The FEM is predominantly used in the satellite industry to perform structural analysis, but it can also be very beneficial for thermal-stress problems. Structural models typically require a greater amount of detail than equivalent thermal models, which means that the structural features will drive the size of the model and analysis for a thermal-stress problem. Structural models contain features such as bolt holes, chamfers, and fillets. Thermal models tend to be more simple representations of satellites versus structural models.

FDM codes are preferable for thermal modeling by itself. FEM codes cannot use just a single node for simulation, like FDM codes can. FEM codes will also generally be larger than necessary for a typical thermal analysis. Each element face must share a complete border with another element, which causes the model to be more complex than needed. FDM codes also require fewer surfaces to model curved surfaces such as cones

and cylinders than FEM codes do. An FDM code can represent these simple surfaces with a single node of 360 degrees that contains the actual surface description, which is all that is needed for radiation codes to calculate radiation-interchange factors. Modeling these surfaces in FEM codes forces increased detail that unnecessarily leads to greater computational cost [14].

Most modern thermal analysis programs contain a model builder, orbital display capabilities, a radiation analyzer, a thermal analyzer, and postprocessing software that displays heat flux plots and the temperature distribution on the model. Many of these software packages utilize FDM codes, though IDEAS TMG for NX uses FEM codes. Some surface generating routines include PATRAN and SURTRAN [1]. ESATAN, ESARAD, and ThermXL are recommended by the ESA, and can be coupled to mathematical modelling and orbit plotting tools [22]. Other commercially available software packages, that utilize FDM codes, include TSS, Thermal Desktop, THERMICA, FEMAP/SINDAG, ITAS, and SINDA. This thesis study focuses on utilizing Thermal Desktop, which uses AutoCAD for modelling and SINDA as a thermal solver, described in Section 6 [26].

3.3.2. Modeling Iterations. The process of creating an accurate and representative thermal model can begin with creating a simplified thermal model, which can be useful in the early design stages. A simple first-order thermal model uses a simplified geometric shape such as a cube, sphere, cylinder, or several flat surfaces that are representative of the satellite [18]. Operational and non-operational temperature requirements for components must be identified, as well as the orbit parameters, the preliminary baseline mission profile for the environmental heating of the satellite, and the internal heat generation of the satellite. The energy balance equation can be used to calculate the temperature of the simple satellite model propagated through the steps of the orbit. Different cases can be run, adjusting surface and other parameters with each case to determine what attributes drive the temperature of the model. The resulting temperatures should be compared with satellite temperature requirements, though a more complex model may be needed to provide more realistic temperature predictions.

Multiple iterations of the thermal model can be constructed with the assistance of thermal modeling software, starting with the simplest model. Each subsequent model can

incrementally incorporate surfaces, complexity, and nodal resolution. The purpose of this gradual process is to ensure accuracy of the model before it becomes more complex. The nodal resolution necessary for the final model can be determined by conducting a convergence study. The temperature results for each iteration are compared to the results from the previous iteration until the difference between them is within a certain tolerance.

3.3.3. Spatially Averaged Properties. Thermal models require optical and thermophysical properties for surfaces and components to calculate the radiation and conduction heat exchange in the satellite as well as the radiation heat rejection from the satellite. For models that lump these parameters for multiple surfaces, the spatial average of a property for the surfaces must be calculated to more accurately represent each of the surfaces in the simplified model, if testing for the effective properties cannot be done [1]. Effective values for optical properties can be predicted by taking the area averages. For example, the components that make up a solar panel may be lumped together in a simple model and the effective optical properties for the surface must be calculated to take into account the optical properties for component that makes up the outward facing surface: solar cells, printed circuit board, and thermal tapes. The percentage of the total surface area made up by an individual component will determine its contribution to the effective value of the optical property. Equations 14 and 15 show the calculation for effective absorptivity and effective emissivity for n surfaces, respectively.¹

$$\alpha_{effective} = \sum_{j=1}^n \left(\frac{A_j}{A_{total}} \right) \alpha_j \quad (14)$$

$$\varepsilon_{effective} = \sum_{j=1}^n \left(\frac{A_j}{A_{total}} \right) \varepsilon_j \quad (15)$$

¹ Dr. Derek Hengeveld in discussion with the author, 2016.

Thermal conductivity and specific heat must also be predicted for a lumped parameter situation. The percentage of the volume that a component makes up in a surface will determine the component's contribution toward the specific heat of the effective surface, as shown in Equation 16. The effective conductivity of multiple layered surfaces in parallel is found using the method of parallel resistors, where A is the cross-sectional area and t is thickness, as shown in Equation 17². For multiple layers in series, the effective conductivity can be found using Equation 18.

$$c_{p_{effective}} = \sum_{j=1}^n \left(\frac{M_j}{M_{total}} \right) c_{p_j} \quad (16)$$

$$k_{effective} = \frac{t_{effective}}{A_{effective}} \sum_{j=1}^n \frac{k_j A_j}{t_j} \quad (17)$$

$$\frac{1}{k_{effective}} = \frac{A_{effective}}{t_{effective}} \sum_{j=1}^n \frac{t_j}{k_j A_j} \quad (18)$$

3.4. VERIFICATION OF RESULTS

3.4.1. Simplified Thermal Analysis. Reduced versions of detailed models are helpful for parametric, tradeoff, and interface studies. Simplified numerical analyses can also be used to verify computer results, detecting errors and subtleties in more complex computer models [1]. Analyzing a single isothermal node model constructed using numerical methods is a useful means for testing assumptions before considering more a more complex analysis. However, a single node model for a satellite will not provide

² Dr. Derek Hengeveld in discussion with the author, 2017.

adequate temperature calculations to analyze and design the thermal control for a satellite. Even small or simple satellites will require the creation of a mathematical multi-node thermal model [18].

3.4.2. Thermal Balance Test. A thermal model must be verified before flight, which is achieved through performing a thermal balance test to confirm that the analysis method is valid and that the satellite temperatures will indeed not exceed the mission requirements [1]. At this point, it is expected that any discrepancies between the model results and the test results will be minor. If necessary, slight design alterations can be made. Intermediary and system level tests can also be performed before this step to confirm hardware properties and performance.

The thermal balance test must be performed in a vacuum chamber equipped with heating sources and cryogenic surroundings to simulate space background and orbital heating fluxes. The vacuum air pressure should be in the range of 10^{-6} torr [1]. The thermal balance test is generally performed on flight hardware, and typically only the main satellite electronics canister is tested [14]. Nonflight attachments may be tested along with the canister that are designed to be heated or cooled to mimic the thermal effects of deployed structures. Some heat exchanges that might occur in a test configuration but are absent on orbit can be minimized using guard heaters, reflective shields, and isolators [1].

During the test, individual conditions are simulated and thermal data are collected during the temperature transition for correlation with the transient analysis and at equilibrium for steady-state analysis correlation [14]. Verification of the thermal control subsystem also requires performance verification of thermal hardware including heaters, thermal sensors, radiators, louvers, heat pipes, and cryogenic systems. The simulation conditions include hot and cold operational phases, cold non-operational phases, transitions between conditions, and safe mode phases. The test typically begins with the cold phase, to simulate the temperature decreasing from launch into ascent, though it can start with the hot operational phase instead to increase material outgassing of the spacecraft. Test processes and profiles are described in more detail, with recommended test levels, in guidelines published by the Department of Defense [27], [28]. An example of a simple thermal balance test profile is shown in Figure 3.1 [14].

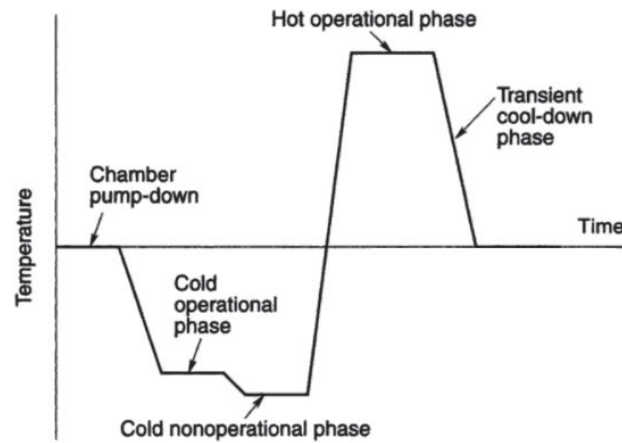


Figure 3.1. Simple Thermal Balance Test Profile [14]

The success criteria for the test depends on the demonstration of the thermal system in operational and survival conditions as well as correlation of the resulting test data with the thermal model. The correlation process includes altering the thermal model to make predictions for the satellite under the environment and configuration of the test chamber. Some modifications to the thermal model for this purpose include removing hardware that will not be included in the test such as propellant and solar arrays, adding nodes to represent test hardware that includes test stands and heater lamps, adding nodes to represent cabling for guard heaters and for chamber walls, and altering radiation view factors to account for blockages resulting from test equipment and stowed hardware. Correlation of the results to the model predictions should be within $\pm 3^{\circ}\text{C}$ [14].

A lack of model and test correlation may result from deficiencies in the model, test setup, or satellite hardware. Areas with large temperature discrepancies should be scrutinized first. Testing conditions should be checked, as well as any obvious omissions in the model. If the issues persist, the thermal model should be adjusted in the direction to make the model temperatures agree with the test temperatures. Conductance values and view factors can be modified to alter the paths of heat transfer in areas with high uncertainty, such as paths across complex geometries and interfaces.

Changes made to the model should be minor, and major changes should never be made to force a model to match test data. Any changes made to the model must maintain agreement with the satellite hardware. Changing object parameters in a model to something other than a recommended value suggests that other error sources should be investigated instead. A significant amount of changes often indicates that a thermal mode lacks sufficient detail to accurately model the satellite [14]. While the goal of making these corrections to the thermal model is to bring temperature predictions into agreement with the test values, the ultimate purpose is to ensure that the thermal model is capable of accurately predicting flight temperatures.

4. SATELLITE THERMAL CONTROL

Satellites must use certain thermal control methods and hardware to regulate temperatures to ensure that the satellite components function properly during the mission. Thermal engineers must choose and apply hardware elements while meeting cost, mass, and power constraints [18]. As small satellite designs mature, thermal control techniques must be able to meet smaller constraints on mass, volume and power. To achieve volume efficiency, many small satellites must rely on primary structural components not only for carrying mechanical loads but also as the primary component for thermal control and radiation shielding. Traditional thermal control methods may need alteration for application in smaller platforms, though some methods can easily be applied to small satellites [10].

4.1. THERMAL CONTROL HARDWARE

The thermal control system on a satellite generally uses two basic approaches for temperature management: passive and active thermal control. Many satellite thermal control systems use a combination of passive and active control, though the passive control methods make up the majority of the system with supplemental active control methods for equipment with small temperature tolerances [22]. Small satellites most commonly employ passive control methods, though these methods may need more surface area or assistance from deployable systems to radiate heat away from the satellite. Some active thermal control systems can be more compact, but most are often heavy and power intensive [6].

4.1.1. Passive Thermal Control. Passive thermal control techniques include material property selection, controlling the path of heat transfer, and using insulation systems to ensure that temperatures remain within acceptable limits [22]. Techniques including the use of multilayer insulation (MLI) and thermal coatings have a long heritage on traditional satellites, but may require modifications for use in small satellites. The performance of these techniques in small satellites may be compromised because the effectiveness of the materials may tend to decrease when they are applied to small surface

areas, but many companies that produce MLI blankets and surface coatings have had their products demonstrated on small satellite missions [6].

4.1.1.1 Insulation. Insulation systems are designed to minimize heat exchange in the vacuum of space [22]. Thermal insulation acts as a barrier to radiation and prevents excess heat dissipation. MLI blankets are the most common insulation, though single layer barriers are sometimes used where lesser degrees of insulation are required because they are lighter and less expensive [18].

MLI is composed of layers of low-emittance films, as shown in Figure 4.1 [14]. A simple MLI blanket consists of layers of about ¼ mm thick embossed Kapton or Mylar sheets that each have vacuum deposited aluminum finish on one side. The embossing of the sheets causes them to only touch at a few points, which minimizes conduction between the sheets. The sheets are only aluminized on one side so that the sheet material acts as a low conductivity spacer. A more complex and higher performance construction consists of sheets that are metalized with aluminum or gold on both sides and silk or Dacron net between the sheets acting as the low conductivity spacer [14]. An outer cover encloses the stack to form the MLI blanket, which is held together with non-metallic thread, intermittent taping along the edges, or non-metallic snap buttons [1]. The outer cover can be made from Teflon, aluminized Kapton, black Kapton, or Beta cloth, which is a Teflon coated glass fabric [14]. The blanket assembly is typically secured to the satellite by bonding or using Velcro strips. Grounding straps are added to reduce the electrostatic charge on the insulation during orbit [1].

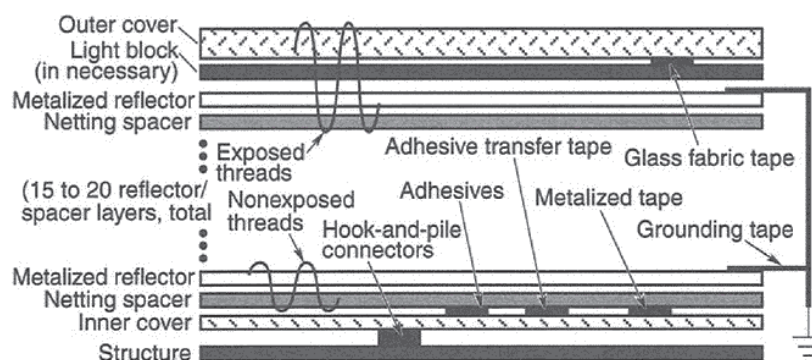


Figure 4.1. Typical MLI Blanket Composition [14]

Heat transfer through MLI occurs as a combination of conduction and radiation. The radiation heat transfer is minimized by using as many sheet layers as is possible and practical between the surface or object being insulated and its surroundings. Conduction heat transfer is minimized by using low density material for the spacers and by ensuring that the embossing of the sheets is sufficient to minimize contact between the layers [14]. Because these heat transfer methods are occurring simultaneously, the thermal conductivity of the insulation system is difficult to define. An effective thermal conductivity $k_{effective}$ or effective emissivity ϵ^* is typically used to describe the heat transfer through the MLI. These values can be derived experimentally, and are generally also provided by the manufacturer.

Materials used for fabrication of an MLI blanket should always be treated as flight-critical hardware from the moment they are received. The materials should never be handled with bare hands and should never be exposed to uncontrolled and corrosive environments in order to avoid contamination and material degradation. Actions such as pulling or unnecessarily wrinkling the material should be avoided as this can cause stress in the layers and defects that may not appear until launch. Fabrication should occur in a temperature and humidity monitored Class 100,000 clean room to preserve the cleanliness and optical properties of the material. The fabrication area requires tables large enough to support the largest blanket being manufactured. All tools, equipment, templates, holding fixtures, and tables should be cleaned with a solvent that has a nonvolatile residue that does not exceed 0.02 g/L. The solvent must be compatible with the materials to avoid damaging the materials during normal cleaning operations. Clean white gloves or powder-free latex gloves suitable for clean room use must be used when handling the material, and clean room lab smocks must be worn [14].

The effectiveness of an MLI blanket cannot be determined through visual inspection. The efficiency of an assembled insulation can only be measured by an actual performance test. The construction of a reliable MLI blanket is typically achieved by experienced manufacturers [1]. Although, Dunmore Aerospace corporation has recently engineered, through their developments with STARcrest Spacecraft Materials, a SATKIT that contains MLI blanket materials for small satellite applications [10]. The materials have previously been flown, and the kit is considered to be “flight qualified” through

testing and demonstration, but has not been “flight proven” by successful operation during a satellite mission [29].

The performance of MLI blankets tends to drop in efficiency as their size decreases, so they do not perform as well for small satellites as they do on larger platforms. They can also be delicate so engineers must take caution when using MLI on the external surfaces of small satellites, especially satellites that will be launched from a small satellite deployment system. Surface coatings tend to be more appropriate for small satellite exteriors because they are less delicate. Surface coatings can also replace MLI for internal surfaces that do not receive direct solar radiation. Low emissivity coatings perform almost identically in this context, use less volume, and cost less [10].

4.1.1.2 Surface coatings and finishes. Surfaces can be tailored to emit and absorb energy at specific rates. Thermal control coatings are typically classified as solar reflectors, flat coatings, or solar absorbers. Solar reflectors have a low solar absorptivity and a high emissivity, which makes them useful in solar and albedo environments because they reflect much of the incoming radiant energy while continuing to reject waste heat. Flat coatings reflect and absorb almost equally, and are frequently used inside of satellite enclosures to enhance radiant heat sharing. Solar absorbers have a high solar absorptivity and a low emissivity, making them nonideal for satellite surfaces but excellent for extendable elements. Solar absorbers are also sometimes used with other coatings in combination patterns to tailor surface properties, as shown in Figure 4.2 [1]. Over the past few decades, a wide range of materials, coatings, and paints with almost every combination of absorptivity and emissivity have been produced that can be used for thermal control [22].



Figure 4.2. Surface Coating Combination Patterns [1]

4.1.1.2.1 Common surface treatments. Almost all interior and exterior surfaces of a satellite have thermal control surface finishes applied to them. Space qualified paints are available in a wide range of colors, but black and white are the most commonly used. Specialty finishes are also occasionally used in satellite thermal control. The typical optical properties for different surface treatments are shown in Figure 4.3 [14].

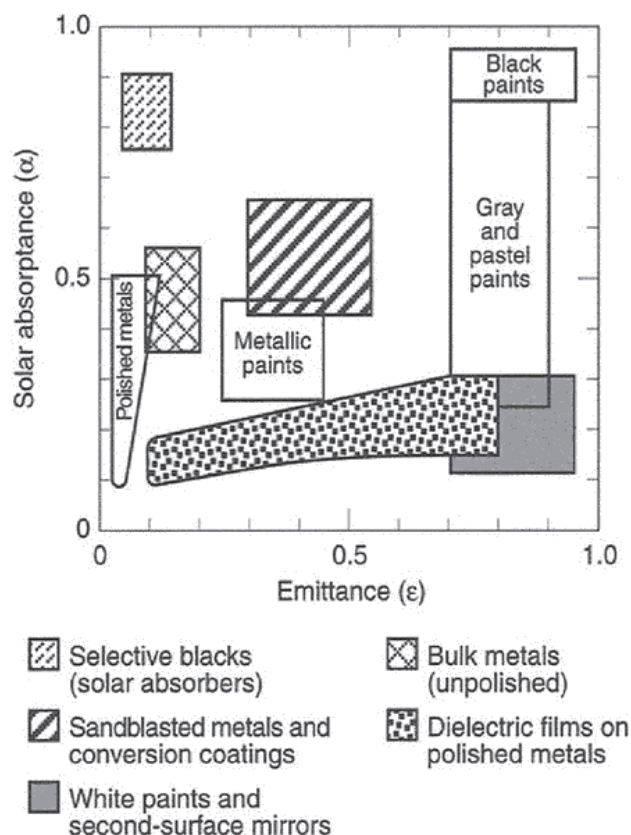


Figure 4.3. Optical Properties of Common Surface Treatments [14]

External surfaces may include the outer layer of insulation blankets, radiator coatings, and paints. The outer cover layer of an MLI blanket can be chosen based on optical properties. Aluminized Kapton has a moderate solar absorptance and a high emittance, while Black Kapton has a high solar absorptance due to being loaded with

carbon to improve electrical conductance for grounding purposes. Beta cloth has a low solar absorptance and high emittance. Radiator coatings are usually white paint or second-surface mirrors, which use a visibly transparent material to achieve a high emissivity and a reflective coating on the back for low solar absorptance. Quartz glass or Teflon can be used for the transparent material, and aluminum or silver coating as the reflective material [14].

Internal surfaces including electronics boxes and the structural panels they are attached to are typically coated with high emittance coatings and paints [14]. Black paints are the conventional choice for this purpose, though most paints have high emittance regardless of color. Paint selection typically depends on solar absorptance, ease of application, and the electrical conductivity requirements for grounding. Internal components, such as propellant tanks and lines, that are temperature sensitive and do not dissipate large amounts of heat are often coated with low emissivity finishes of gold or aluminum, or covered with Kapton tape that has a vapor deposited gold or aluminum coating.

Metallic finishes are also available for use in many situations. Finishes with low emissivity can be used in locations on the satellite where radiative heat transfer must be minimized, including bare or polished aluminum, bare stainless steel, or aluminum tapes. Metallic finishes are not typically used on large external surfaces, however, due to their high ratio of absorptivity to emissivity. Small exterior surfaces or components will sometimes have metallic finishes, but only if they are conductively coupled to the satellite [14].

Surface finishes are available with a variety of optical property combinations for different uses. Finishes with high absorptivity and low emissivity can be used to raise the temperature of a surface exposed to solar radiation. Aluminum paints or silicon oxide coated aluminum, that has moderately low absorptivity and emissivity, can be used for mitigating swings in temperature on exposed surfaces of the satellite structure. Anodize and alodine processes can be used on aluminum surfaces where other coatings are not allowed. Engineers should use manufacturer-provided surface property information for anodized and alodined surfaces, because the optical properties are highly dependent on the specific process used to create these finishes [14]. If the process is tightly controlled,

as those that follow military specifications are, then the process is repeatable and the resulting surface properties will be the same each time. Military specifications for anodic coatings and chemical conversion coatings include [31] and [32]. Appendix B provides a list of space qualified finishes, paints, and coatings and their corresponding optical properties.

4.1.1.2.2 Surface degradation and contamination. Thermal control finishes on the surfaces of a satellite may degrade or become contaminated over time due to the effects of the orbit environment including charged particles, radiation, and high vacuum as well as contamination from satellite debris, erosion from atomic oxygen, and delamination of bonded materials [1], [14]. Contamination can affect all surface treatments, though the level of contamination depends on temperature and proximity to the contaminating source. Surface degradation typically causes an increase in absorptivity, with little effect on emissivity. This degradation becomes particularly noticeable for Kapton and white paints that use organic binders [14].

Optical degradation of satellite surfaces is most often caused by contamination effects. Contaminants typically come from particles and compounds that are outgassed by satellite materials. These particles condense on surfaces at a greater rate when the surface is in the presence of sunlight. The solar radiation will enhance chemical binding of particles to the surface and will cause contaminants to darken over time, increasing the absorptivity of the surface. Contamination can be minimized by selecting low outgassing materials [14]. Atomic oxygen damage is very prevalent in the LEO space environment, which causes erosion of externally applied organic films, advanced composites, and metalized surfaces [14], [25]. Atomic oxygen forms when solar radiation causes a dissociation of molecular oxygen.

Degradation and contamination effects can be reduced by placing radiator with critical coatings in locations on the satellite surface where solar radiation and contamination are not excessive. Adhesive coatings on radiators should be applied in vacuum to avoid trapping air. Air pockets in adhesive tapes can cause cracking and delamination. Visible pockets and wrinkles can be punctured and worked out with a hard roller. Black paint is very susceptible to erosion by atomic oxygen and should be used

only for internal surfaces or radiators that do not face the Sun. White paints are also vulnerable to solar radiation and atomic oxygen degradation [1].

In order to avoid damaging surface coatings and finishes on the ground, handling procedures should be strictly enforced. Protective covers should be used for white paints and quartz mirrors. Flight radiators that are exposed during vacuum testing should be cleaned and their properties confirmed again before being covered. Properties of primary radiators should be monitored during extended periods of assembly and storage on the ground. Coatings and finishes with flight heritage should be chosen over those whose history is based on lab data. Simulated degradation and accelerated testing do not always accurately represent what occurs in space [1].

4.1.1.2.3 Electrical grounding. Satellites in LEO may fly through regions of high space plasmas that can cause electrical charge buildup on the external surfaces of the satellite. If a large charge builds up on the surface, static electricity charges through the surface finish to the satellite structure can occur, which can damage electrical components. Surface finishes should be grounded to avoid this issue. Some surface finishes, such as certain black and white paints and black Kapton, are electrically conductive so the surface charges readily bleed off to the structure. Other materials and finishes act as electrical insulators and require special grounding methods, such as applying a thin indium tin oxide coating over the material and providing a connection from the coating to the satellite structure. This coating can be easily damaged, however, and can be degraded from minimal handling and even cleaning. In some instances, grounding requirements may prevent the use of surface finishes that might have been the best choice for thermal control.

4.1.1.3 Tapes. Adhesive tapes can be used for satellite thermal control to close MLI blanket edges, to aid in MLI blanket grounding, and to block radiation on a surface [14]. Tapes can be purchased from a manufacturer, but can also be made from the blanket material by applying a transfer adhesive to a cut piece of material when tapes are needed for use with MLI. In this situation, the tape material should match the optical properties of the MLI, to ensure that the performance of the MLI blanket is not affected by the tape. Electrically conductive tape will be needed for grounding applications. Aluminum or gold-coated tapes can be used when low emittance is required. Other coatings for tapes

can be tailored for various optical properties, conductivity, non-conductivity, and corrosion resistance [30]. Surfaces should be clean and free of oils before tapes are applied, to ensure good bonding. A hard roller should be used to help with application of the tape to prevent bubbling, which can reduce the effectiveness of the tape [14].

4.1.1.4 Sunshields. Sunshields offer shading for a satellite from direct solar impingement and the radiation environment of space [6]. Traditional sunshields have been made from a thin aluminum, titanium, or stainless-steel substrate, with a low absorptivity and high emissivity coating of silvered Teflon or white paint on the outer surface [1]. Sunshields for small satellites must unfold from a smaller form factor than their traditional counterparts. The implementation of sunshields for small satellites applications is fairly new, though Sierra Lobo has flown deployable sunshields on a few small satellite missions [10].

4.1.1.5 Radiators. Waste satellite heat is rejected to space through the use of radiators. Regardless of the radiator configuration, be it a satellite structural panel or a flat plate radiator mounted to the satellite exterior, radiators reject heat from their surfaces by IR radiation. The optical properties determine the power of the radiator. Radiators must reject waste heat from the satellite while also rejecting heat impinging on the satellite. Most radiators have a high emissivity to maximize heat rejection and low absorptivity to limit heat loads from the space environment. Typical finishes include quartz mirrors, white paint, and silvered or aluminized Teflon [14].

The simplest and most common radiators are the existing panels of the satellite exterior. For example, an exterior aluminum honeycomb panel can serve as a structural panel as well as a radiator. The face sheets of the panel distribute away from electronics boxes that are mounted to it, with the outside panel face acting as the radiating surface. The face sheets can also be made thicker to increase the heat distribution. Separate plates called “doublers,” typically made of aluminum, can also be added under high heat dissipating electronics boxes to help distribute the heat. These measures may result in mass increases that will not fit within the satellite mass budget. Heat pipes can be considered in this situation to distribute spread the heat.

4.1.1.6 Heat pipes. Heat pipes involve liquid phase change in a closed flow cycle to transport heat from one location to another, thus greatly improving heat sharing in a satellite. Heat pipes can be used in conjunction with radiators to transport heat from dissipating components to the radiator and to distribute the heat across the radiator panel [14]. A heat pipe is a sealed pipe or tube with an interior wick that is saturated with a liquid, and a vapor space. As heat is applied to one end, a differential pressure is created that drives the vapor to the cooler end of the pipe where it condenses back into the wick. Because of the liquid loss at the end where heat is being applied, called the evaporator, the meniscus there depresses which results in a capillary pressure head that drives the condensed liquid back from the cooler end, called the condenser, to the heated end causing the cycle to repeat [1]. A schematic of this process is shown in Figure 4.4 [14].

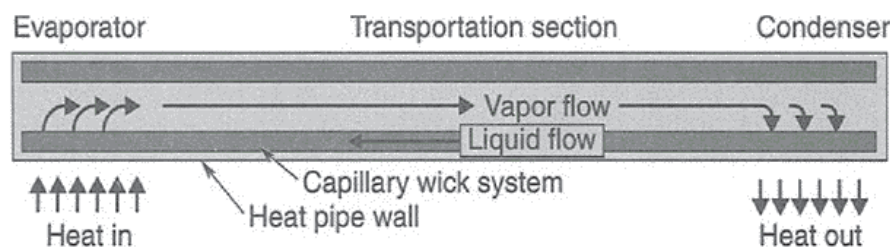


Figure 4.4. Heat Pipe Schematic [14]

The most basic heat pipes have a working fluid, a wick structure, and an envelope, and move heat from one location to another or is used to make a surface isothermal. This is called a “constant conductance heat pipe” [14]. Variations of this concept include the variable conductance heat pipe and the heat pipe diode. Schematics of these variations are shown in Figures 4.5 and 4.6 [1]. In a variable conduction heat pipe, the condenser end of the pipe has a reservoir of incondensable gas. The gas front moves in and out of the active pipe section following a pressure change with heat input. In a liquid trap diode, one end of the pipe has a disconnected wick that blocks the working fluid thus shutting off operation if the condenser and evaporator switch roles because of a change in the distribution of heat [1].

Most heat pipes use a wick design that consist of axial grooves in the wall of the tubing. Heat pipes are typically made from aluminum and use ammonia as the working fluid, because it has excellent heat transport capabilities [1]. Heat pipes must be secured as leak-proof pressure vessels, with advanced welds around the fill valves and end caps, to avoid an ammonia leak.

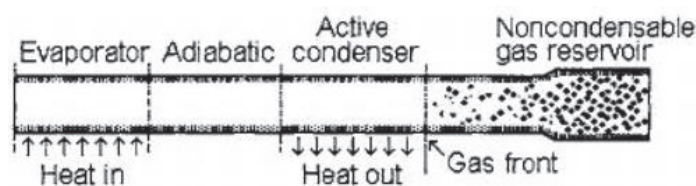


Figure 4.5. Variable Conductance Heat Pipe Schematic [1]

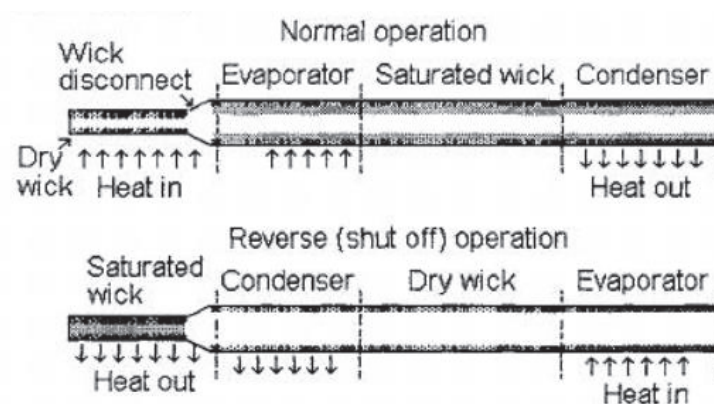


Figure 4.6. Liquid Trap Diode Schematic [1]

Traditional cylindrical heat pipes are not always considered useful for small satellite applications [6]. Flat plate heat pipes, that utilize rectangular stainless-steel tubing with a working fluid sandwiched between aluminum plates, have been successfully developed specifically for small satellites. Though the technology has been demonstrated on a microsatellite, it may require additional fabrication and testing for smaller satellite applications [10].

4.1.1.7 Phase change materials. Phase change materials (PCM) can be useful for providing stable temperatures or in conjunction with radiators to decrease their sizing [14]. They are typically made from hydrocarbon wax, but many substances covering a wide range of temperature requirements are available. PCMs function by absorbing or releasing energy during solid-liquid phase changes [19]. For example, a cyclically operating electronic component could be mounted to a PCM to allow the component to operate isothermally through time. When the component dissipates heat the PCM would store the energy by phase change. Once the component stops dissipating heat, the energy is removed by a radiator, or other means, which allows the PCM to refreeze. This alternative melting and freezing of the PCM is what allows the electronic component to remain isothermal [14]. In this manner, PCMs can be used in conjunction with precisely calibrated instruments for spaceflight experiments to maintain thermal stability.

When used in conjunction with radiators, PCMs can allow the radiator to be smaller than it would usually be. Radiators are typically sized in order to successfully remove heat even during peak thermal loading conditions. By integrating a PCM into the radiator, it can instead be sized for the mean thermal loading condition since it can store the heat from the peak thermal loading in the PCM to be radiated to space at a later time [14].

PCM systems typically result in mass savings when compared to systems utilizing a solid heat sink or conventional radiator and heater. Although, the cost and complexity of developing a PCM system can be high. And in the case of small duty cycles, the mass of the component being cooled may be great enough that it will be able to absorb the heat dissipation directly and survive the small temperature rise, making the PCM system unnecessary. PCM systems may also result in large volumetric changes in melting or freezing [14].

4.1.1.8 Heat switches. Heat switches are devices that can switch between being good thermal insulators and good thermal conductors as needed. They achieve temperature control by creating or removing a conduction path. For example, when sandwiched between a heat dissipating component and a heat sink, the change in thermal conductance of the heat switch can control the temperature of the component [14]. Heat switches are typically passive devices that self-regulate their conductance when operating

in normal spacecraft temperature ranges, not needing signals from a controller in order to react.

Heat switches are typically used to control the temperature of an individual component. The heat switch can be mounted between the component and a sink, or between an electronics box and a sink, such as a satellite structural panel or a radiator. The heat switch will control the temperature to a point chosen during the manufacturing process [14]. When the temperature of the component or box exceeds that temperature, the heat switch conductance will increase, which will allow the excess heat to travel through the switch to the sink and radiate out to space. When the temperature is below that specified point, the heat switch will have a low conductance, which will cause the component or box to be kept warm by its own heat [14].

4.1.2. Active Thermal Control. Active thermal control uses mechanical or thermoelectric devices to maintain acceptable temperatures. These devices use power and may have moving parts, which makes them inherently less reliable than passive thermal control methods [6]. Active systems should only be used when it is not possible to use passive systems alone [22]. Typically, active systems are used for temperature sensitive equipment and for specialized payload components such as infrared sensors.

4.1.2.1 Heaters. Heaters are often the simplest device to use for active thermal control [19]. Their main function is to maintain satellite components in the required temperature range, but they can also be used to warm up components that are dormant before their activation, to control temperature differences to greater stability, and to dissipate excess satellite power [1]. Heaters are the only active thermal control hardware that have been successfully miniaturized for use on small satellites [6].

4.1.2.1.1 Heater types. The most commonly used type of heater is the patch heater. Patch heaters consist of an electrically resistant element bonded between two sheets of flexible electrically insulating material [14]. The electrically resistant element is typically an etched foil, such as Nichrome, and the insulating material is typically a Kapton film [1]. The heater often contains two or more independent circuits for redundancy or for varying heating levels. Redundancy is sometimes provided externally by using two separate patch heaters. Film adhesives are typically used for bonding the heating to the intended surface, though clamps or bolts can be added to secure the corners

and prevent them from lifting. A few examples of custom shaped patch heaters are shown in Figure 4.7 [14]. In most instances, a patch heater will be a simple rectangle of standard dimensions.

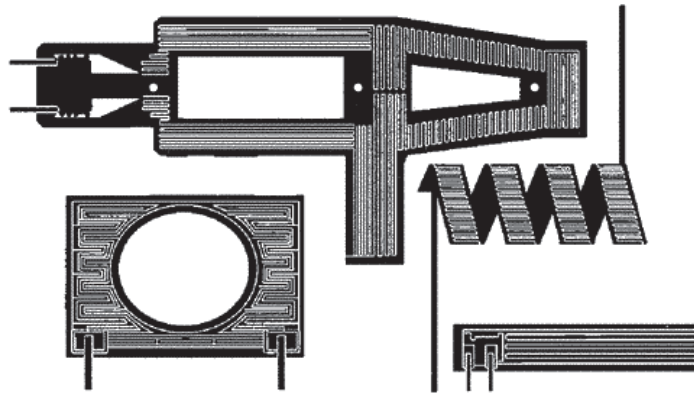


Figure 4.7. Custom Shaped Patch Heaters [14]

Cartridge heaters, or shunt heaters, are sometimes used in high temperature regions of satellites where adhesive bonds may not be reliable. They are typically used to heat blocks of material, for high temperature components, or to dissipate excess solar array power. These heaters are in the shape of a cylindrical cartridge with wound resistors encased in a metal housing [1]. They are usually only a few inches long, and a quarter-inch or less in diameter. Cartridge heaters are attached by drilling a hole into the component to be heated and potting the cartridge in the hole [14]. They can also be attached by using a clamp or bracket.

4.1.2.1.2 Heater control. Heater control capability typically involves enabling or disabling the power being supplied to the heater by commanding a relay from the ground, a fuse to protect the satellite in the event of a short circuit, and a thermostat or controller to turn the heater on and off at specified temperatures [14]. More sophisticated satellites can use onboard computers to monitor temperatures and control the heater using relays. The simplest possible method of heater control only involves the heater, a fuse, and a ground controlled relay to turn the heater on and off. This setup is typically used

when heaters only need to be activated for special events or for heaters than can be left on. Most heater applications on satellites will require at least some automatic heater control to keep the heated component at the necessary temperature and to minimize unnecessary power consumption. Historically, satellites used mechanical thermostats as their control device, but solid-state controllers are becoming more common [14].

4.1.2.1.3 Heater system failure modes. Caution must be exercised when designing a system of heaters and controllers. The failure of a wire in a patch heater can cause damage and failure in adjacent elements. Damage can be reduced by adequately spacing elements within the limits of affecting heating uniformity [1]. When mounting thermostats or other sensing elements, common bonds should be avoided when local damage could affect nearby units. When considering covering a heater with MLI, it should be kept in mind that MLI does not typically have uniform effectiveness. If the insulated surface has a low thermal conductivity, low effectiveness of the MLI in the area where temperatures are being sensed may lead to the heater remaining on. Areas with a higher effectiveness of the MLI may then rise to excessive temperatures [1]. Mechanical thermostats occasionally fail closed, leaving the heater on, or fail open, leaving the heater off. Solid-state controllers eliminate this risk of mechanical failure, and are more reliable and have a higher life expectancy [14].

4.1.2.2 Thermoelectric coolers. Thermoelectric coolers (TECs) provide localized cooling to components or devices, such as star trackers and infrared sensors, that require cooler temperatures in order to operate [14]. The cooling provided by TECs is created by the Peltier effect, which is the cooling that results when an electric current is passed through the junction of two dissimilar metals (typically semiconductors). A simple TEC setup between one “p-type” material and one “n-type” material is shown in Figure. 4.8 [14]. TECs are simple, reliable, compact, lightweight, noiseless, and they do not vibrate while operating. They have no moving parts, and their use is mainly limited by their low efficiency. TECs are best suited for systems with modest heat loads and cold temperatures not falling below 150 K.

TECs are usually mounted by bonding or clamping, though their fragile nature makes them difficult to work with. Any differences in the coefficient of thermal expansion between the TEC and the mounting surface can cause internal stresses and

fatigue, and ultimately failure of the device. The TEC manufacturer should be consulted to determine the best mounting process for any particular device in order to avoid damage or degradation of the TEC [14].

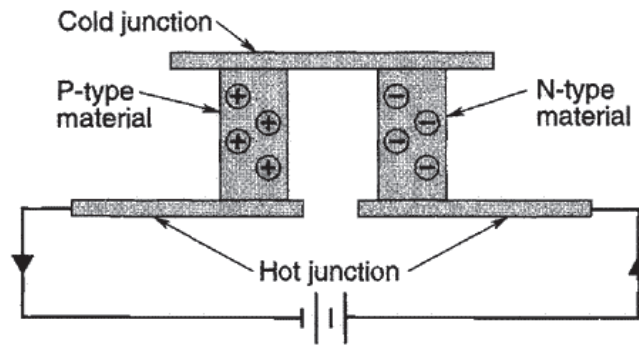


Figure 4.8. Peltier Thermoelectric Couple [14]

4.1.2.3 Louvers. Louvers are mechanical devices that are most commonly placed over external satellite radiators to control the effective emittance of a radiator in response to its temperature [22]. Louvers can also be used to modulate the heat transfer between the internal surfaces of a satellite or from internal surfaces directly to space through openings in the exterior walls of the satellite [14]. A louver is typically an array of metallic blades analogous to venetian blinds, as shown in Figure 4.9 [1]. The array of highly reflective blades is fitted with a frame and includes central shafts that are tightly fit in to the center of bimetallic spring actuators that are calibrated to expand and contract to different angular positions at certain temperatures. The actuators are contained in a housing that is thermally coupled to the radiator, while being isolated from the external environment by a housing cover [1]. The temperature within the housing rises as the radiator heats up, causing the actuators to heat up as well. This causes the actuators to generate thermal torques that rotate the blades to the open position, which allows the radiator surfaces to radiate more heat to space. The actuators move the blades back to the closed position when the temperature of the radiator decreases, blocking the view to space. The automatic opening and closing of the blades keeps the temperature within a

narrow range, and compensates for any changes in environmental heating and dissipation [1]. The system can be a single-actuation system, where all the blades are controlled by a single actuator, or multiple-actuation, where multiple actuators are used and the failure of a single actuator would not affect all of the blades [14].

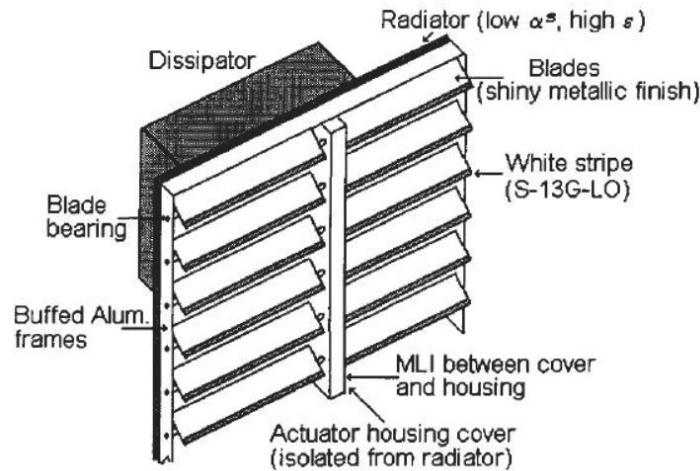


Figure 4.9. Venetian Blind Louvers [1]

Louvers can be built in different sizes, with as few as a single row of blades and with different thicknesses. The frame material is typically made from polished 2024-T4 aluminum, and blades are typically made from 5052-H38 aluminum that is highly buffed to reduce emittance and anodized on the interior side [1]. The actuator is generally coated black to enhance the interchange of radiation [14].

Although using louvers can be advantageous to reduce power consumption, the resulting reduced radiation area from mounting the louver over the radiator should not be underestimated [1]. As a solution, engineers will design combinations of louvered and non-louvered radiators. Louvers have other benefits as well. Because they are calibrated to respond to specific temperatures, louver blades will automatically close to counterbalance available power reductions. Louvers will also offset heat losses caused by underestimated effectiveness of MLI [1].

4.1.3. Emerging Technologies for Small Satellite Use. Many traditional thermal control techniques have been miniaturized for implementation on small satellites. Of these techniques, there are some that currently require additional development and testing in order to be considered “flight proven” [10]. The following technologies are variations of traditional technologies that are under development specifically for small satellite applications.

4.1.3.1 Thermal straps. Thermal straps are a passive thermal control technology that are common on traditional spacecraft [6]. They consist of flexible strips of fibers or metal foil of any length that are used to passively transfer heat. The thermally conductive path on the strap provides a method of mitigating hot spots in a satellite [10]. Straps made from aluminum and copper foils and copper braid have been developed and tested, as well as straps with greater thermal conduction efficiency made from k-Core encapsulated graphite, and some designs have recent flight heritage [33]. Thermal straps are currently considered to be flight qualified [6].

4.1.3.2 Deployable radiators. Passive radiator technologies traditionally rely on large surface areas to radiate waste heat away from the satellite into space. Small satellites do not typically have large enough external surface areas to effectively radiate a sufficient amount of heat away from the satellite [6]. Passively deployable radiators have been designed to expand a small satellite’s surface area for radiating waste heat. An actuator utilizing shape memory alloy and a bias spring is used to move the radiator from the stowed position to the deployed position when the temperature increases. The design has been tested, and is considered to be a prototype demonstrated in a relevant environment, but has not been demonstrated in a space environment [6], [29].

4.1.3.3 Fluid loops. Traditional pumped fluid loops use forced liquid convective cooling to transfer heat between two points [14]. A simple pumped fluid loop consists of a pumping device, heat exchanger, and a radiator. A coolant is used to transport the dissipated thermal energy from a component to a heat sink. An expendable coolant would then be rejected from the satellite. A nonexpendable coolant would be recirculated in the system after the thermal energy has been radiated to space through a radiator [14].

Traditional mechanical pumped fluid loops tend to have a high power consumption and mass, and are therefore not applicable for small satellites [10]. A circular pump is being developed for closed cycle cryocoolers that can circulate gas as part of a single or two-phase thermal management system. The pump will have a very low mass and low power consumption, making in very practical for small satellite applications. The pump is still in the design phase and must undergo rigorous testing before being considered a functional prototype [10], [29].

4.2. MOUNTINGS AND INTERFACES

Developing optimal conductive interfaces between components, baseplates, and the satellite structure is a critical concern when designing a thermal control system. Engineers must consider the effects of uniform pressure between surfaces in vacuum, using bolts versus screws to join surfaces, the effects of fluid in gaps between surfaces, and the use of fillers in interface gaps [14].

4.2.1. Thermal Contact Conductance. Heat transfer from electronic components to radiating surfaces on the exterior of the satellite occurs predominantly by conduction [14]. This thermal energy must travel through the baseplate, or electronic box, to which the component is mounted, through the satellite structure, and finally to the radiating surface to be rejected into space. Conduction from one surface to another, such as from the surface of the electronics box to the surface of the satellite structure, is called “contact conductance.” The conductance at the interface must be determined in order to predict the heat transfer between two surfaces that are pressed together under uniform pressure. This contact conductance C in W/K is characterized by the product of the heat transfer coefficient h in W/m²K and the surface area A , as shown in Equation 19. Imperfections of machined surfaces can affect the conductance between two surfaces [14].

$$C = hA \quad (19)$$

4.2.2. Bolted-Joint Conductance. Two surfaces that are bolted together experience nonuniform pressure across the interface, creating a more complex problem. As demonstrated in Figure 4.10 [14], bolted plates deform elastically at a macroscopic level. Separation of the contacting plates will occur at small distances from the bolts, though this is exaggerated in the figure. This bolted-joint problem can be considered as a contact conductance problem with nonuniform pressure at the interface.

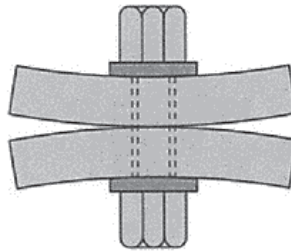


Figure 4.10. Bolted-Joint Interface [14]

The thermal conductance across a bolted interface depends upon screw size, as well as other parameters. Table 4.1 [14] provides conductance values for a variety of screw sizes used for mounting to small stiff surfaces and large thin surfaces. These values can, however, be increased or decreased depending on screw torque, materials, surface finishes, and surface flatness. When using these conductance values in thermal modeling, each contact location between two surfaces should be modeled individually. When two panels are connected at their edges, an edge conductance can be modeled using the conductance value of an individual screw multiplied by the total number of screws across the edge.³

4.2.3. Interface Filler Conductance. Filler materials can be used to improve contact conductance between two plates. These materials fill the microscale voids created by surface imperfections and roughness [14]. A wide variety of filler materials are available, but some materials may have a lower heat transfer coefficient than the bare

³ Dr. Derek Hengeveld in discussion with the author, 2018

unfilled joint. These materials can be used as insulators and may be useful for situations where thermal isolation is desired. Classes of fillers include greases, gaskets, and silicone compounds. The silicone compounds are also known as cured-in-place room temperature vulcanized (RTV) silicone compounds [14].

Table 4.1. Screw Thermal Conductance Design Guideline [14]

Screw Size	Conductance [W/K]	
	Small Stiff Surface	Large Thin Surface
2-56	0.21	0.105
4-40	0.26	0.132
6-32	0.42	0.176
8-32	0.80	0.264
10-32	1.32	0.527
¼-28	3.51	1.054

While fillers can improve contact conductance, they can also create problems that did not exist for a bare interface. Fillers can interfere with grounding, create new structural loads, cause contamination and outgassing, and can eliminate or create difficulty in the ability to remove the attached surfaces from each other for rework [14]. Although, private companies such as Carbice Technologies are working to develop nanotube-based thermal interface materials that will allow for the ability to perform rework with ease [34]. Greases not containing silicone mitigate some contamination issues, but thermal gaskets and cured-in-place RTV silicone compounds are preferred for satellite applications.

Thermal gaskets do present other issues as well. Though they improve contact conductance near the bolts, separation between the gasket and surface can occur at some distance from the bolt. Thermal gaskets also require high pressure in order to compress the gasket between the surfaces. This can lead to structural loads that cause undesired bowing of the mounting panel [14].

Cured-in-place RTV silicone compounds can provide almost continuous contact between two surfaces without the issues presented by the other filler methods. The process for applying these compounds calls for cleaning and drying the surfaces to be attached, using a primer on both surfaces, installing a mesh screen or using washers at screw locations for grounding, application of the compound, application of torque, and finally allowing the compound to cure in place [14]. The compound conforms to the profile of the space between the surfaces resulting from the bolt torque action.

5. THERMAL DESIGN PROCESS

The basic approach to the thermal design process starts with defining the requirements for the thermal control system, followed by iteratively analyzing, designing, and reanalyzing the system, and ends with a physical verification test of the design [18]. Figure 5.1 depicts a flow chart of the analysis and design process for a simplified model, but can largely be followed for a more complex model as well, using thermal modeling software for the computations. This outline of tasks required for the thermal design process can be invaluable in keeping the design and analysis efforts on track as the process unfolds [14].

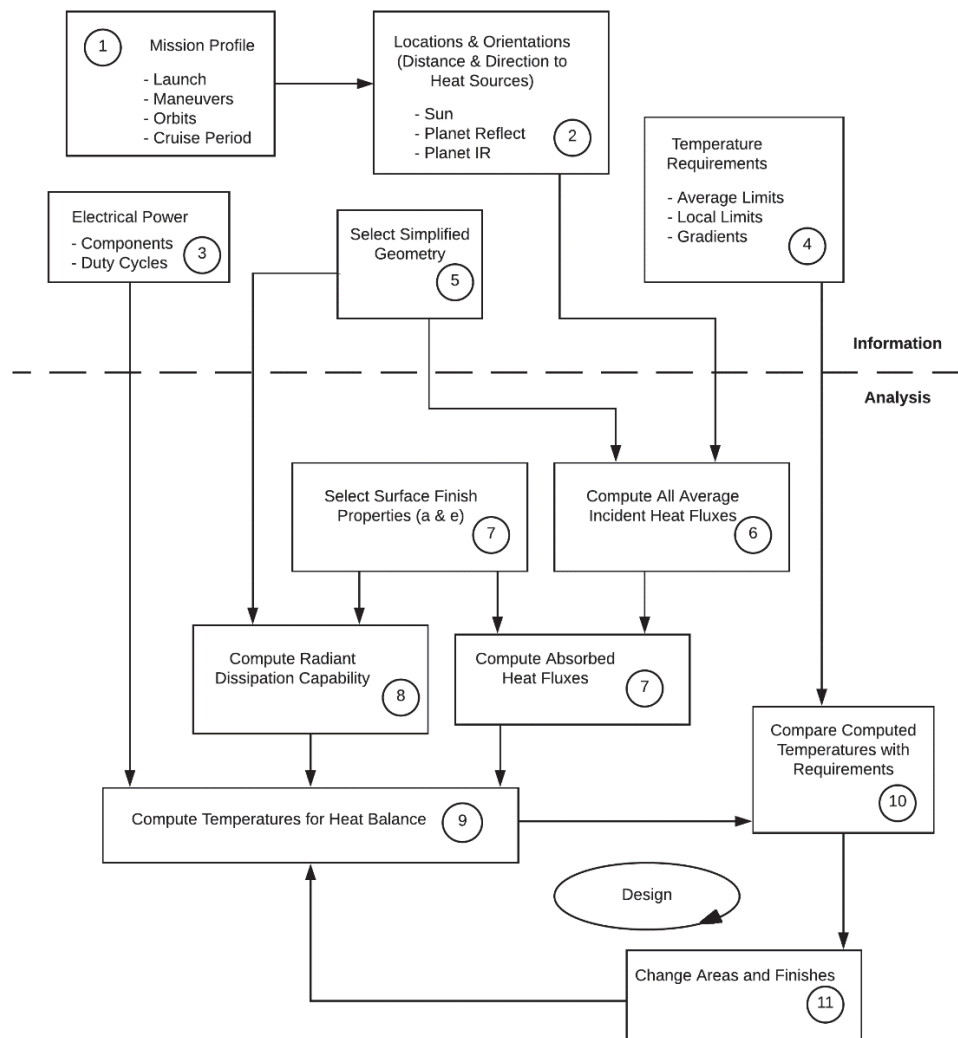


Figure 5.1. Thermal Analysis and Design Process [18]

The first step in the process involves establishing the thermal design requirements and constraints [14]. This involves identifying the temperature requirements of all the satellite components and the satellite heating environment. While most components will operate at or near room temperature, some may have narrow temperature ranges in which they will be able to function properly [18]. When compiling this list of component temperature ranges, it is important to identify a component's operating temperature range as well as its survival temperature range. The operating temperature range defines the temperature that a component must be at in order to effectively perform its required function. The survival temperature range represents the range across which a component is expected to survive. If a component remains within the survival temperature range, it is expected to experience no performance degradation once it returns to its operational temperature range [14]. If the temperature of a component exceeds the survival temperature range in either direction, it will likely no longer operate as expected or fail to operate entirely.

The preliminary baseline thermal environment that the satellite will experience throughout its mission must also be defined. Major changes to this mission profile could result in a drastically different thermal environment for the satellite, and may require major design changes [18]. The satellite orbit, altitude, and beta angle are all important parameters that will be needed to determine the external heat sources. Internal satellite heating from individual component power dissipations will need to be identified or estimated.

During the thermal design process, thermal engineers must use analyses to select the necessary thermal control methods and hardware that will maintain the satellite temperature within the assigned specifications even under the worst potential heating and cooling conditions [1]. The first analysis step will involve determining the maximum and minimum temperatures that the satellite will experience during its mission lifetime. Surface property estimates will need to be determined for the satellite surfaces in order to estimate the absorbed and emitted radiation. A first-order analysis approximation can be constructed, using a simplified geometric shape to represent the satellite, such as a cube, sphere, hexagonal structure, or cylinder [18]. The satellite shape should be propagated through the orbit with its established orientations relative to heating sources, and the

thermal heating environment calculated at each step. Thermal modeling software and or other computer programs are available to help with these computations. The modeling and analysis methods discussed in Section 3 can be followed for this step as well.

The first step of the design process involves adjusting surface finishes and testing the implementation of other passive thermal control methods. Thermal engineers are responsible for selecting the simplest and safest system design that will suffice, therefore, passive designs should be chosen when possible [14]. A passive design that relies on tailored surface finishes, insulation blankets, and other passive methods will be lighter, more reliable, and easier to implement and test than a design involving active thermal control methods, though passive heat pipes should be avoided when possible as well for mass savings.

Multi-node thermal models should be constructed for the next step of the analysis process. These models should include individual node power levels rather than averages, surface properties of individual satellite surfaces, and a network of node connections representing internal radiation and conduction [18]. At this step, the engineer should determine radiation and conduction couplings throughout the satellite that, when combined with external properties and power dissipations, can provide acceptable satellite temperatures. If necessary, the engineer may consider recommending component relocations and active thermal control elements to bring the temperatures into an acceptable range [18].

The design resiliency should be tested by varying the conduction and radiation couplings, surface properties, component power dissipations, and environmental heat loads. Different mission mode parameters should be tested in the model to verify that the thermal control design will be sufficient for every aspect of the mission. After verifying that the modeled thermal design will provide adequate satellite temperature ranges, physical testing must be performed to verify the performance of the design [18]. Test data should be evaluated, and the thermal model and design should be modified accordingly [14].

Throughout the entire process, the thermal engineer should be sure to maintain working relationships with individuals who provide necessary input information or receive results [14]. Typically, these people will be lead engineers responsible for other

satellite subsystems and payloads, including power, propulsion, structures, and attitude control. Coordinating with these team members to establish goals, understand subsystem requirements, and determine the impact of the thermal system design is important. Failure of communication can lead to wasted time working with out of date designs and information. Working with program management will also be important. As the design and analysis process progresses, cost, mass, power consumption, and schedule should be monitored regularly to measure performance, and so that any slips and changes can be incorporated into the plan for the thermal design process [14].

The ultimate goal of the thermal design process is to provide a reliable thermal control system at minimum cost, mass, and power consumption. The process of analysis, design, and testing are tools used to reach this goal, and any time or money spent without real need should be avoided. A thermal control system design should be no more complex than is absolutely necessary. A thermal model should have the minimum number of nodes needed to accurately verify the design, and when difficulties are encountered in analysis, design, or testing, the thermal engineer should consider whether a simpler route is available. An overly complex design can slow down the design and analysis process [14].

6. CASE STUDY: MR SAT AND MRS SAT

The Missouri University of Science and Technology Satellite Research Team has been working toward the completion of the design and construction of its first satellite mission for launch. The team has been working in conjunction with mentors from the Air Force Research Laboratory, NASA, and other members of the satellite industry. The mission consists of two small satellites referred to as the Missouri-Rolla Satellite (MR SAT) and the Missouri-Rolla Second Satellite (MRS SAT). The primary objective of the mission is to demonstrate proximity operations utilizing a stereoscopic imaging system and a cold-gas propulsion system. MR SAT will serve as an inspector satellite and will perform proximity operations about MRS SAT, which will serve as a non-cooperative resident space object (RSO). Image data collected during the inspection portion of the mission will be used to estimate the relative position of MRS SAT with respect to MR SAT and will be used to generate a 3-D reconstruction of MRS SAT.⁴ This thesis study presents the thermal analysis performed for the current MR SAT design; the thermal analysis for the MR SAT and MRS SAT pair will be performed by the team in the near future. Additional analyses will need to be performed for the final satellite pair design as well, once the design parameters are finalized.

6.1. SATELLITE TEAM HISTORY

The Missouri S&T Satellite Research team (formerly the University of Missouri-Rolla) was formed in 2002. The team submitted its first proposal to the University Nanosatellite Program (UNP), sponsored by the Air Force Research Laboratory (AFRL), in 2005. The team participated in four competition rounds, and finished first place in the Nanosat 8 competition, which concluded in January 2015. The team is currently in the second phase of the project, and is working towards completion and testing of the satellite engineering design unit, which will be followed by integration of the flight unit that will be deployed from the International Space Station (ISS) into low Earth orbit [35].

⁴ “MR & MRS SAT Mission Overview.” Unpublished Document, 2017.

Through the years since the team's inception, the thermal subsystem has taken a few different approaches to thermal design. In the past, the NX I-DEAS TMG software was used for thermal modeling and analysis [36]. In 2017, at the suggestion of industry mentor Dr. Derek Hengeveld, the decision was made to utilize Thermal Desktop for thermal modeling and analysis. This software is widely used in the satellite industry, as well as by university research teams. Cullimore and Ring Technologies graciously agreed to sponsor the team with their Thermal Desktop software at no cost.

The satellite has gone through many design changes between the first proposal submission and the current version. Additional changes have been made since the start of the second phase of the competition including changes to the structure, selection of different electronic components, and repositioning of electronics boxes and components inside of the satellite for various reasons. This thesis study presents and discusses the thermal model and analysis for the latest iteration of the MR SAT satellite design.

6.2. MR AND MRS SAT OVERVIEW

6.2.1. Mission Overview. The goal of the mission is to demonstrate close proximity operations and formation flying using an R-134a-based cold gas propulsion system and a stereoscopic imager. The satellite pair will launch in a mated configuration and separate once in orbit after all system checkouts have been completed. The MR SAT satellite will circumnavigate MRS SAT in demonstration of an inspector satellite surveying and characterizing a non-cooperative RSO. Data collected during this mission will be evaluated for the benefit of future satellite missions.⁵

6.2.2. Overview of Subsystems. The satellite pair is composed of a number of subsystems including structures, propulsion, guidance, navigation, and control (GNC), command and data handling, power, communication, payload, and thermal. The subsystems of integration, ground station, ground support equipment, and test support the mission as well.

The satellite mounted pair structure is shown in Figure 6.1. MR SAT is a hexagonal prism, and is the larger of the two, with an envelope of about 65 cm x 55 cm x

⁵ "MR & MRS SAT Executive Summary." Unpublished Document, 2017.

47 cm and a mass of 42.4 kg. MRS SAT is a smaller rectangular prism with an envelope of about 19 cm x 22 cm x 14 cm and a mass of 4.1 kg. The two are mounted to each other using three TiNi E500 Ejector Release Mechanisms. The load bearing body of each satellite is made from 6061-T6 aluminum. The base plate of MR SAT is made from 7075-T73511 aluminum, in accordance to the ISS Cyclops deployment requirement.

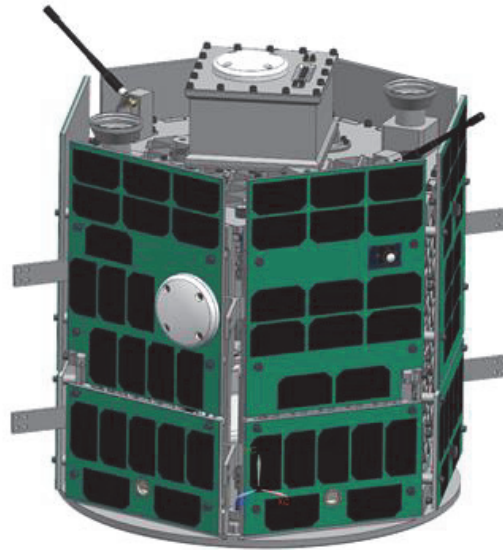


Figure 6.1. Satellite Pair in Mated Configuration

MR SAT is equipped with solar cells on each of the eight side panels to provide power for its internal components during the mission, notably the propulsion system and the communication radios. The internal configuration of MR SAT consists of electronics boxes for housing printed circuit boards (PCBs), the propulsion system, battery boxes, and torque coils. MR SAT also carries communication antennas, cameras and camera baffles for the stereoscopic imager, a magnetometer, Sun sensors, and thrusters. MRS SAT is equipped with a minimal number of components, consisting of a battery, PCB, a Pumpkin/Near Space Launch EyeStar radio and antenna, and a GPS receiver and antenna.⁶

⁶ “MR & MRS SAT Structures Conceptual Design Document.” Unpublished Document, 2017.

The MR SAT propulsion system consists of a cold gas thruster system with R-134a refrigerant, which is used as a two-phase propellant. The system utilizes a propulsion tank, propellant lines, a pressure transducer, isolation valves, a pressure regulator, a distributor, and 12 thruster solenoids. The system is designed to provide three-axis translational orbital control and three-axis attitude control, for a full six degrees-of-freedom of control, for the satellite, allowing MR SAT to circumnavigate MRS SAT during the mission.⁷

The GNC subsystem is responsible for commanding the thrusters and torque coils after processing sensor data provided by the inertial measurement unit (IMU), magnetometer, GPS receiver, and the stereoscopic imager.⁸ The subsystem uses a navigation filter and translational guidance and attitude control algorithms to determine the necessary acceleration and/or torque that must be applied on the satellite during a given mission mode by the thrusters or torque coils.

The command and data handling subsystem is responsible for data operations and issuing commands to the other subsystems. On MRS SAT, this is done through the use of a central computer communicating over two universal asynchronous receiver-transmitter (UART) data buses. On MR SAT, the flight computer uses an inter-integrated circuit (I²C) bus for most communication, and a UART bus when large amounts of data must be passed between systems.⁹ A serial peripheral interface (SPI) bus is used for communication with the IMU, an ethernet cable is used for communication between the flight computer and the imager, and the thermal sensors are connected to the flight computer using a 1-Wire bus. The MR SAT flight computer consists of two Raspberry Pi CM3 Lites, and an ATMEGA644 microcontroller is used as the flight computer for MRS SAT.

The power subsystem is accountable for generating, storing, and distributing power throughout the satellite in a way that will sustain mission operations. For MR

⁷ “MR & MRS SAT Propulsion Conceptual Design Document.” Unpublished Document, 2017.

⁸ “MR & MRS SAT GNC Conceptual Design Document.” Unpublished Document, 2016.

⁹ “MR & MRS SAT Command and Data Handling Conceptual Design Document.” Unpublished Document, 2017.

SAT, Spectrolab ITJ solar cells will be used for power generation and lithium-ion batteries will be used for power storage. The power subsystem also includes power regulators and a distribution unit, housed in a component box. MRS SAT's power system only includes lithium-ion batteries.¹⁰

The communication subsystem relays information and commands between the ground station and the satellite pair in orbit. During the course of the mission, commands and collected data will be transmitted via a primary communication link between the ground station and MR SAT. The radio used for uplink and downlink from MR SAT is a GomSpace AX100. A separate simplex beacon will be used to downlink position information from MRS SAT to the ground station using the Eyestar radio through the Globalstar satellite communications network.¹¹

The mission payload onboard MR SAT is the stereoscopic imager, consisting of two cameras, that is used for measuring the relative position of MRS SAT. The imager is also used to capture images of MRS SAT from multiple angles to generate a three-dimensional model, which will be created post-mission after downlink. This demonstrates the ability of a stereoscopic imager to be used for assessment and identification of an RSO's purpose and capabilities.

6.3. THERMAL SUBSYSTEM OVERVIEW

The thermal subsystem is tasked with measuring the temperatures of the satellite components throughout the mission using temperature sensors, and ensuring that the temperatures of the satellite components do not exceed their specified ranges. In order to successfully accomplish these tasks, a thermal model of the satellite must be constructed and thermal control methods applied to maintain the satellite temperature. Thermal Desktop was used for constructing the thermal model of the current MR SAT design, which is presented in this thesis study.

¹⁰ "MR & MRS SAT Power Conceptual Design Document." Unpublished Document, 2017.

¹¹ "MR & MRS SAT Communication Conceptual Design Document." Unpublished Document, 2017.

6.3.1. Satellite Temperature Specifications. The specified temperature ranges of the components on MR SAT constrain the acceptable temperature of the satellite on orbit. The operational temperature range for each critical component is listed in Table 6.1. Survival temperatures for many components were not available. The maximum survival temperature for the TiNi separation devices varies depending on whether the devices have been actuated or not. In the analysis presented in this thesis study, the devices were assumed to have already been actuated. The most constraining minimum operational temperature comes from the solar cells, which must remain over 10°C. The most constraining maximum operational temperature comes from the batteries and the cameras, which must both remain below 45°C. It should be noted that all operating and survival temperatures presented in this thesis study came from manufacturer specification sheets, and were not verified by the research team for accuracy through testing.

Table 6.1. MR SAT Critical Component Operational Temperatures

Component	Min Operating [°C]	Max Operating [°C]	Min Survival [°C]	Max Survival [°C]
TiNi Separation Device	-65	70	-150	Pre actuation: 70 Post actuation: +150
MCU Digital	-40	85	-65	150
Isolation Valves	-18	49	-	-
Thruster Valves	-18	49	-	-
Propellant Tank	-40	65	-	-
Pressure Transducer	-29	82	-	-
Comm Radio	-30	70	-30	85
GPS Receiver	-40	85	-55	95
GPS Antenna	-55	85	-55	85
Flight Computer R-Pi	-25	80	-	-
IMU	-40	85	-	-
Sun Sensor Cameras	-10	70	-40	95
Sun Sensor Boards	-10	70	-40	95
MCU Analog	-40	85	-65	150
Magnetometer	-55	85	-	-
Magnetic Torque Coil (Top Panel)	-50	60	-	-
Magnetic Torque Coil (Panel 5)	-50	60	-	-
Magnetic Torque Coil (Panel 6)	-50	60	-	-
Camera	0	45	-30	60
Payload R-Pi	-25	80	-	-
EPS Board	-40	105	-	-
Solar Cells	10	80	-180	150
Lithium-Ion Batteries	0	45	-20	60

6.3.2. Thermal Environment and Heating Fluxes. The thermal environment that the satellite will experience depends on the orbit parameters. It is expected that the MR and MRS SAT pair will be deployed from the International Space Station. Because the orbit beta angle of the ISS varies, different orbit heating environments were considered. It is, however, known that the orbit is nearly circular and at an altitude of approximately 400 km.

The thermal analysis presented in this thesis study considers the mission phases where the heating of MR SAT will be most critical. The phase with the longest duration will take place during the time when MR SAT's Panel 2, which includes the GPS antenna, is facing away from the Earth. During this time, MR SAT's Panel 8, the top panel, will be facing in the same direction as the positive velocity vector.¹² The numbered panels of MR SAT are shown in Figure 6.2.

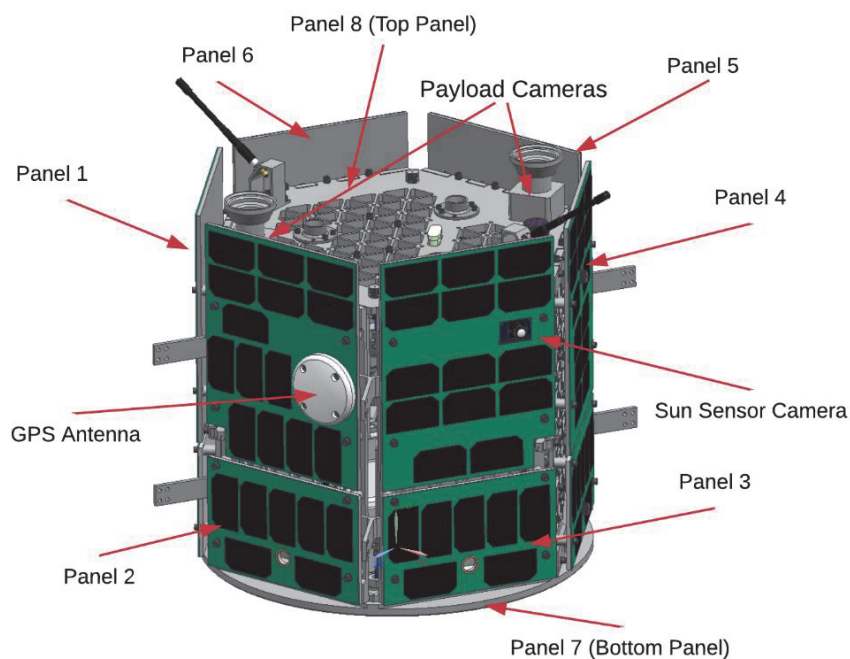


Figure 6.2. MR SAT Panel Numbering

¹² "MR and MRS SAT Concept of Operations." Unpublished Document, 2018.

It is important to consider the most extreme environments that a satellite may encounter during its mission lifetime. For this reason, the orbital parameters and mission mode internal heat generation that result in the highest and lowest temperatures were analyzed for MR SAT. The parameters considered for these extrema cases include orbit beta angle, solar flux, albedo factor, and internal heat loads.

6.3.2.1 Hot case. Because it is expected that the satellite pair will be deployed from the ISS, the heating conditions from the resulting orbit must be considered. The orbit beta angle of the ISS can reach as high as 60 degrees, and occasionally exceeds 60 degrees. Because it is not known what the beta angle of the ISS will be when the satellite pair is deployed, a beta angle of 60 degrees was used for the hot case since the beta angle of the ISS does not often exceed 60 degrees. Figure 6.3 depicts the beta angle of the ISS versus day for an inclination of 51.6° , 0° RAAN, and an altitude of 400 km.¹³

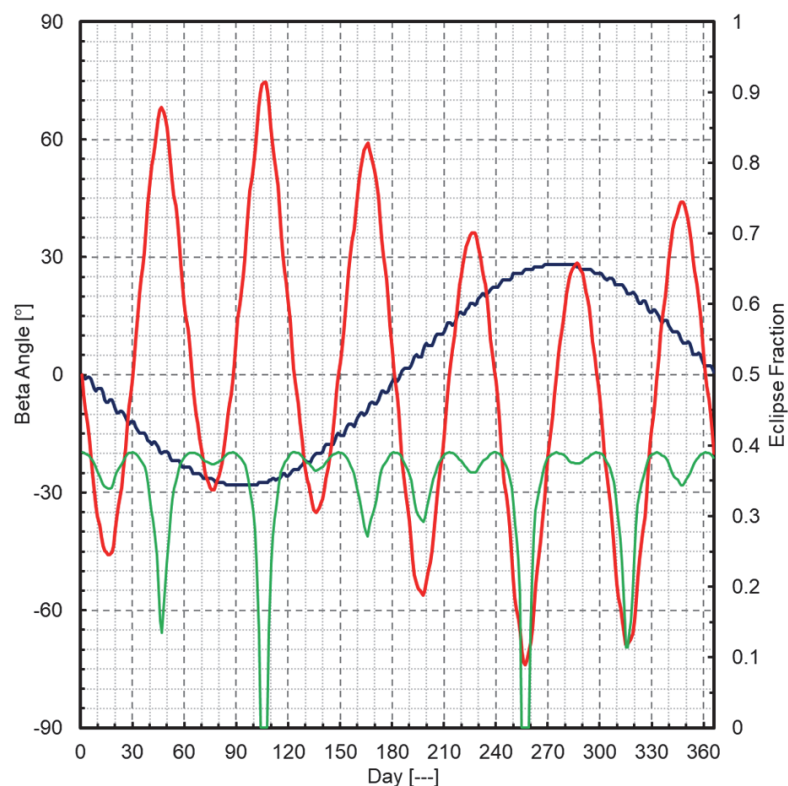


Figure 6.3. ISS Beta Angle Versus Day

¹³ Dr. Derek Hengeveld in correspondence with the author, 2018

At the time of year where the Earth is closest to the Sun the solar flux may be as high as 1419 W/m^2 , so this value was chosen for the hot case. The highest realistic albedo factor was also chosen for this case, at 0.55 [25]. The internal satellite heating loads for the hot case were taken from the mission mode that uses the greatest amount of power, which is the second mission mode. For cases that use a lumped heat load, the total sum of the internal heat loads was used, which was 22.4385 watts for the hot case.

6.3.2.2 Cold case. A satellite will experience the greatest amount of time in eclipse at an orbit beta angle of zero degrees, which will lead to the coolest thermal environment. The albedo heat load and solar heating will typically not contribute to the satellite heating during eclipse. At the time of year where the Earth is farthest from the Sun the solar flux may be as low as 1317 W/m^2 , so this value was chosen for the cold case. An albedo factor of 0.18 [25], the lowest realistic factor, was chosen for this case. The internal heating loads for the cold case were taken from the mission mode that uses the least amount of power, which is the safe mode. For cases that use a lumped heat load, the total sum of the internal heat loads was used, which was 6.594 watts for the cold case. A summary of the thermal environment extrema cases is shown in Table 6.2, and the total internal heating loads for the satellite electrical components for each case are shown in Table 6.3. Earth emitted radiation is calculated and implemented by the Thermal Desktop software.

6.4. THERMAL ANALYSIS USING THERMAL DESKTOP

Thermal modeling of the current MR SAT design was accomplished using Thermal Desktop 6.0, with SINDA/FLUINT 5.8. The process was guided by trusted industry professional Dr. Derek Hengeveld, who has experience working with Thermal Desktop to perform thermal analyses for spacecraft. The modeling process began with the construction of a simple single node model of the satellite to determine the approximate temperatures that the satellite will experience during the different heating cases. Subsequent models were constructed, incrementally incorporating more complex surfaces and increasing nodal resolution. The most complex model presented includes individually modeled surfaces and components representative of those in the satellite design. Table

6.4 presents the details of each model revision. Geometries and material properties for all panels, boxes, and components are presented in Appendix C.

Table 6.2. Orbit Parameters for Extrema Environment Cases

Parameter	Hot Case	Cold Case
Altitude [km]	400	400
Beta Angle	60°	0°
Solar Flux [W/m ²]	1419	1317
Albedo Factor	0.55	0.18

Table 6.3. MR SAT Electrical Components Total Heat Loads for Extrema Cases

Component	Mission Mode 1 [W]	Safe Mode [W]
TiNi Separation Device	0	0
MCU Digital	0.25	0
Isolation Valves	1.91	0
Thruster Valves	7.62	0
Pressure Transducer	0.12	0
Comm Radio	0.05	0.4
GPS Receiver	0.33	0.33
GPS Antenna	0.6	0.6
Flight Computer R-Pi	2.9	2.9
IMU	0.1	0.1
Sun Sensor Cameras	0.21	0.21
Sun Sensor Boards	0.21	0.21
MCU Analog	0.23	0.23
Magnetometer	0.3	0.3
Magnetic Torque Coil (Top Panel)	0	0
Magnetic Torque Coil (Panel 5)	0	0
Magnetic Torque Coil (Panel 6)	0	0
Camera	2.64	0
Payload R-Pi	2.9	0
EPS Board	1	1
Lithium-Ion Batteries	1.0685	0.314

Table 6.4 Model Revision Information

		Model Revision			
		A	B	C	D & E
Nodal Resolution	Single Node	x			
	Eight Node		x		
	Multi-Node			x	x
Parts	Lumped Panels and Solar Cells	x	x		
	Isogrid Aluminum Panels			x	x
	Solar Panel PCB			x	x
	Solar Cells			x	x
	Honeycomb Aluminum Panel			x	x
	Component Boxes				x
	Electrical Components				x
Heating Loads	Lumped Heating Loads	x	x		
	Individual Component Heating Loads			x	x
Contact Conduction	Between Top and Side Panels		x	x	x
	Between Bottom and Side Panels		x	x	x
	Between Side Panels at Bracket Points			x	x
	Between Solar Panel and Honeycomb			x	x
	Between Honeycomb and Side Panel			x	x
	Between Boxes and Side Panels				x
	Between Components and Side Panels				x
	Between Components and Boxes				x

Each model constructed was heavily parameterized, using symbols to represent each input value. This allowed for easy manipulation of the model when changes to input values needed to be made. Using symbols also enables an Excel sheet to be used to change input values when running an analysis, which makes the process of performing parametric studies much easier [37]. Symbols are created in Thermal Desktop using the Symbol Manager. It is important to note that when entering symbols, the engineer must select “done” rather than using “x” to close the window in order to save the symbols. Using “x” to close the window will result in a loss of the symbols entered. This is necessary when entering optical and thermophysical properties into the respective databases as well.

The steady state and transient temperatures calculated for each iteration are compared with the results from the previous iterations and with the component temperature specifications. Locations of higher and colder temperatures are discussed, and passive thermal control through the use of surface finishes for the final model revision are presented.

6.4.1. Extrema Case Construction. Each MR SAT thermal model revision was analyzed for hot and cold extrema cases, with the same parameters used for each revision analysis. For the hot and cold cases, the respective parameters specified in Section 6.3.2 were applied in the Heating Rate Case Manager. The hot case orbit is shown in Figure 6.4, and the cold case orbit is shown in Figure 6.5. A simplified geometric shape model is shown at 12 different points on the orbit. Each panel is a different color, for easier visualization. Panel 1 is yellow, Panel 2 is green, Panel 6 is orange, the top panel is red, and the bottom panel is blue.

6.4.2. Single Node Analysis – Model Revision A. In order to get an idea of the approximate temperatures the satellite as a whole will experience on orbit, a single node model was created for MR SAT. The model represents the properties of the exterior satellite surfaces, as well as the satellite internal heat generation, all “lumped” into a single node. As was shown in Table 6.4, this thermal model revision lumps together the properties of the each of the side panels, including the isogrid aluminum panels, solar panel PCB, solar cells, and honeycomb aluminum panels. Steady state and transient analyses were run for the model for the thermal environment extrema cases.

6.4.2.1 Model construction. In order to create a single node thermal model in Thermal Desktop, each of the sides of the satellite was created, and their nodes merged together onto a single node to represent the entire satellite. Side panels were constructed using Thermal Desktop Rectangles, each with a single node. The effective optical properties for each panel were calculated to reflect the outward facing surfaces of the panel. As can be seen in Figure 6.6, the space-facing side of one of the rectangular satellite side panels primarily consists of the solar panel PCB and the solar cells. The effective optical properties used for the space-facing side of the lumped panel were calculated from the optical properties of the solar panel PCB and the solar cells. The interior facing side of the panel primarily consists of the aluminum isogrid panel, so the optical properties for the isogrid aluminum panel are used for this face of the lumped panel in the thermal model. While the honeycomb aluminum panel adhered to the back of the solar panel PCB is not included in the calculated optical properties for the lumped panel, it is included in the calculated mass, effective thermal conductivity, and effective specific heat of the lumped panel.

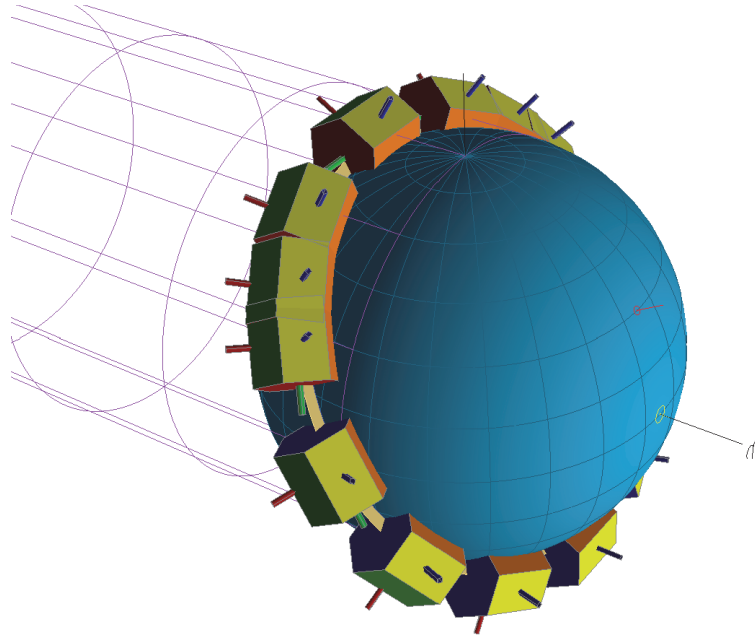


Figure 6.4. MR SAT Hot Case Orbit – Beta Angle of 60°

A heat load was applied to the node on the bottom panel to represent the internal satellite heating, most of which is generated by batteries and components mounted on the bottom panel. The lumped heat load of 22.4385 watts was applied for the hot case, and 6.594 watts for the cold case. The wireframe thermal model, before the nodes were merged, is shown in Figure 6.7. The model after merging the nodes onto a single node is shown in Figure 6.8. Input parameters for the model geometry and lumped material properties are shown in Appendix D.

6.4.2.2 Analysis results. Steady state and transient analyses were performed for the thermal model, applying the parameters for both the hot and cold case. The steady state analysis resulted in a temperature of 10.15°C for the hot case, and -17.45°C for the cold case. The results of the transient analyses are shown for the hot and cold cases over a period of four orbits in Figures 6.9 and 6.10, respectively. The two red lines in the figures depict the most constraining operational temperature range for the satellite electrical components; with an upper limit of 45°C and a lower limit of 10°C . A thermal uncertainty margin was not included for the analyses. For traditional satellites a thermal uncertainty margin of 11°C is recommended [1]. Including this margin would drastically

narrow the allowable temperature margin for the satellite, which is why it was not included for this analysis, but may be considered in the future.

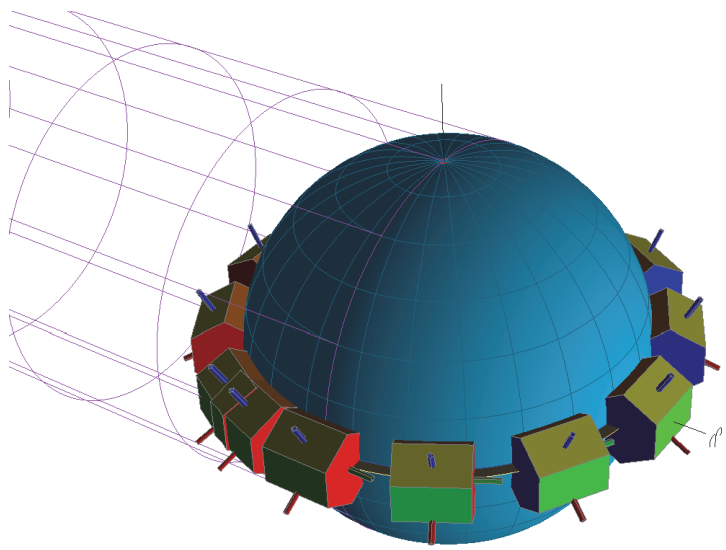


Figure 6.5. MR SAT Cold Case Orbit – Beta Angle of 0°

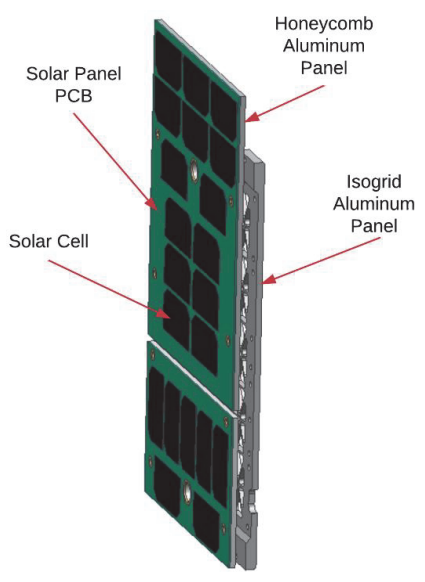


Figure 6.6. MR SAT Side Lumped Model Panel Components

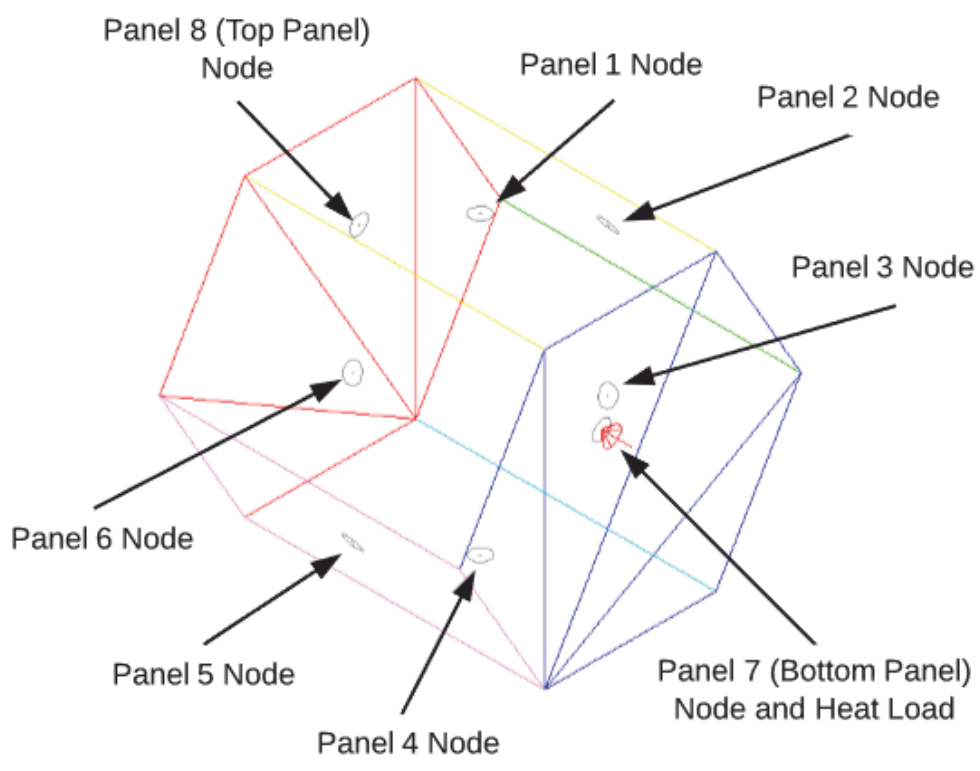


Figure 6.7. Wireframe Single Node Thermal Model Before Merging Nodes

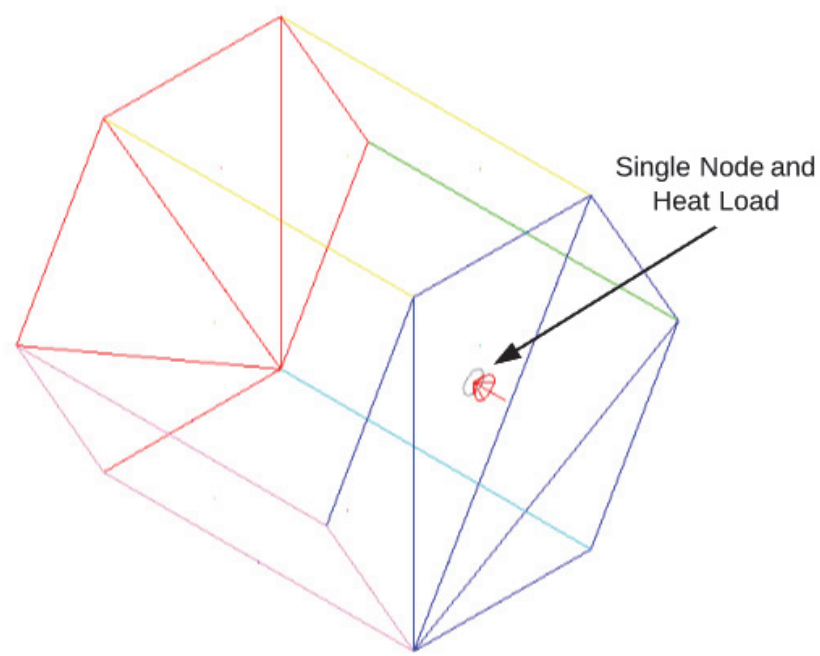


Figure 6.8. Wireframe Single Node Thermal Model with Merged Nodes

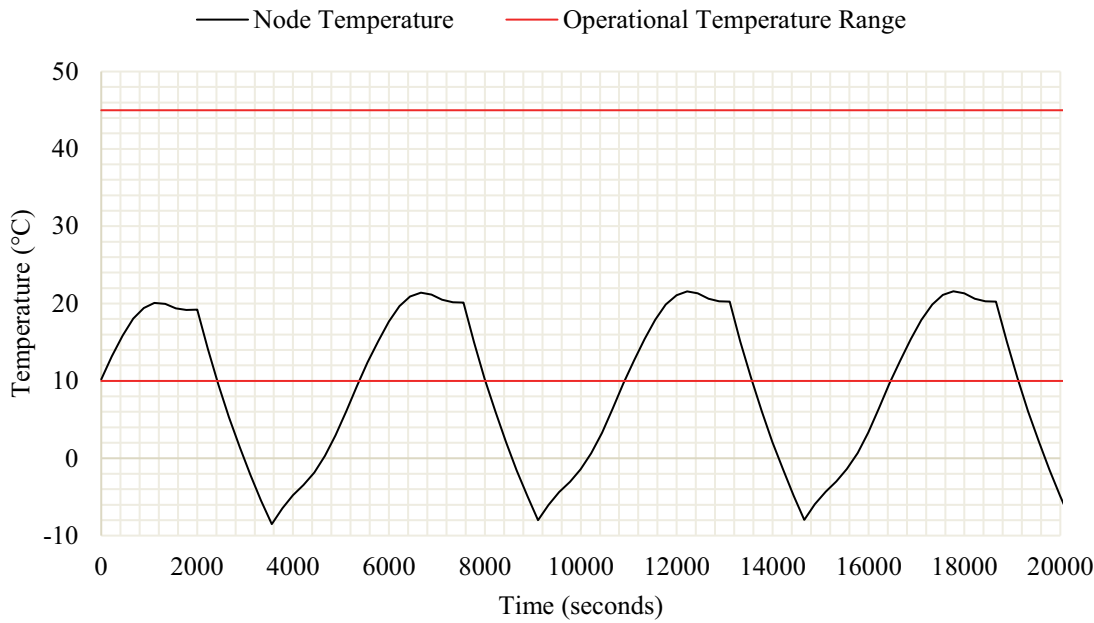


Figure 6.9. Model Revision A – Hot Case Transient Analysis

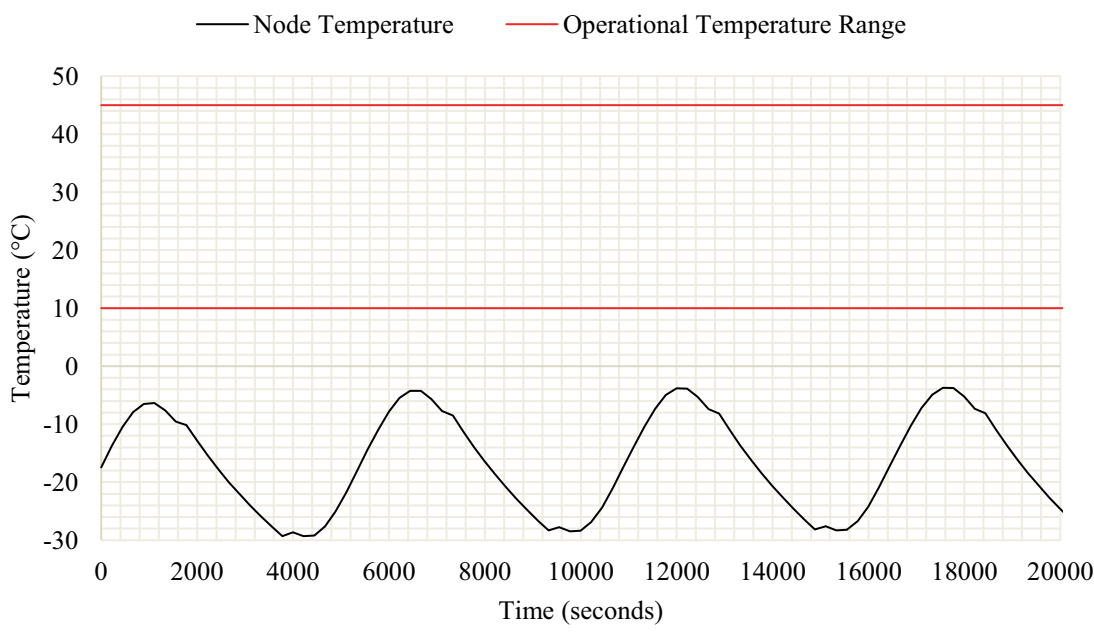


Figure 6.10. Model Revision A – Cold Case Transient Analysis

6.4.2.3 Discussion. As can be seen in Figures 6.9 and 6.10, the single node thermal model of the satellite results in temperatures lower than needed for the satellite components to function properly on orbit. Because the thermal model is of very low fidelity, it is not overly concerning that the temperatures are so low. This single node model lumps the properties of the external panels together, excluding interior boxes and electrical components. Conduction between panels is also not considered.

6.4.3. Eight Node Analysis – Model Revision B. The next model revision for MR SAT consists of eight panels representing the exterior surfaces of the satellite, each with a single node where the panel properties are lumped (the same as the eight panels used to construct the single node model). The same lumped heat load from model revision A is applied to the bottom panel, representing where the majority of the heating is expected to occur. Conduction is included in this model between the side panels and the bottom panel as well as between the side panels and the top panel.

6.4.3.1 Model construction. Model revision B was constructed using the panels created for the first thermal model. Each panel has a single node where the properties for each of the components of the panel is lumped. The calculated properties were the same as those used for thermal model revision A, shown in Appendix D. Conduction was applied between the side panels and the top panel and between the side panels and the bottom panel using Thermal Desktop edge contactors, as shown in Figure 6.11. Location “1” is where conductance values calculated for use between the side isogrid panels and the bottom panel are applied, and location “2” is where conductance values calculated for use between the side isogrid panels and the top panel are applied. Conductance between the panels was calculated in W/K, and is shown in Appendix C.

6.4.3.2 Analysis results. The temperatures resulting from the steady state analyses are presented in Table 6.5. The transient analysis temperature results for the hot and cold cases are presented in Figure 6.12 and 6.13, respectively. The color of each panel in previous sections corresponds with the colors representing each panel in the figures.

6.4.3.3 Discussion. The resulting range of temperatures from the analysis of thermal model revision B does not fall entirely within the acceptable temperature range set by the most temperature sensitive electronic components within MR SAT. The results

are in a similar range compared to those from model revision A. For the cold case, the temperatures are entirely outside the acceptable range. At this stage, it becomes clear that thermal control methods will likely be necessary to manipulate the properties of the satellite to result in higher temperatures. However, this model revision involved applying a lumped heat load to the bottom of the satellite. Applying the heat loads at the actual locations of the electrical components will distribute the heating throughout the satellite. The next thermal model revision provides a more accurate prediction of the panel heating throughout the orbit.

6.4.4. Multi-Node Analysis. The next step in the thermal model construction involved increasing complexity of the model with explicit rather than lumped modeling, increasing nodal resolution, and by applying heat loads for individual components. Figure 6.14 shows the internal layout of the satellite components. The four battery boxes, each containing eight batteries, are mounted to the bottom panel. The component box stack mounted on top of the battery boxes consists of two boxes with the bottom box housing the EPS board and the top box housing the communication radio, GPS receiver, IMU, Sun sensor boards, both the digital and analog MCU boards, and both the flight computer and payload Raspberry Pi boards. The propellant tank is mounted on top of the box stack, with a propulsion bridge holding the pressure transducers and isolation valves on top of the tank. The GPS antenna is mounted on the outward face of the Panel 2 solar panel, and the Sun sensor cameras are mounted on the outward face of the solar panels on Panels 3 and 6.

6.4.4.1 Explicit panel modeling – model revision C. The third thermal model revision that was constructed involved increasing complexity by more explicitly modeling the side panels of the satellite shown in Figure 6.2. The panels from model revision B became the isogrid panels in model revision C by applying the material properties for the isogrid panels from the table in Appendix C, and explicitly modeling the solar panel PCB and honeycomb aluminum.

6.4.4.1.1 Model construction. The solar panels, consisting of solar panel PCB and solar cells, were modeled using Thermal Desktop rectangles, and applying the lumped material properties for the solar cells and PCB, shown in Appendix E. The optical properties for the back of the panel are those for the PCB by itself because the solar cells

are only located on the front of the panel, the property values of which are listed in Appendix C. The solar panels on the satellite consist of an upper portion and a lower portion, with the lower portion being the same for each side panel. The upper solar panel portions were modeled with centered nodes equidistant from each other, with eight nodes along the x-direction of the panel and eight nodes along the y-direction of the panel for a total of 64 nodes on the panel. The lower solar panel portions were also modeled with centered nodes equidistant from each other, with eight nodes along the x-direction and four nodes along the y-direction, for a total of 32 nodes on the panel. The entire thermal model contained a total of 2294 nodes.

The honeycomb aluminum panels were modeled as an upper and lower portion as well, using Thermal Desktop rectangles. In order to more accurately model honeycomb aluminum, the panel numbering was set to use different numbering IDs on either side of the panel, which was selected on the Numbering tab of the Thin Shell Data window for editing the Thermal Desktop rectangle. The material properties for the honeycomb aluminum skin sheets and core are then applied separately in the Cond/Cap tab, with the skin properties and thickness entered for the Top/Out and Bottom/In materials. The core properties are entered for the Separation material. Optical properties applied in the Radiation tab are selected for the panel skins.

The conduction applied between the side isogrid panels and top isogrid panel as well as conduction between the side isogrid panels and the bottom isogrid panel were applied during construction of the previous thermal model revision. Conduction between isogrid side panels is applied for this model revision using node-to-node conduction contactors. This represents the connection between the panels by the brackets shown in Figure 6.15, where one of the solar panels is removed to showcase the bracket mounting locations.

Conduction was also applied between the solar panel PCBs and the honeycomb aluminum panels, as well as between the honeycomb aluminum panels and the isogrid aluminum side panels. A face-to-face contactor was used between the PCB and the honeycomb to represent the epoxy used to adhere the two together. Node-to-node contactors were used between the honeycomb and isogrid panels to represent the bolts connecting the two. Standoffs are used between the solar panel assembly and the isogrid

panels, as can be seen in Figure 6.15, preventing the panels from contacting each other at any other points than the bolt locations, which is why node-to-node contactors were used. Conductivity values calculated for the contactors are shown in Appendix C.

Figure 6.16, shown with a solar panel removed for visibility, depicts the location of node-to-node contacts for a side panel and face-to-face contactors for a side panel. These contactors are applied for each of the side panels on the satellite. The figure also illustrates a few locations of heat loads applied on nodes, representing where the electrical components are mounted. For this case, heat loads are applied at nodes throughout the satellite rather than as a single lumped node on the bottom of the satellite. The heat loads are applied at the node locations of the electrical components depicted in Figure 6.14, though the heat loads for the electrical components on the bottom panel are all applied at the center node of the bottom panel because the component box stack is centered on the bottom panel. Values used for the heat loads are presented in Appendix F.

6.4.4.1.2 Analysis results. The results of the steady state analyses are shown for the hot and cold cases in Tables 6.6 and 6.7, respectively. Only the most extreme temperature from each panel component is shown in the table. The hottest temperature on each of the solar panel PCBs, honeycomb aluminum panels, and isogrid aluminum panels is presented, and the coldest temperature on each of the panel components is presented. The results of the transient analysis for the hot case are shown for each of the three panel components in Figures 6.17 through 6.19, and for the cold case in Figures 6.20 through 6.22.

6.4.4.1.3 Discussion. The resulting temperatures of most of the panel components fall below the required temperature range, though the solar panel PCB and honeycomb aluminum on Panels 1 and 6 exceed the temperature range during the hot case for a portion of the orbit. Panels 1 and 6 receive the highest solar flux due to their position relative to the Sun. The resulting temperatures of the solar panel PCB and honeycomb aluminum are nearly identical due to the thermal coupling of the panel faces by adhesive. The isogrid panels are separated from the solar panel assembly by standoffs, and are not in direct sight of the solar radiation, causing the temperature of the isogrid panels to be somewhat cooler.

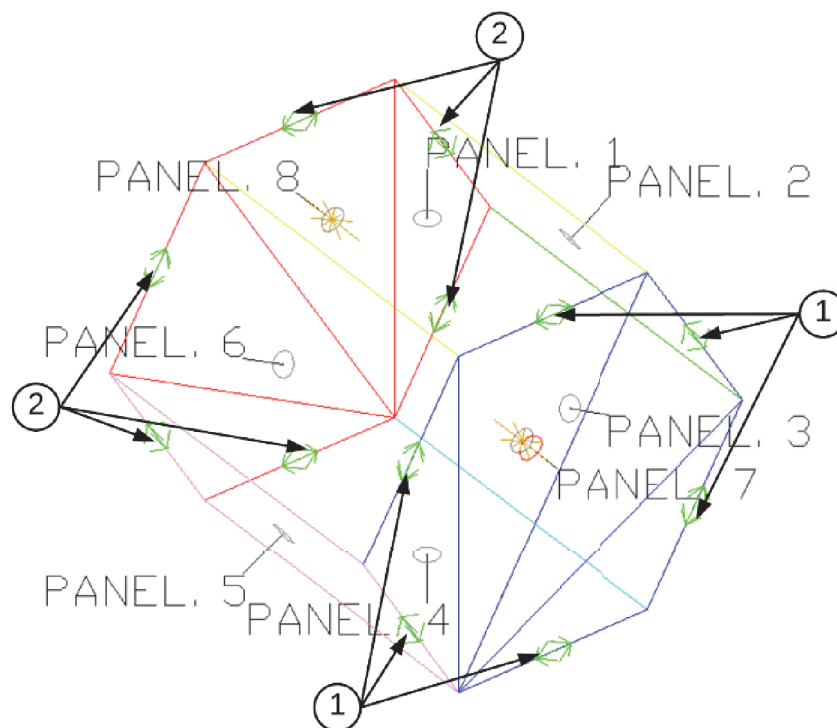


Figure 6.11. MR SAT Model Revision B – Edge Contactors

Table 6.5. Model Revision B – Steady State Analysis

Panel	Case Temperature [°C]	
	Hot Case	Cold Case
1	19.94	-23.55
2	-0.54	-18.14
3	-6.13	-24.32
4	-1.62	-26.06
5	4.23	-22.21
6	20.69	-26.14
7	3.23	-24.05
8	2.25	-25.19

6.4.4.2 External surface and internal components – model revision D. The next thermal model revision involved the explicit modeling of the MR SAT internal component boxes and electronic components. Nodal resolution of the panels remained the same. Heat loads for this model were applied to the appropriate components. Panels and conduction modeled in revision C remained the same for this model.

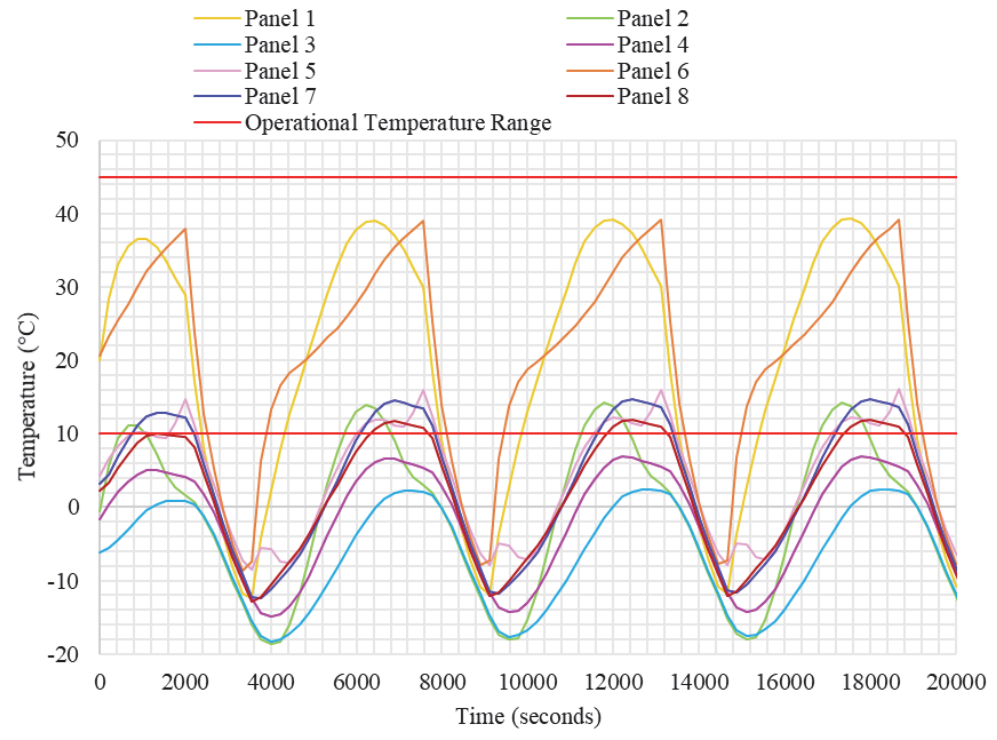


Figure 6.12. Model Revision B – Hot Case Transient Analysis

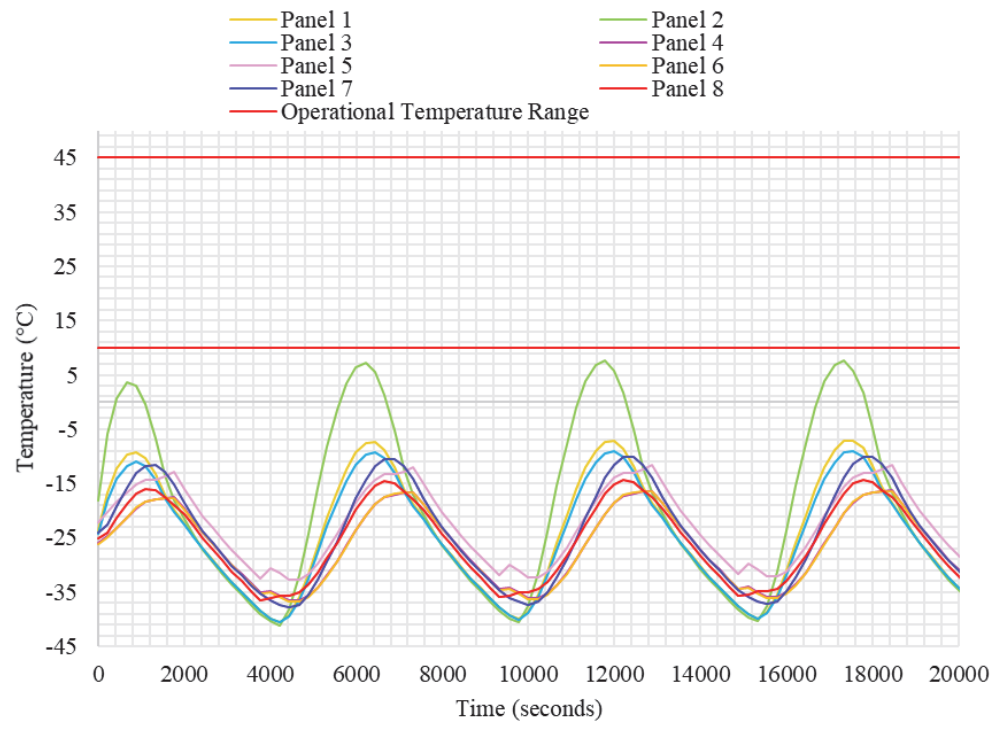


Figure 6.13. Model Revision B – Cold Case Transient Analysis

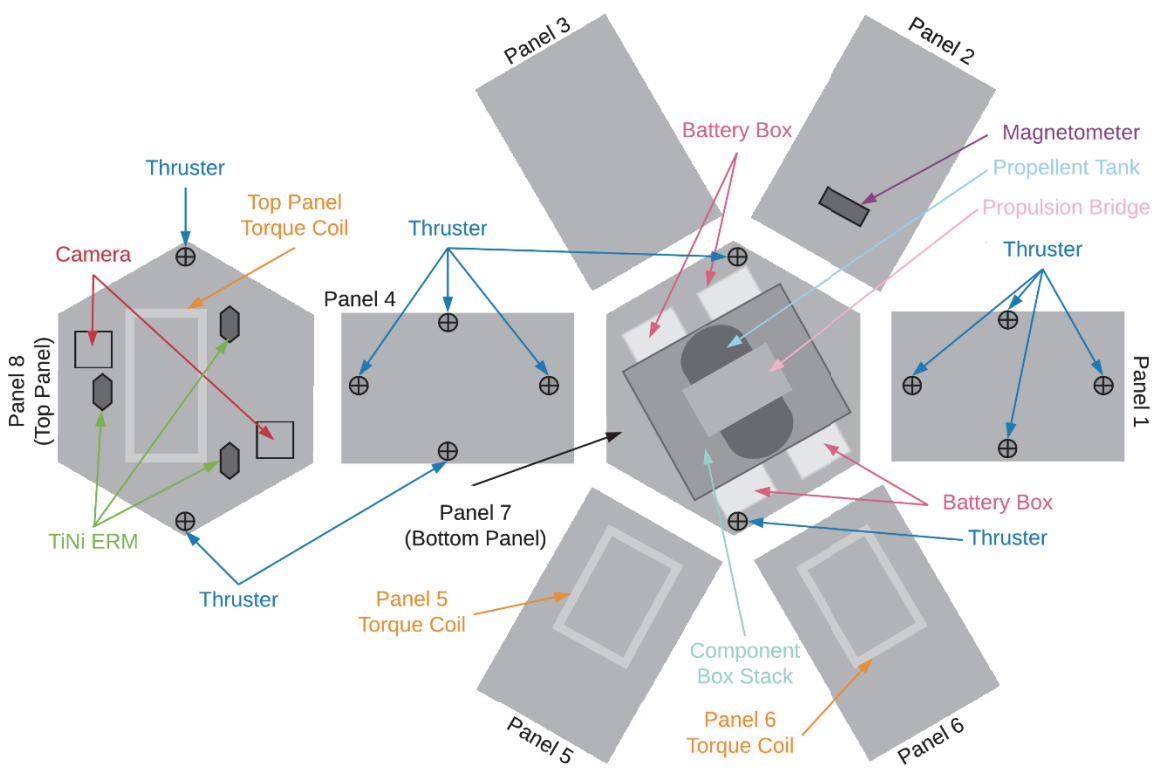


Figure 6.14. MR SAT Internal Component Layout

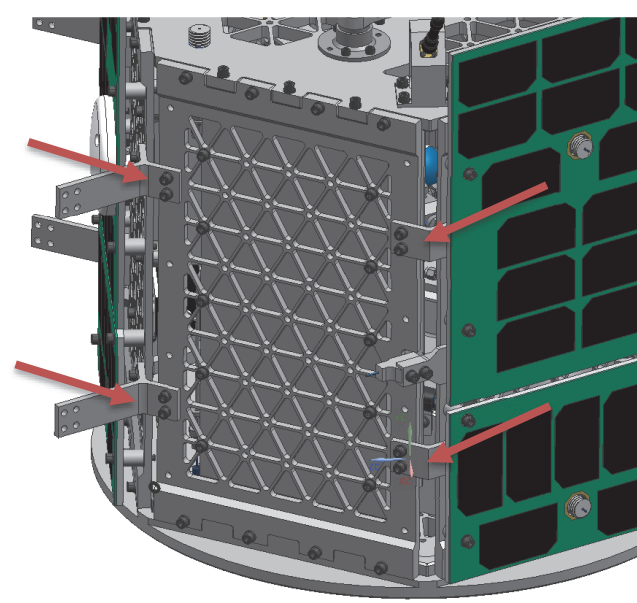


Figure 6.15. MR SAT Side Panel Brackets

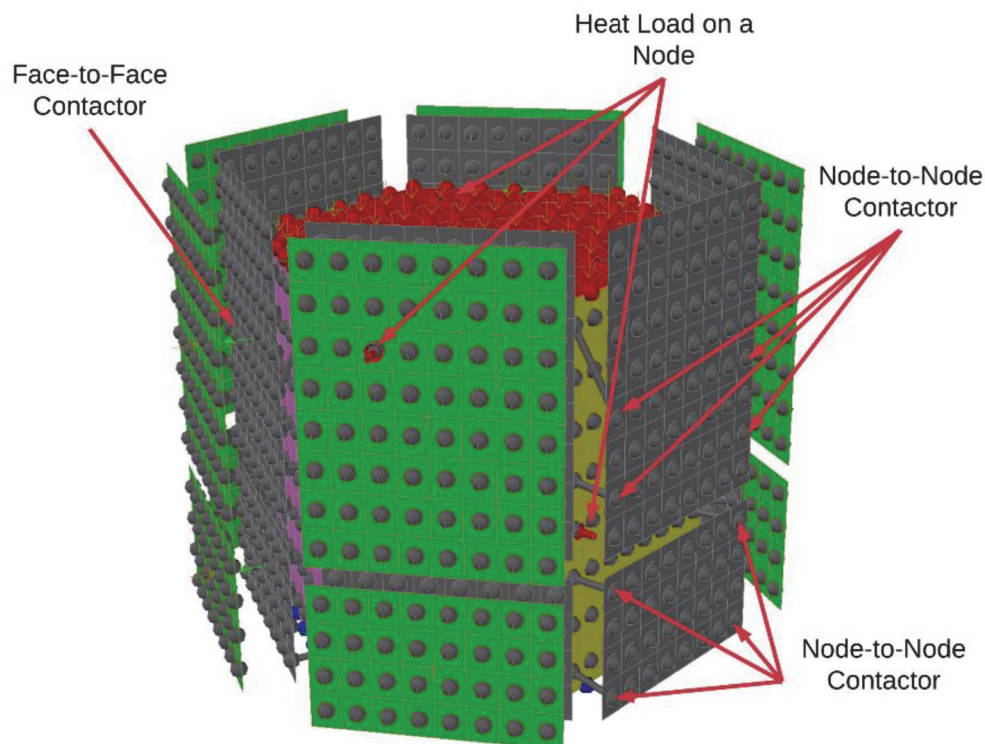


Figure 6.16. MR SAT Model Revision C – Conduction and Heat Load Locations

Table 6.6. Model Revision C – Hot Case Steady State

Panel Number	Maximum Panel Temperature [°C]		
	Solar Panel (PCB and Solar Cells)	Honeycomb Panel	Isogrid Panel
1	40.16	40.16	8.67
2	0.93	0.94	2.19
3	-4.70	-4.63	-1.51
4	-1.30	-1.27	-0.03
5	5.66	5.66	3.52
6	42.36	42.36	8.92
7	-	-	3.54
8	-	-	4.93

6.4.4.2.1 Model construction. Component boxes were modeled using Thermal Desktop boxes with edge nodes. Electronic components were created using the Thermal Desktop brick, Thermal Desktop cylinder, and Thermal Desktop rectangle with the

dimensions and material properties presented in Appendix C. Each component has a single arithmetic node, because temperature gradients across components are not examined in this thermal model revision. Conduction was applied between components, component boxes, and the satellite panels using face-to-face contactors. Because there are no standoffs between faces, as there were between the solar panel and isogrid, node-to-node contactors were not necessary. The conductance values are presented in Appendix C. There was a total of 2432 nodes in this constructed thermal model.

Heat loads were also applied to the individual electrical components, using the values presented for the hot and cold case in Appendix C. The locations of the electrical components are shown in Figure 6.23. Figure 6.24 shows the thermal model with panels removed for easier viewing of the internal modeled components. A few locations of face-to-face contactors and heat loads on nodes are annotated.

6.4.4.2.2 Analysis results. The results of the steady state analysis for thermal model revision D are shown in Appendix G. The transient analysis results for the electrical components are shown in Tables 6.8 and 6.9. The maximum and minimum temperatures for each panel component are shown in Figures 6.25 through 6.30.

6.4.4.2.3 Discussion. Only two orbits were propagated for this analysis in order to reduce the analysis run time. The resulting temperatures of the electrical components in Table 6.8 and 6.9 are compared with their respective maximum and minimum operating temperatures. The cells of temperatures that do not fall outside out the acceptable range are highlighted in green. Those that are outside of the acceptable operating range are highlighted in orange. This allows the engineer to see where thermal control methods must be employed on the satellite in order to regulate these temperatures. This is detailed in Section 6.4.4.3.

The temperatures of the panel components for this thermal model revision did not differ significantly from the results of the previous revision because the construction of the panels in the model did not change. The temperature of the solar panel PCB and solar cells is of concern because the operating temperature of the solar cells lies between 10°C and 80°C. The solar cells will likely function beneath the minimum operating temperature, but the efficiency of the cells may be lower than necessary for power generation.

Table 6.7. Model Revision C – Cold Case Steady State

Panel Number	Minimum Panel Temperature [°C]		
	Solar Panel (PCB and Solar Cells)	Honeycomb Panel	Isogrid Panel
1	-21.39	-21.40	-21.78
2	-18.38	-18.41	-20.70
3	-21.30	-21.30	-21.72
4	-26.35	-26.35	-22.63
5	-20.92	-20.93	-22.11
6	-26.70	-26.70	-22.52
7	-	-	-21.85
8	-	-	-22.57

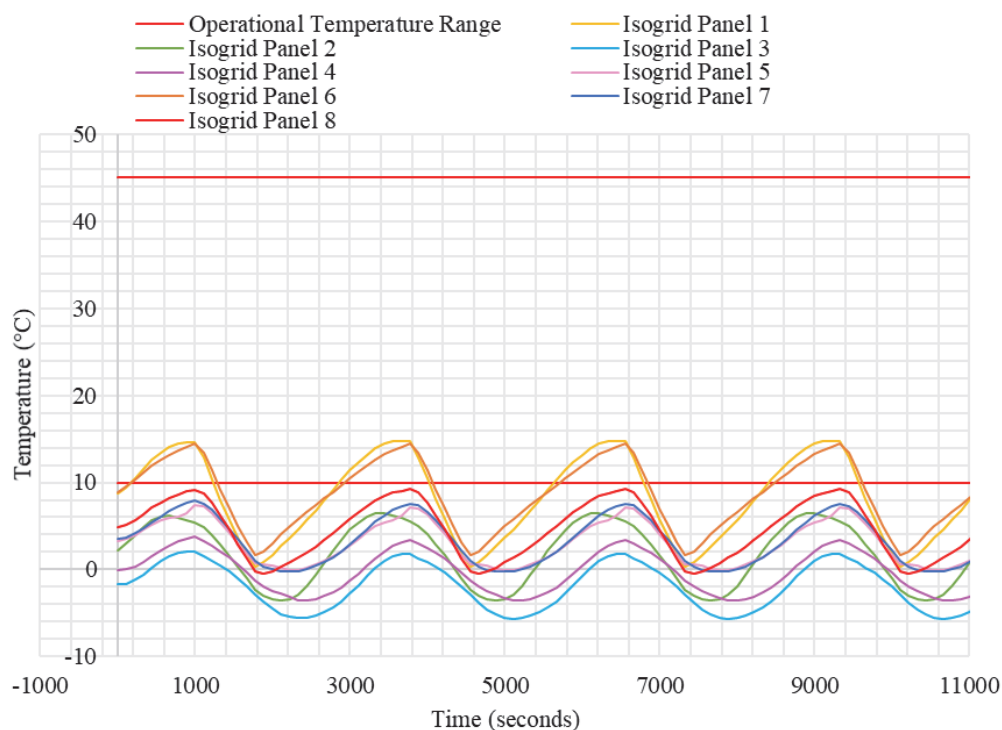


Figure 6.17. Model Revision C Hot Case Transient – Isogrid Panels

6.4.4.3 Model revision E – potential thermal control system design. The thermal control methods for MR SAT were restricted to the utilization of tailored surface coatings and minor design changes. Thermal control hardware such as MLI was deemed too costly to use for the mission. Heaters had been considered in the past, but were

deemed too unreliable for the mission should the heaters fail in the “on” position and cause overheating.

Surface finishes were applied to components and panels in order to bring the temperatures of the satellite components within the operational temperature range, as many of the components are too cold in many of the cases. Some potential design changes were also identified that were used to improve the temperatures as well. Future work may include determining other possible combinations of surface finishes and design changes to alter the resulting temperatures if the thermal design presented is deemed unfeasible for the other subsystems.

6.4.4.3.1 Surface properties and design changes. Altered surface finishes are presented in Appendix H. The original optical properties and finishes are presented, along with the finishes selected for thermal control. All of the changes made were done in order to raise the temperatures of the components. Surface finishes were selected from [14] based on their optical properties. Figure 4.3 was consulted to assist in the selection process.

The surface finish for all aluminum components including panels and component boxes was changed to a plain anodic coating rather than a clear anodic coating in order to reduce the emissivity and increase the absorptivity of the surfaces. The Sun sensor boards and cameras were coated with black Kapton film in order to increase their absorptivity as well. Copper foil tape was applied around the thrusters in order to increase their absorptivity and decrease their emissivity to space so that they will not lose as much thermal energy to radiation.

The previous thermal model revisions show that the solar panel PCBs and solar cells do not reach the necessary temperature required for proper solar cell operation. Changes to the model were made in an attempt to increase the temperatures of each solar panel PCB and solar cell assembly. The solar panel PCBs were coated with black paint on their space-facing side in order to increase absorptivity as well. A different coating with similar optical properties may need to be selected for the PCB if it is determined that the selected paint cannot be used on the PCBs. This coating will be applied before attaching the solar cells in order to reduce the risk of contaminating the cells and reducing their efficiency. Black tape was applied to the back of the solar panel PCB in an

attempt to increase the emissivity of the surface and to increase the transfer of thermal energy to the inside of the satellite. It is likely that this tape may act as an insulator between the PCB and the aluminum panel, but was included in this thesis study to demonstrate the effect of altering surface finishes on panels.

Other changes to the satellite design included adding boxes around the Sun sensor cameras to assist in the prevention of energy loss to space by radiation. The box created on Panel 3 was coated with a plain anodic coating, but the box created on Panel 6 was coated with a black anodic coating on the external surface and a green anodic coating applied on the internal surface. The Sun sensor camera on Panel 6 was cooler in revision D than the Sun sensor camera on Panel 3, so a different coating was chosen in order to absorb more incident radiation from the Sun. The green anodic coating on the internal surface of the box was chosen because of its lower absorptivity in order to prevent absorption of thermal energy from the Sun sensor camera, and a higher emissivity in order to increase the amount of radiation being transferred from the box to the Sun sensor camera.

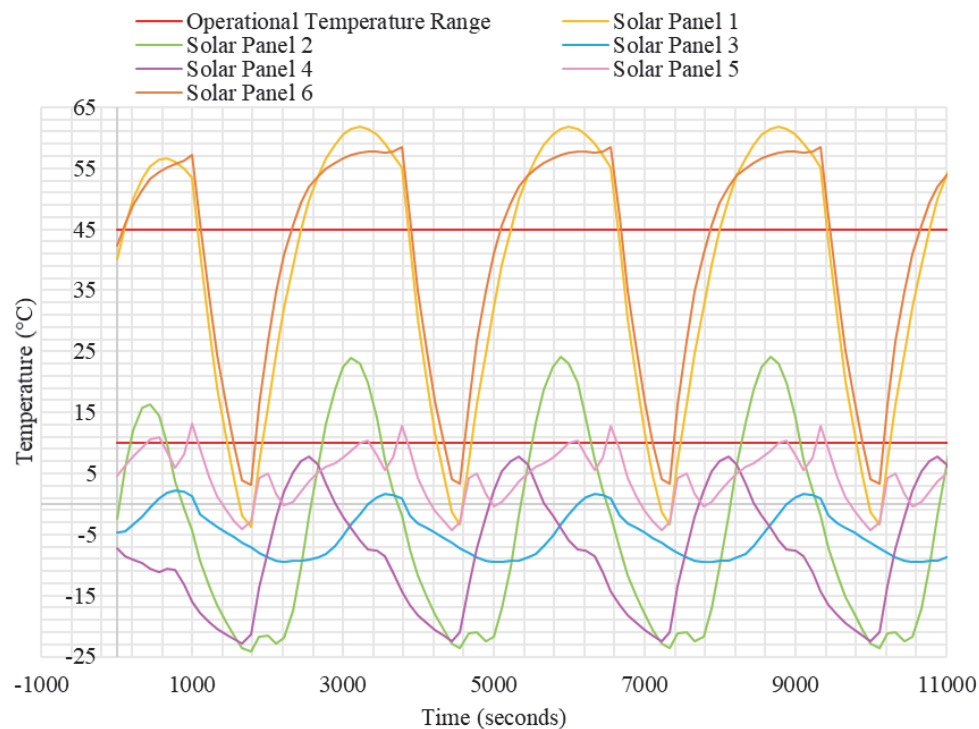


Figure 6.18. Model Revision C Hot Case Transient – Solar Panel PCB

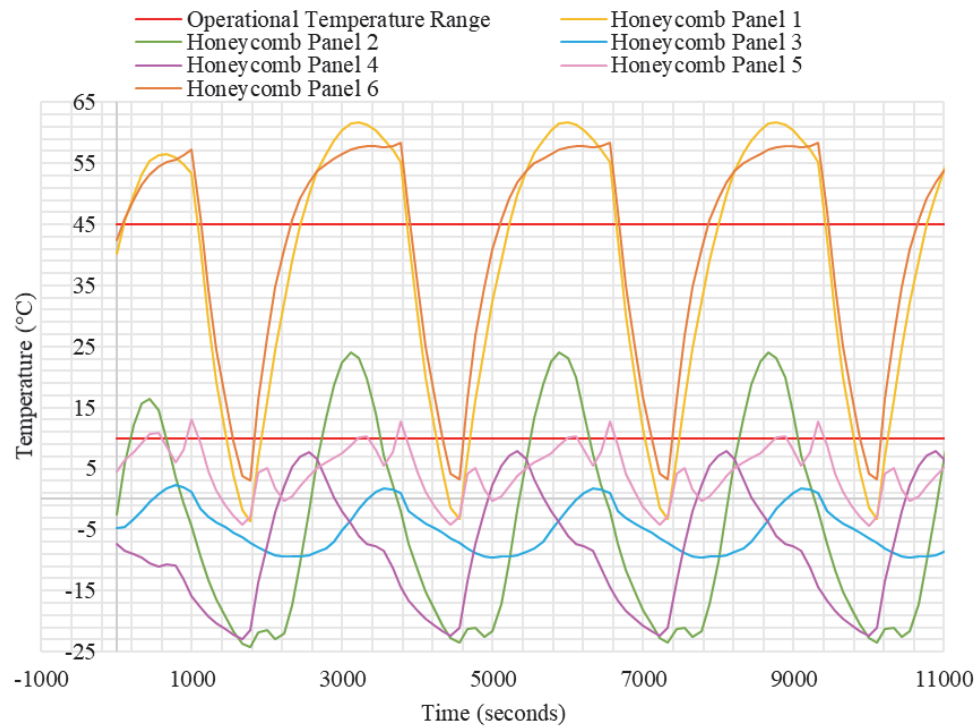


Figure 6.19. Model Revision C Hot Case Transient – Honeycomb Panels

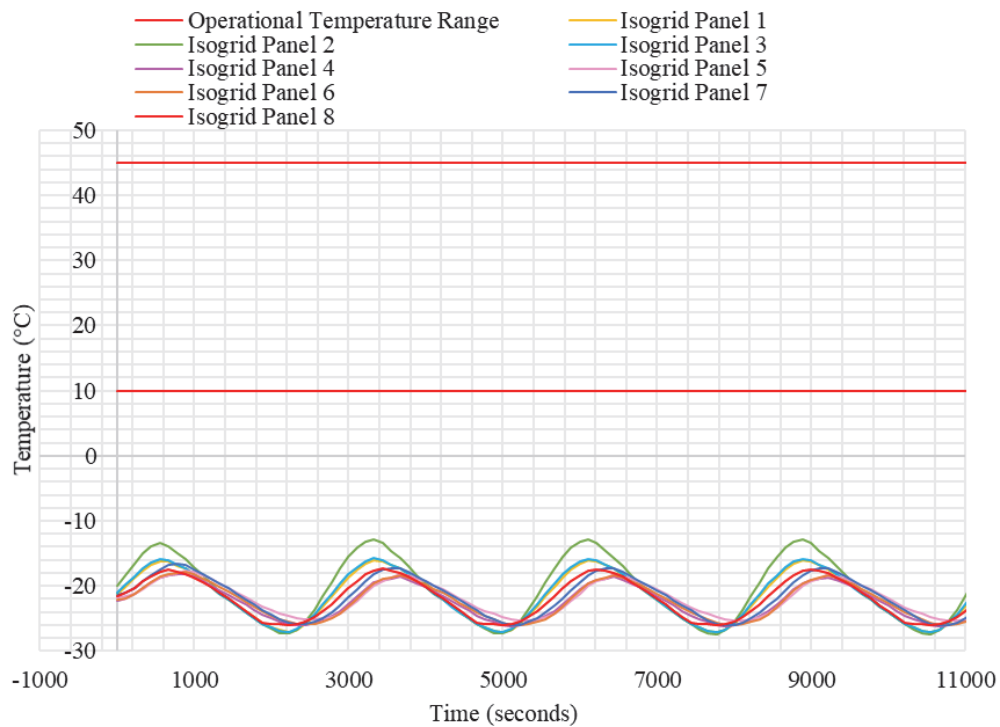


Figure 6.20. Model Revision C Cold Case Transient – Isogrid Panels

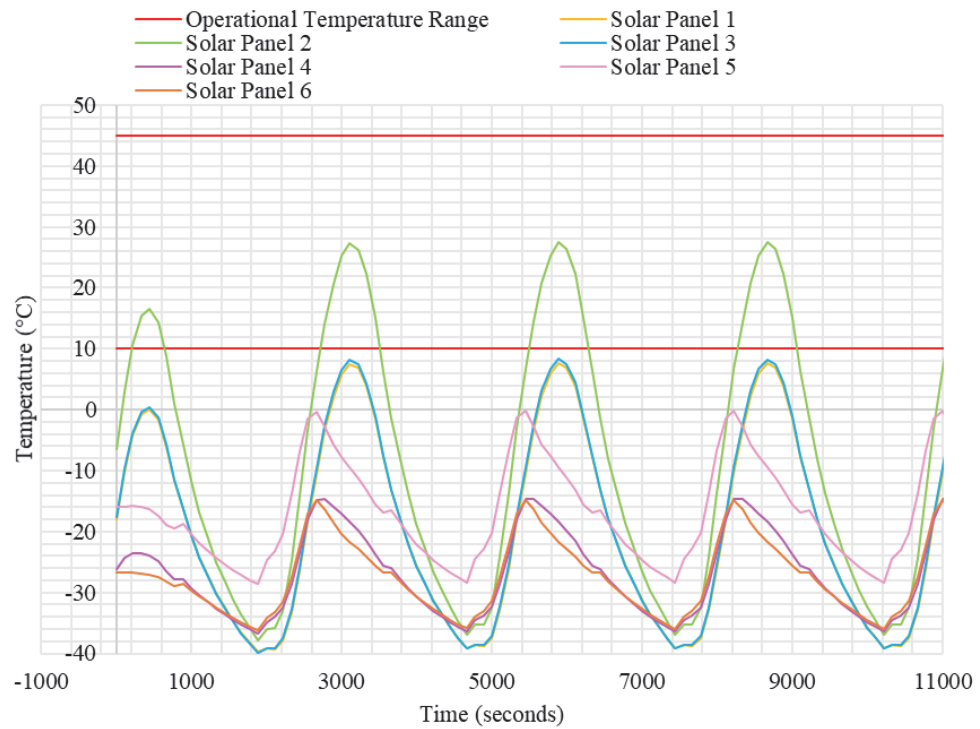


Figure 6.21. Model Revision C Cold Case Transient – Solar Panel PCB

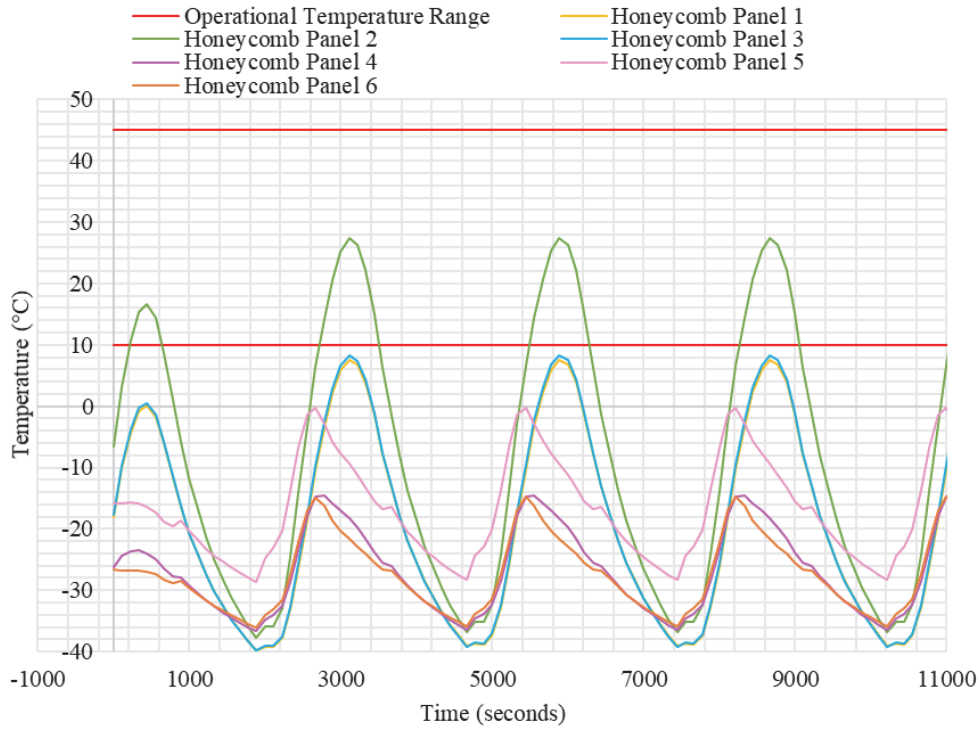


Figure 6.22. Model Revision C Cold Case Transient – Honeycomb Panels

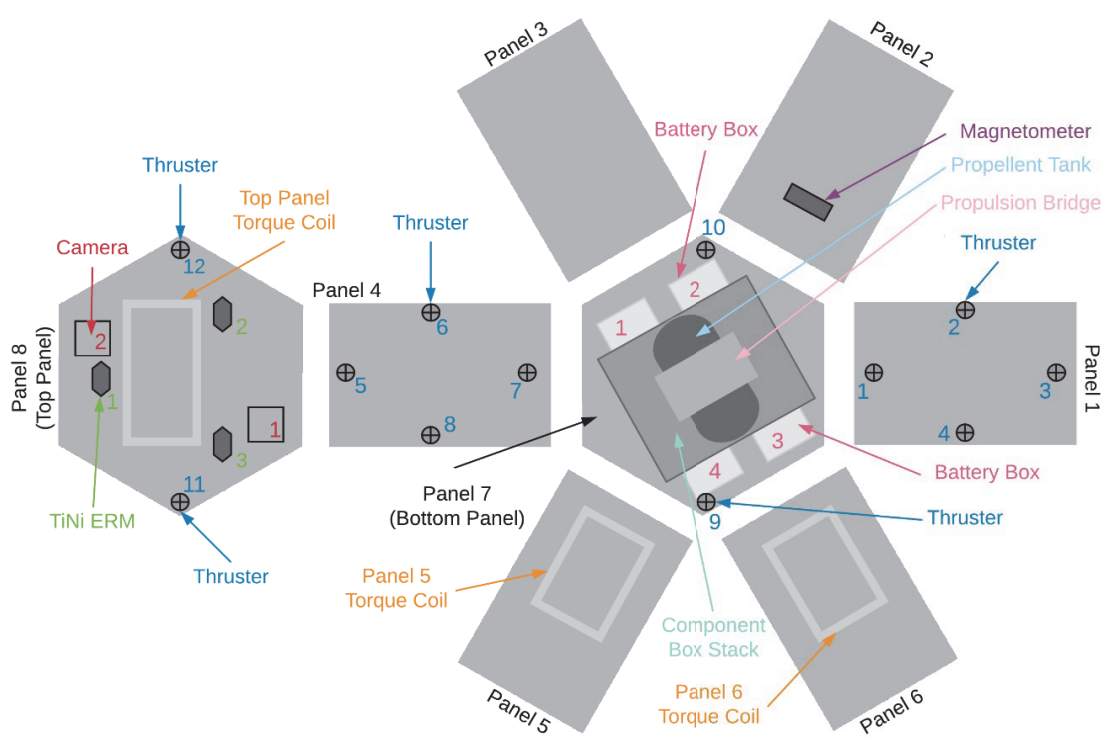


Figure 6.23. MR SAT Internal Electrical Component Mounting Locations

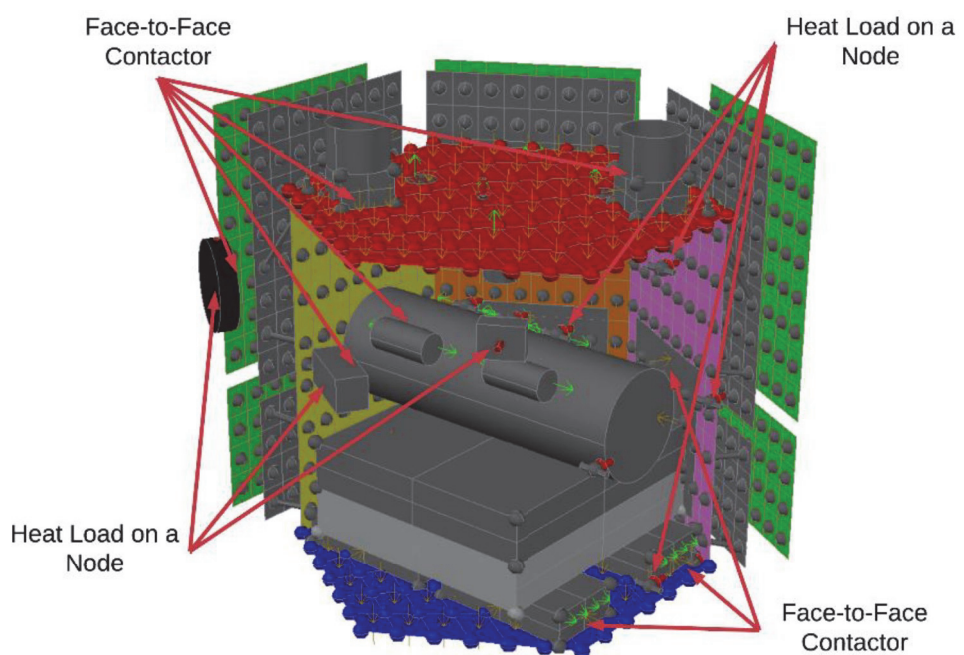


Figure 6.24. MR SAT Model Revision D – Conduction and Heat Load Locations

Table 6.8. Model Revision D – Transient Analysis Results for Electrical Components

Component	Max Temp [°C] - Hot Case	Min Temp [°C] - Cold Case	Max Operating Temp [°C]	Min Operating Temp [°C]	Max Survival Temp [°C]	Min Survival Temp [°C]
Box 1 - Battery 1	5.1223	-24.5763	45	0	-20	60
Box 1 - Battery 2	5.1241	-24.5723	45	0	-20	60
Box 1 - Battery 3	5.1260	-24.5731	45	0	-20	60
Box 1 - Battery 4	5.1233	-24.5730	45	0	-20	60
Box 1 - Battery 5	5.1253	-24.5737	45	0	-20	60
Box 1 - Battery 6	5.1199	-24.5758	45	0	-20	60
Box 1 - Battery 7	5.1223	-24.5763	45	0	-20	60
Box 1 - Battery 8	5.1199	-24.5758	45	0	-20	60
Box 2 - Battery 1	6.0558	-24.5556	45	0	-20	60
Box 2 - Battery 2	6.0560	-24.5527	45	0	-20	60
Box 2 - Battery 3	6.0594	-24.5532	45	0	-20	60
Box 2 - Battery 4	6.0554	-24.5533	45	0	-20	60
Box 2 - Battery 5	6.0588	-24.5536	45	0	-20	60
Box 2 - Battery 6	6.0520	-24.5558	45	0	-20	60
Box 2 - Battery 7	6.0558	-24.5556	45	0	-20	60
Box 2 - Battery 8	6.0520	-24.5558	45	0	-20	60
Box 3 - Battery 1	7.3151	-24.1578	45	0	-20	60
Box 3 - Battery 2	7.3415	-24.1608	45	0	-20	60
Box 3 - Battery 3	7.3455	-24.1611	45	0	-20	60
Box 3 - Battery 4	7.3415	-24.1608	45	0	-20	60
Box 3 - Battery 5	7.3455	-24.1611	45	0	-20	60
Box 3 - Battery 6	7.3108	-24.1575	45	0	-20	60
Box 3 - Battery 7	7.3151	-24.1578	45	0	-20	60
Box 3 - Battery 8	7.3108	-24.1575	45	0	-20	60
Box 4 - Battery 1	6.4003	-24.1106	45	0	-20	60
Box 4 - Battery 2	6.4015	-24.1074	45	0	-20	60
Box 4 - Battery 3	6.4039	-24.1081	45	0	-20	60
Box 4 - Battery 4	6.4009	-24.1079	45	0	-20	60
Box 4 - Battery 5	6.4033	-24.1086	45	0	-20	60
Box 4 - Battery 6	6.3978	-24.1103	45	0	-20	60
Box 4 - Battery 7	6.4003	-24.1106	45	0	-20	60
Box 4 - Battery 8	6.3978	-24.1103	45	0	-20	60

The standoff between the solar panel assembly and the isogrid panels on the sides of the satellite were removed, and the panels mounted flush to each other as a final effort to increase the heat transfer from the external panels to the internal components of the satellite. The honeycomb panels were replaced with solid aluminum panels to reduce the drastic temperature changes of the panels through the orbit. The thicknesses of the aluminum panels (formerly honeycomb panels) and solar panel PCB were increased to 10 mm each for the same purpose. This design change will very likely be deemed unacceptable by the other subsystems, but was included in this thesis study to demonstrate the effect of altering panel properties and mounting methods.

Table 6.9. Model Revision D – Transient Analysis Results for Batteries

Component	Max Temp [°C] - Hot Case	Min Temp [°C] - Cold Case	Max Operating Temp [°C]	Min Operating Temp [°C]	Max Survival Temp [°C]	Min Survival Temp [°C]
TiNi 1	7.1070	-25.8499	70	-65	-150	150
TiNi 2	3.6698	-25.8867	70	-65	-150	150
TiNi 3	5.1413	-25.5146	70	-65	-150	150
MCU Digital	9.6494	-19.5565	85	-40	-65	150
Isovalve 1	9.8847	-19.5659	49	-18	-	-
Isovalve 2	9.8850	-19.5658	49	-18	-	-
Isovalve 3	9.8850	-19.5659	49	-18	-	-
Thruster 1	11.6540	-26.3161	49	-18	-	-
Thruster 2	14.4910	-26.9643	49	-18	-	-
Thruster 3	12.3195	-26.3839	49	-18	-	-
Thruster 4	15.5643	-26.8803	49	-18	-	-
Thruster 5	2.3908	-25.5215	49	-18	-	-
Thruster 6	2.3505	-25.7899	49	-18	-	-
Thruster 7	3.9226	-25.6375	49	-18	-	-
Thruster 8	2.6744	-25.5844	49	-18	-	-
Thruster 9	5.7565	-25.3458	49	-18	-	-
Thruster 10	6.8773	-25.5736	49	-18	-	-
Thruster 11	4.2547	-25.4769	49	-18	-	-
Thruster 12	7.0776	-26.1666	49	-18	-	-
Pressure Transducer 1	9.4240	-19.5725	82	-29	-	-
Pressure Transducer 2	9.4273	-19.5713	82	-29	-	-
Comm Radio	9.4561	-19.1743	70	-30	-30	85
GPS Receiver	9.7028	-19.2589	85	-40	-55	95
GPS Antenna	20.0389	-36.3315	85	-55	-55	85
Flight Raspberry Pi	12.1279	-16.8200	80	-25	-	-
IMU	9.5954	-19.3693	85	-40	-	-
Sun Sensor Camera 1	-13.2369	-38.4079	70	-10	95	-40
Sun Sensor Camera 2	56.4123	-34.0477	70	-10	95	-40
Sun Sensor Board 1	9.7393	-19.0958	70	-10	95	-40
Sun Sensor Board 2	9.4663	-19.4555	70	-10	95	-40
MCU Analog	9.6302	-19.3355	85	-40	-65	105
Magnetometer	6.3479	-26.8240	85	-55	-	-
Torque Coil - Top Panel	5.4649	-25.7916	60	-50	-	-
Torque Coil - Panel 5	7.2184	-24.6578	60	-50	-	-
Torque Coil - Panel 6	13.4455	-25.4730	60	-50	-	-
Camera 1	4.1560	-26.1962	45	0	-30	60
Camera 2	6.0732	-26.5537	45	0	-30	60
Payload Raspberry Pi	12.1312	-16.8183	80	-25	-	-
EPS Board	8.2338	-21.1660	105	-40	-	-

The modeling of the battery boxes was changed from Thermal Desktop Boxes to Thermal Desktop Bricks in order to more accurately represent the boxes in which the batteries will be mounted. Appendix H presents new geometries and contactors for the satellite thermal model revision E.

These potential thermal control design changes must still be presented to and analyzed by other subsystems to determine their feasibility, which will be included in

future work to be done. Replacing the honeycomb panels with solid aluminum panels will increase the overall mass of the satellite, and will affect the moment of inertia of the satellite. Placing the Sun sensor cameras in boxes could potentially reduce the sensor's field of view. Mounting the solar panel assembly directly to the isogrid panels without using standoffs may affect the performance of the structure during vibration testing/ascent. All of these design changes must be fully vetted at both subsystem levels and a systems level before being implemented in the final satellite design.

6.4.4.3.2 Analysis results. The adjusted satellite thermal model was analyzed for the same hot and cold cases as the previous models, though only transient analyses were performed to reduce analysis run time. The nodal resolution of the external satellite panels was reduced by half for each panel, to lower the analysis run time as well. The reduction in nodal resolution will not greatly affect the results of the components because most components are not mounted to the side panels. A total of 692 nodes were used in the thermal model, which is shown in Figure 6.31. Future work will include performing a convergence study to determine the optimal number of nodes to use in the thermal modeling and analysis process. Only two orbits were propagated to provide a reasonable analysis time, as two are sufficient because the maximum and minimum temperature experienced by the model occur by the second orbit. The transient analysis results for the batteries are presented in Table 6.11, and for the other electrical components in Table 6.12. The hot case maximum transient results for the panels are shown in Figures 6.32 through 6.34. The cold case minimum transient results for the panels are shown in Figures 6.35 through 6.37.

6.4.4.3.3 Discussion. As can be seen in Tables 6.11 and 6.12, the temperatures of the critical satellite components were brought within their specific operating temperatures necessary for proper operation. Figure 6.32 and 6.35 present the temperatures of the solar panel PCB and solar cell assembly. The temperatures of this PCB and solar cell assembly remain of concern because since the maximum operating temperature for the solar cells is 80°C, and the minimum operating temperature is 10°C. It is likely that the solar cells will continue to operate, though they may not operate as efficiently as expected because of their cold temperature. While the design changes to the external satellite panels and their mounting method show that it is possible to raise the temperatures of the panels, future

work will be required to determine a more appropriate method of raising the solar cell temperatures.

Model revision E shows the effects of applying tailored surface finishes and design changes to manipulate the temperatures of the satellite panels and components. Though these changes have raised the satellite temperature, they must still be vetted on a subsystem and system level before being accepted for use in the final satellite design. Additional design and thermal control method iterations will be necessary before the final thermal control system is approved.

6.4.5. Future Work. Additional model revisions can be made in order to create a more complex model. Electrical components can be more explicitly modeled, and nodal resolution can be increased. Propellant lines can be modeled, as well as less critical components that were not previously included in the model. Although, adding additional complexity to the model can also introduce additional errors. The conduction values, optical properties, and material properties used in this thesis study are estimates, and their inaccuracy can contribute to errors in the model. The model could be improved by determining exact input values through laboratory testing of materials and conductance, though this process can be complex and time consuming. An improved evaluation of the solar array heat loads, including conversion effects, will be included in the updated model as well.

A convergence study will also be performed to determine the optimal number of nodes to use for accurate modeling of components and panels. Necessary uncertainties must also be determined and applied to the model. Additional Thermal Desktop modeling parameters, including rays per node settings and the number of orbital positions included in each orbit, will be evaluated as well.

The proposed thermal control methods, including design changes and surface finish selection, will be presented to the other subsystems, and the manufacturing implications of the design changes and surface finishes evaluated. These control methods will need to be fine-tuned to fit the requirements of the subsystems. The methods will need to be vetted on a system level as well as a subsystem level before being approved for use in the final satellite design.

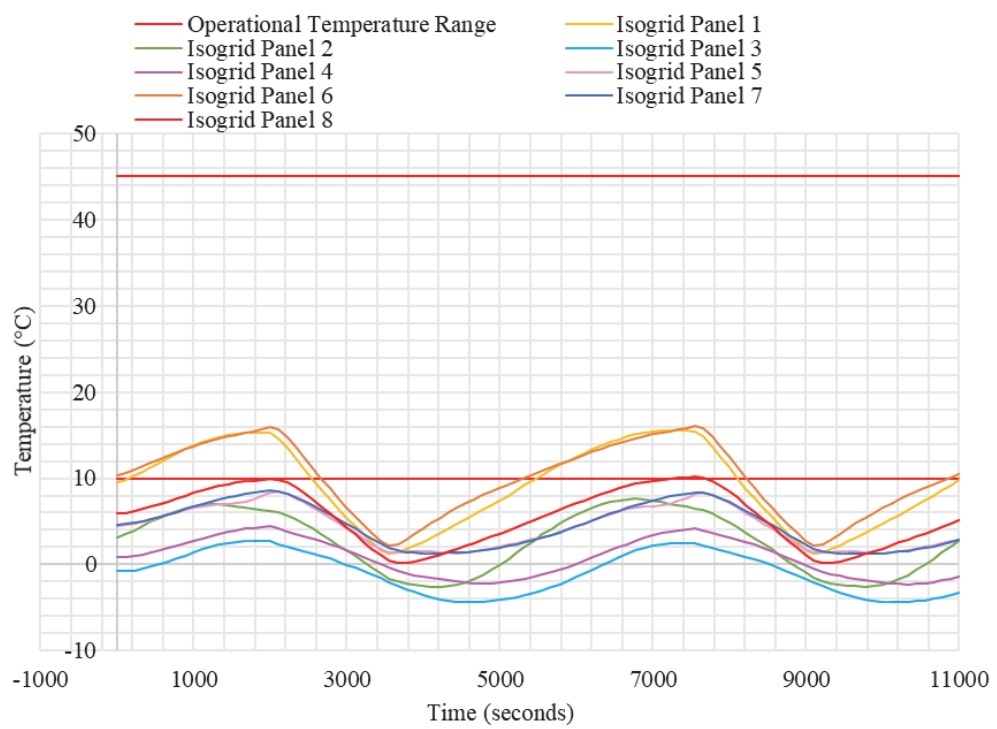


Figure 6.25. Model Revision D Hot Case Transient – Isogrid Panels

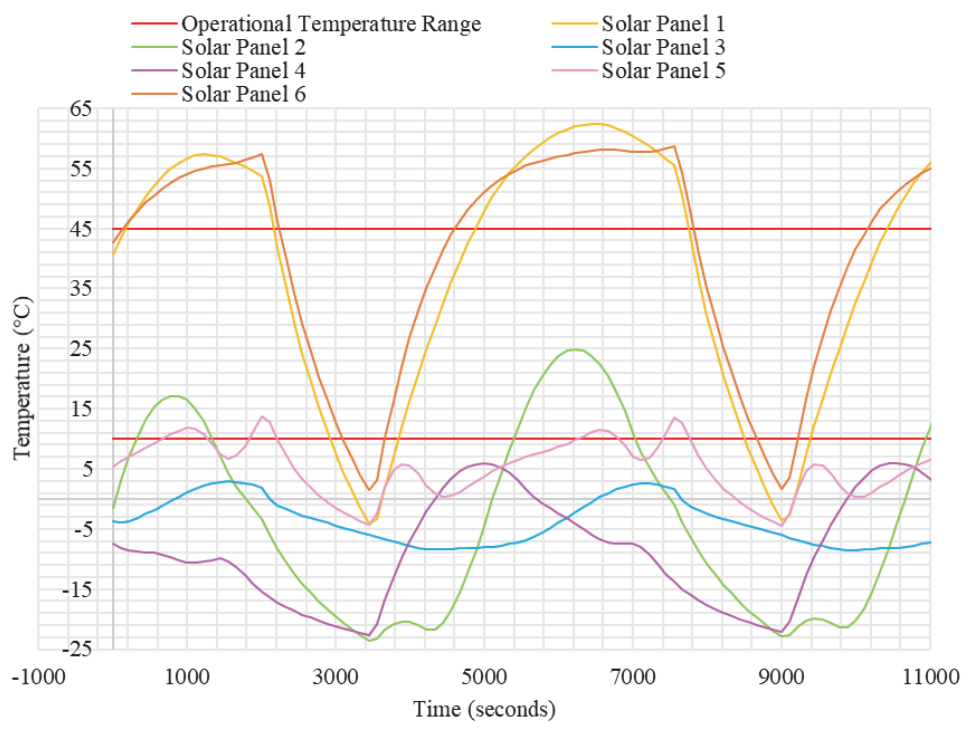


Figure 6.26. Model Revision D Hot Case Transient – Solar Panel PCB

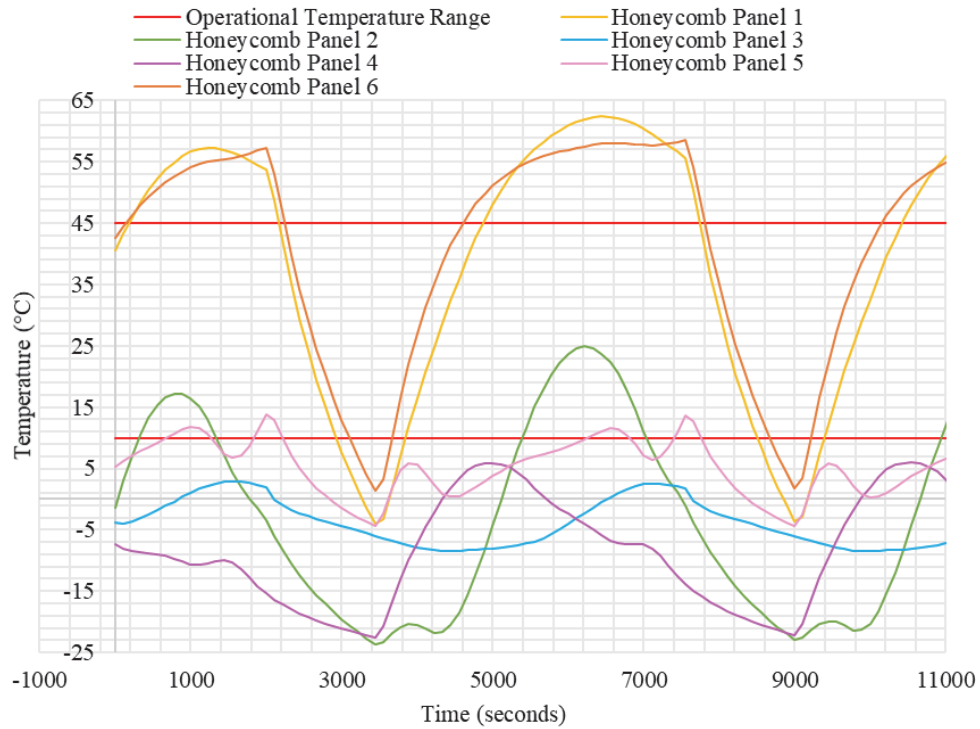


Figure 6.27. Model Revision D Hot Case Transient – Honeycomb Panels

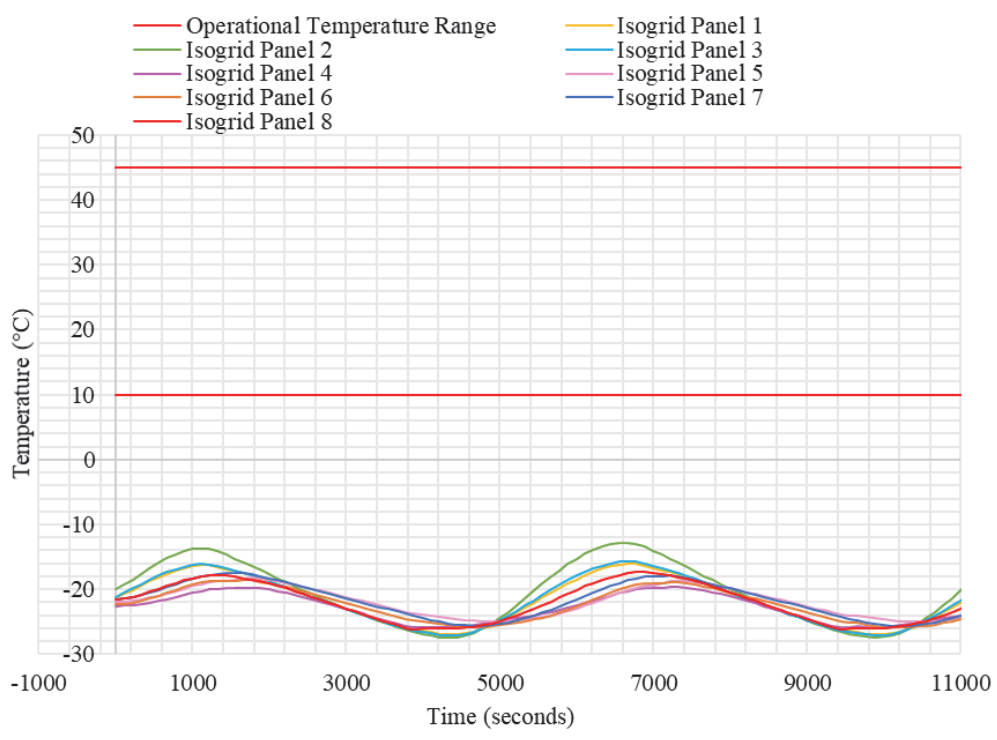


Figure 6.28. Model Revision D Cold Case Transient – Isogrid Panels

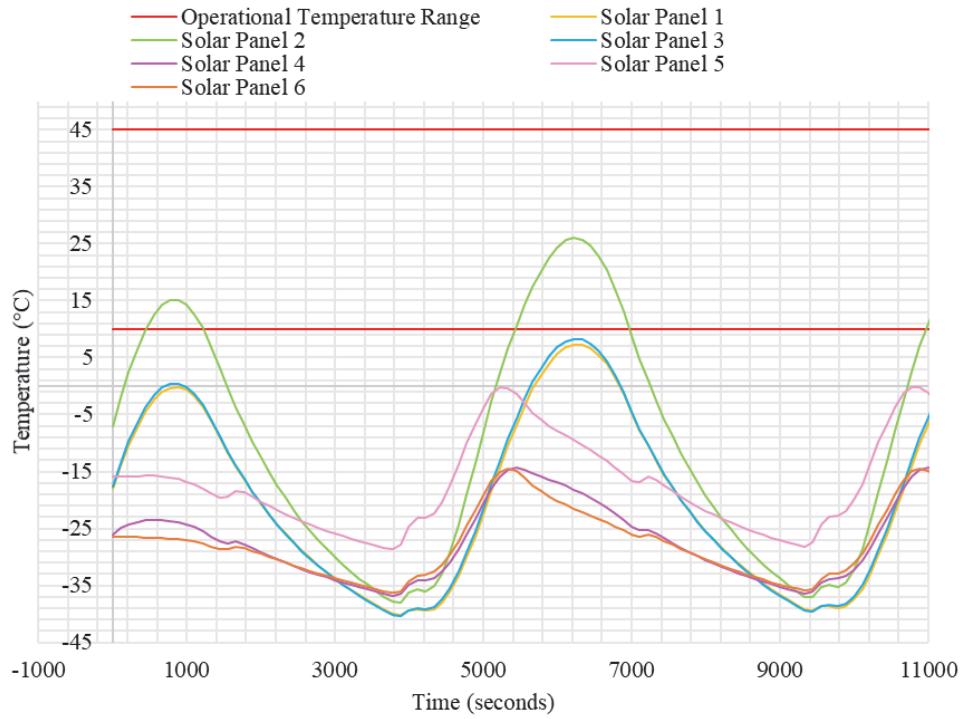


Figure 6.29. Model Revision D Cold Case Transient – Solar Panel PCB

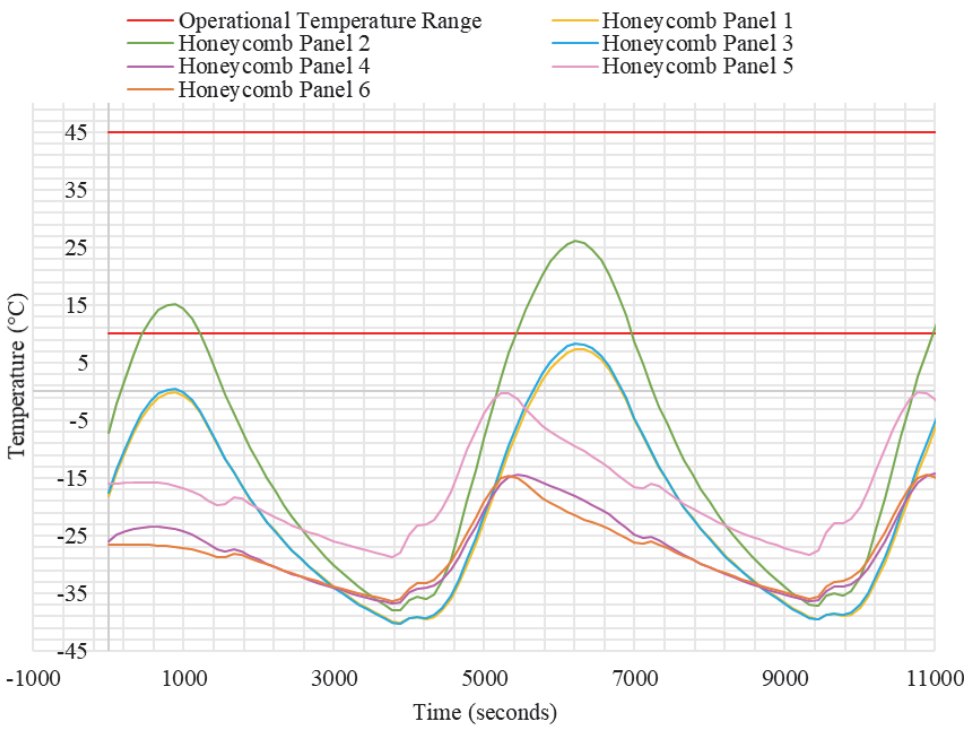


Figure 6.30. Model Revision D Cold Case Transient – Honeycomb Panels

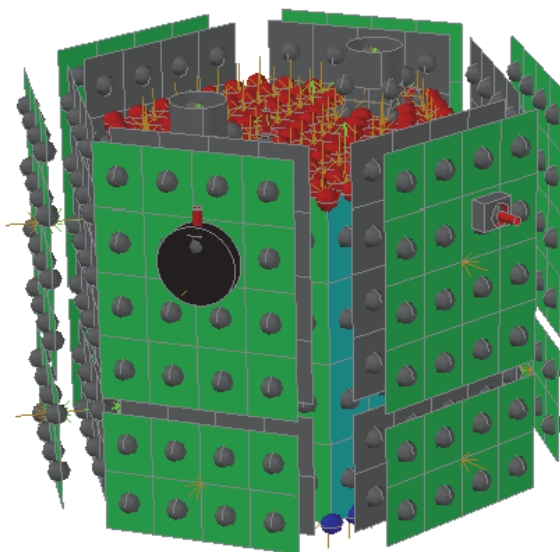


Figure 6.31. MR SAT Thermal Model Revision E

Table 6.10. Model Revision E – Transient Results for Batteries

Component	Max Temp [°C] - Hot Case	Min Temp [°C] - Cold Case	Max Operating Temp [°C]	Min Operating Temp [°C]	Max Survival Temp [°C]	Min Survival Temp [°C]
Box 1 - Battery 1	42.0454	5.4711	45	0	-20	60
Box 1 - Battery 2	42.0454	5.4711	45	0	-20	60
Box 1 - Battery 3	42.0454	5.4711	45	0	-20	60
Box 1 - Battery 4	42.0454	5.4711	45	0	-20	60
Box 1 - Battery 5	42.0454	5.4711	45	0	-20	60
Box 1 - Battery 6	42.0454	5.4711	45	0	-20	60
Box 1 - Battery 7	42.0454	5.4711	45	0	-20	60
Box 1 - Battery 8	42.0454	5.4711	45	0	-20	60
Box 2 - Battery 1	42.6452	5.4923	45	0	-20	60
Box 2 - Battery 2	42.6452	5.4923	45	0	-20	60
Box 2 - Battery 3	42.6452	5.4923	45	0	-20	60
Box 2 - Battery 4	42.6452	5.4923	45	0	-20	60
Box 2 - Battery 5	42.6452	5.4923	45	0	-20	60
Box 2 - Battery 6	42.6452	5.4923	45	0	-20	60
Box 2 - Battery 7	42.6452	5.4923	45	0	-20	60
Box 2 - Battery 8	42.6452	5.4923	45	0	-20	60
Box 3 - Battery 1	42.8676	5.4131	45	0	-20	60
Box 3 - Battery 2	42.8676	5.4131	45	0	-20	60
Box 3 - Battery 3	42.8676	5.4131	45	0	-20	60
Box 3 - Battery 4	42.8676	5.4131	45	0	-20	60
Box 3 - Battery 5	42.8676	5.4131	45	0	-20	60
Box 3 - Battery 6	42.8676	5.4131	45	0	-20	60
Box 3 - Battery 7	42.8676	5.4131	45	0	-20	60
Box 3 - Battery 8	42.8676	5.4131	45	0	-20	60
Box 4 - Battery 1	42.2623	5.4180	45	0	-20	60
Box 4 - Battery 2	42.2623	5.4180	45	0	-20	60
Box 4 - Battery 3	42.2623	5.4180	45	0	-20	60
Box 4 - Battery 4	42.2623	5.4180	45	0	-20	60
Box 4 - Battery 5	42.2623	5.4180	45	0	-20	60
Box 4 - Battery 6	42.2623	5.4180	45	0	-20	60
Box 4 - Battery 7	42.2623	5.4180	45	0	-20	60
Box 4 - Battery 8	42.2623	5.4180	45	0	-20	60

Table 6.11. Model Revision E – Transient Results for Components

Component	Max Temp [°C] - Hot Case	Min Temp [°C] - Cold Case	Max Operating Temp [°C]	Min Operating Temp [°C]	Max Survival Temp [°C]	Min Survival Temp [°C]
TiNi 1	42.3084	2.4930	70	-65	-150	150
TiNi 2	38.6156	2.7749	70	-65	-150	150
TiNi 3	39.9796	2.7160	70	-65	-150	150
MCU Digital	46.7935	10.9856	85	-40	-65	150
Isovalve 1	47.0767	10.9767	49	-18	-	-
Isovalve 2	47.0771	10.9768	49	-18	-	-
Isovalve 3	47.0768	10.9767	49	-18	-	-
Thruster 1	47.5563	1.8898	49	-18	-	-
Thruster 2	46.8478	1.4100	49	-18	-	-
Thruster 3	48.0069	1.5618	49	-18	-	-
Thruster 4	48.9021	1.5535	49	-18	-	-
Thruster 5	34.8042	1.9214	49	-18	-	-
Thruster 6	35.5939	2.1649	49	-18	-	-
Thruster 7	37.3262	2.4853	49	-18	-	-
Thruster 8	36.0827	2.3751	49	-18	-	-
Thruster 9	41.0231	3.5942	49	-18	-	-
Thruster 10	42.4893	3.4262	49	-18	-	-
Thruster 11	38.4595	2.6354	49	-18	-	-
Thruster 12	42.1236	2.2227	49	-18	-	-
Pressure Transducer 1	46.6006	10.9703	82	-29	-	-
Pressure Transducer 2	46.5972	10.9711	82	-29	-	-
Comm Radio	46.6040	11.3703	70	-30	-30	85
GPS Receiver	46.8809	11.3115	85	-40	-55	95
GPS Antenna	39.1379	-1.9531	85	-55	-55	85
Flight Raspberry Pi	49.2888	13.7380	80	-25	-	-
IMU	46.7473	11.1784	85	-40	-	-
Sun Sensor Camera 1	23.1908	-2.2587	70	-10	95	-40
Sun Sensor Camera 2	58.0436	-3.2861	70	-10	95	-40
Sun Sensor Board 1	47.5635	12.0652	70	-10	95	-40
Sun Sensor Board 2	46.6694	11.1045	70	-10	95	-40
MCU Analog	46.7745	11.2067	85	-40	-65	105
Magnetometer	39.4948	1.3307	85	-55	-	-
Torque Coil - Top Panel	40.5600	2.6806	60	-50	-	-
Torque Coil - Panel 5	40.4200	2.9337	60	-50	-	-
Torque Coil - Panel 6	47.6028	2.2410	60	-50	-	-
Camera 1	40.1028	2.6107	45	0	-30	60
Camera 2	42.4532	2.3708	45	0	-30	60
Payload Raspberry Pi	49.2892	13.7377	80	-25	-	-
EPS Board	44.8940	8.9883	105	-40	-	-

The thermal model for MRS SAT must also be constructed by the team, as well as a model including both MR SAT and MRS SAT in their mated configuration. The addition of MRS SAT will likely not have a large effect on the temperatures of electrical components mounted to MR SAT. MRS SAT will not block a large area of MR SAT's external surface and thus is not expected to prevent MR SAT from absorbing much thermal energy from the Sun. MRS SAT may conduct/radiate some absorbed thermal

energy on to MR SAT, but it is not expected that the amount of energy will cause MR SAT to increase in temperature by a large enough margin to cause the failure of any components.

Each of the mission mode heating load cases must be included in the analysis as well, rather than just the two most extreme thermal cases. Any changes made to the internal layout of the component boxes and electrical components must also be incorporated into the model, to ensure an accurate model and accurate temperature predictions for the final satellite pair design.

Final verification will need to be performed following thermal vacuum testing, which will likely occur at the Air Force Research Laboratory in Albuquerque, New Mexico. The model results will be compared with the results of the thermal vacuum test, and adjusted to more closely reflect testing results. This process is discussed in more detail in Section 3.4.2.

6.4.6. Lessons Learned. Many lessons were learned throughout the process of thermal model construction, analysis, and application of thermal control. It is very important to keep up-to-date documentation during the process. Documentation should include information regarding all model input parameters including orbit profile, satellite dimensions, and material properties. It should be very clear in the documentation which parameters are used for which model revision. Each new model revision should be saved as a separate file and should be accompanied by its own documentation. A cohesive naming convention should be chosen for model drawing files and documentation in order to assist with organization. When applying thermal control, documentation should include an explanation of why certain methods were used. This documentation can be greatly beneficial to future engineers working on the mission, and for personal reference.

It is important to keep track of material properties and their sources. Should there be any question regarding the validity of the property, it will be necessary to refer to the original source. As often as possible, property values provided by material or component manufacturers should be used (but carefully vetted for accuracy).

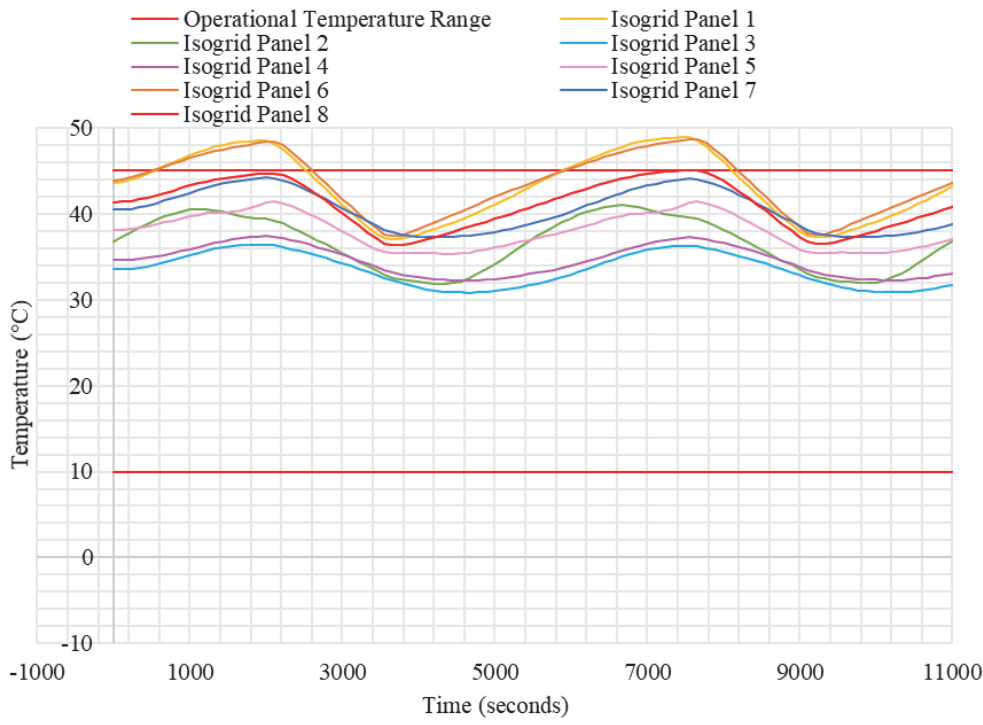


Figure 6.32. Model Revision E Hot Case Transient – Isogrid Panels

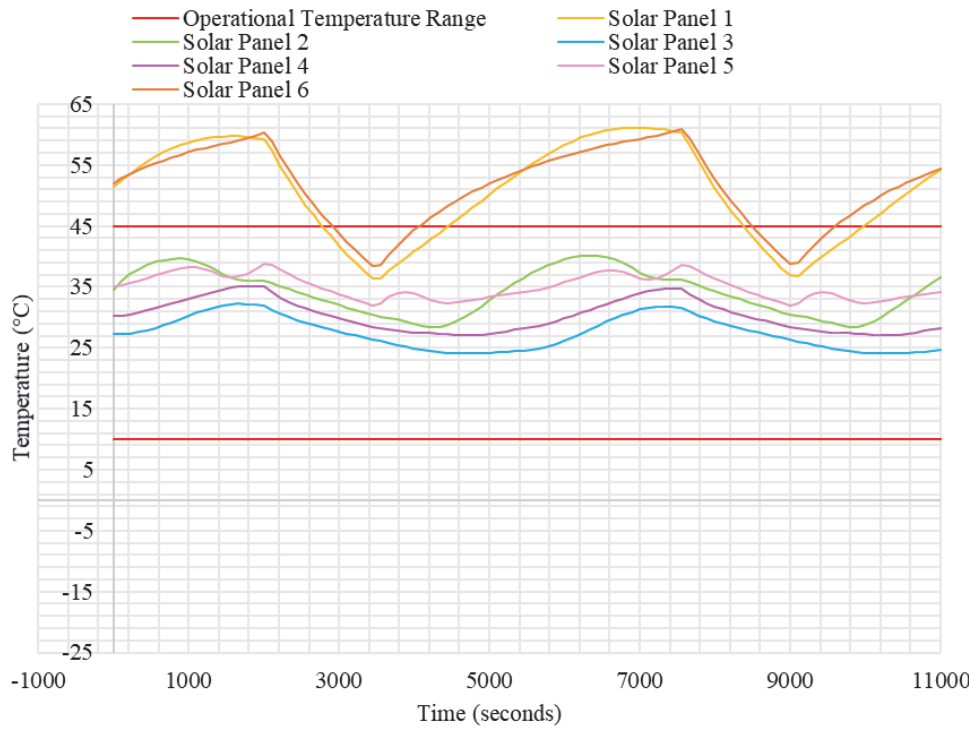


Figure 6.33. Model Revision E Hot Case Transient – Solar Panel PCB

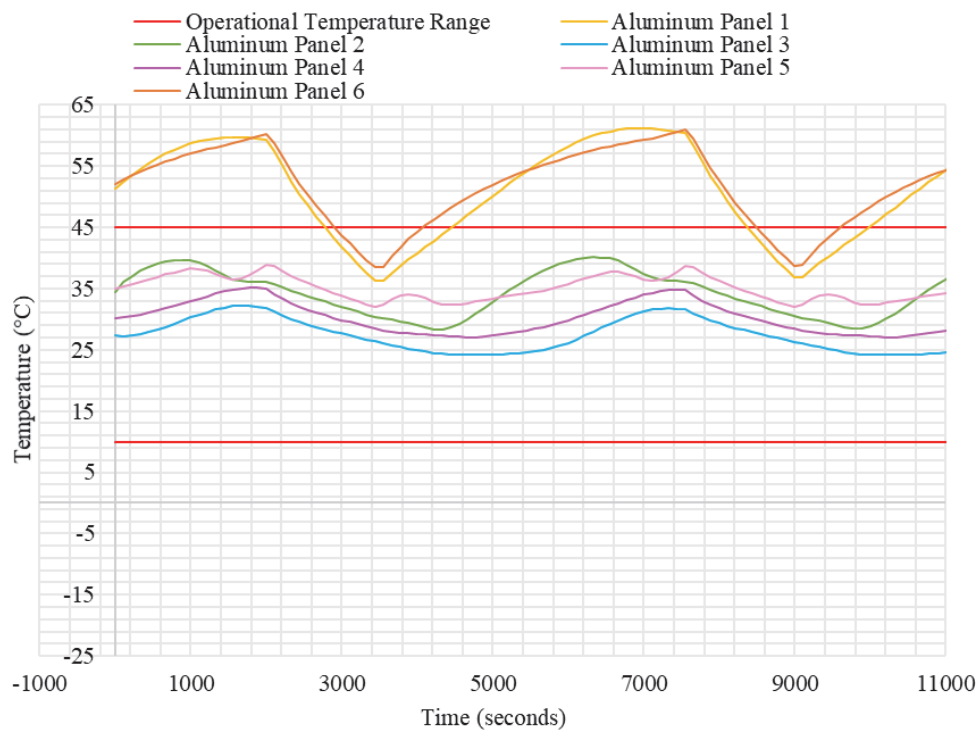


Figure 6.34. Model Revision E Hot Case Transient – Aluminum Panels

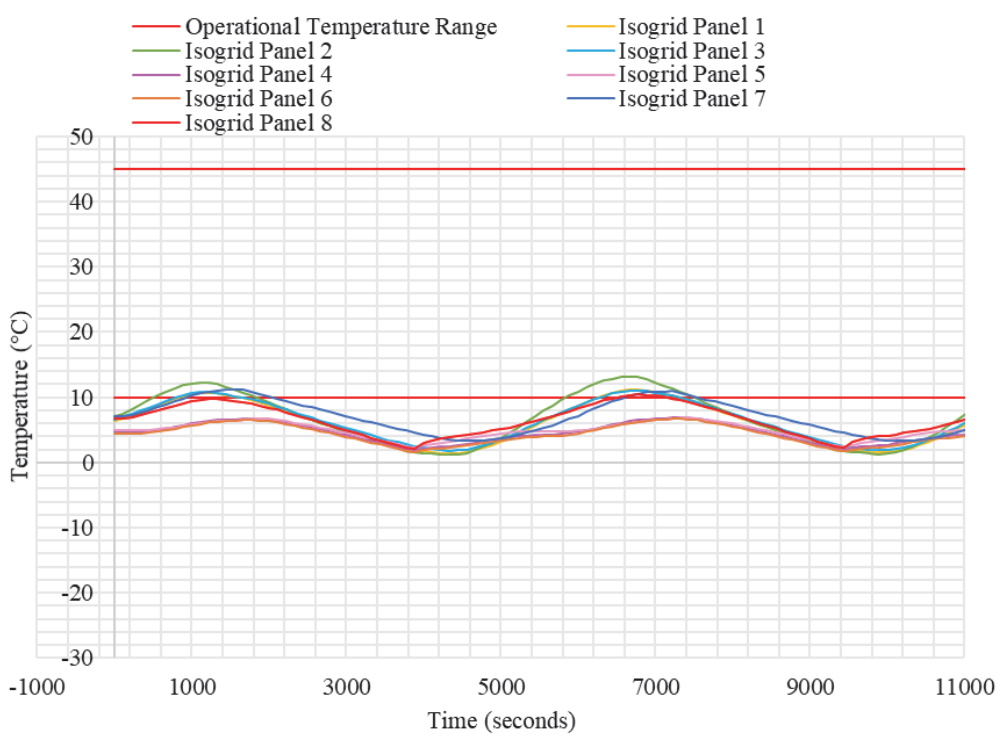


Figure 6.35. Model Revision E Cold Case Transient – Isogrid Panels

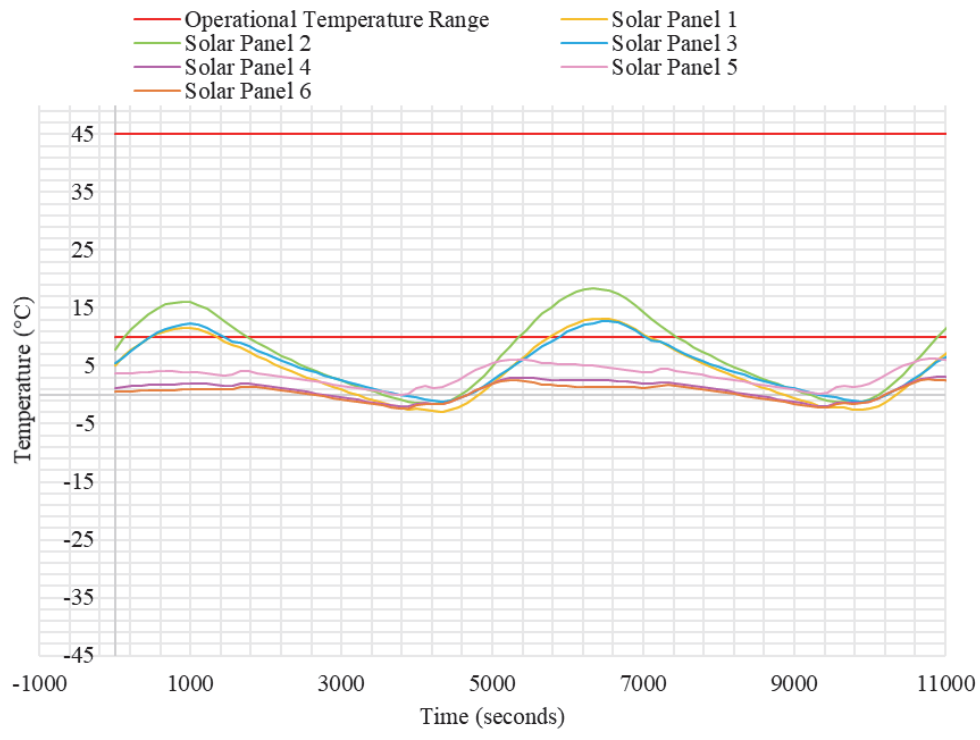


Figure 6.36. Model Revision E Cold Case Transient – Solar Panel PCB

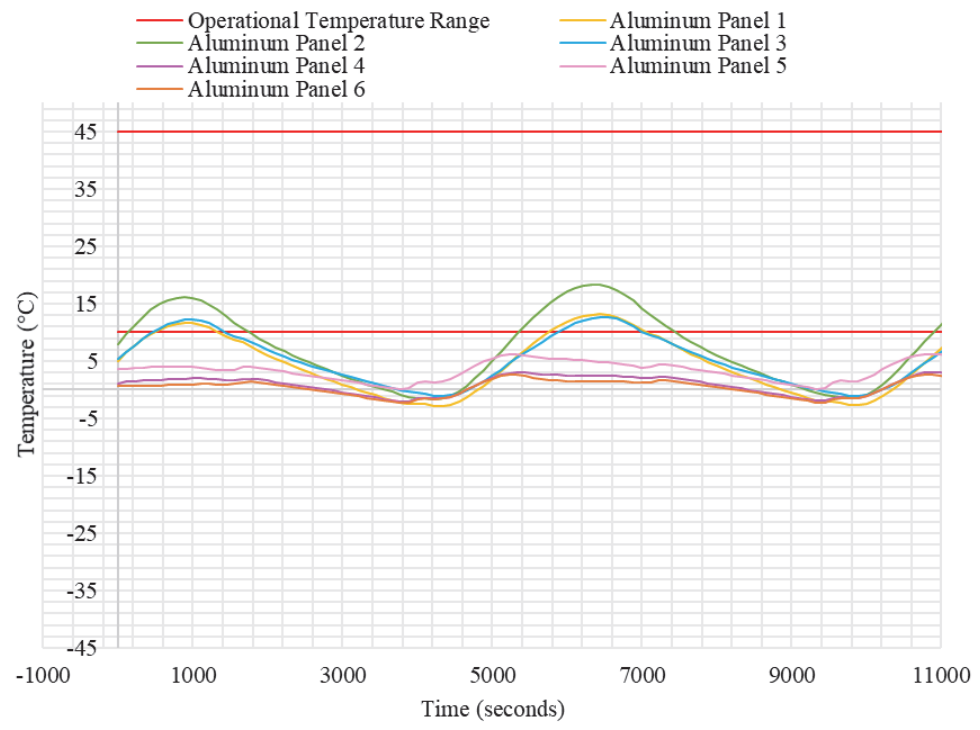


Figure 6.37. Model Revision E Cold Case Transient – Aluminum Panels

Parameterizing a model from the very beginning can be very useful for quickly altering models in the future. Using the Symbol Manager in Thermal Desktop allows for the creation of symbols. An Excel sheet can then be used to drive the values of the symbols when running an analysis in the Case Set Manager. These symbol values can easily be changed in the Excel sheet, allowing for the user to more quickly alter the model for another analysis run.

Thermal Desktop is a very powerful and useful tool for thermal modeling and analysis. Becoming familiarized with the software before beginning the model construction and analysis process is very important. The Thermal Desktop User's Manual offers helpful tutorials that introduce the user to the capabilities of the software and teach the user how to set up simple models and analyses [37].

7. CONCLUSION

7.1. THESIS SUMMARY

Proper thermal analysis and control for spacecraft is essential for successful mission performance. Thermal control methods for traditional satellites are well documented, but many methods for small satellite applications are still in the development stages. This thesis study presents proven methods of thermal analysis and control specifically relating to small satellites in low Earth orbit in order to act as a resource for future reference.

Satellite thermal analysis typically involves using analytical processes assisted by computer software to determine temperatures at nodes in the model by applying a numerical approximation method, typically the finite difference method. The solar vector, albedo factors, satellite component dissipation, orbit beta angle, and orbit altitude all affect the outcome of the thermal analysis. Thermal extrema cases define the upper and lower bounds on temperature predictions. The results of thermal models are then verified through testing, and the thermal model adjusted to more closely reflect the test results.

Satellite thermal control methods are used to regulate temperatures to ensure that components function properly throughout the mission. Thermal control systems on a satellite can use both passive and active thermal control. Small satellites most commonly employ passive methods as they tend to be lighter, more reliable, and do not require power. Passive thermal control methods include the use of multilayer insulation, thermal surface coatings and finishes, tapes, sunshields, radiators, heat pipes, phase change materials, and heat switches. Active thermal control methods should only be used when passive methods alone are not enough to control the temperature of the satellite. Active methods include the use of heaters, thermoelectric coolers, and louvers. Some traditional thermal control methods are being miniaturized for use in small satellites including thermal straps, deployable radiators, and fluid loops.

The thermal design process involves defining the requirements of the thermal control system, followed by iteratively analyzing, designing, and reanalyzing the system. The temperature requirements of all satellite components must be identified, as well as

the satellite heating environment. Analyses are used to select the necessary thermal control methods and safest design that will suffice should be chosen when possible.

The case study of MR SAT and MRS SAT, a microsatellite mission in development by the Missouri S&T Satellite Research Team, is presented to demonstrate the process of satellite thermal modeling, analysis, and control. The process began by identifying the operating temperatures of the critical electronic components on board the satellite. Thermal extrema environment and heating cases were identified, as well as the orbit profile. A simple single node model of the satellite was constructed using the Thermal Desktop software, followed by subsequent models that incrementally incorporated more complex surface modeling and increased nodal resolution. Potential thermal control methods were applied to the most complex model in an attempt to bring the satellite electrical component temperatures within their specified operating ranges. Analysis results for each model are presented, in order to show the effect of increasing model complexity on the satellite temperature. Results of the final model show how altered surface finishes and modified design change the calculated component and external surface temperatures.

7.2. CONTRIBUTIONS TO THE SMALL SATELLITE COMMUNITY

The goal of this thesis study has been to provide a resource to guide the small satellite thermal control system design and analysis process. Inexperienced engineers and academic teams will be able to use this thesis study as the starting point for their work in the thermal analysis and control of their small satellite designs. Basic heat transfer concepts and satellite heating environments are discussed for the benefit of student engineers still learning about the topics. Thermal analysis processes from various sources are summarized and presented, as well as a case study to demonstrate the use of these practices and an outline of the practical application of model construction, analysis, and design in Appendix A. Thermal control methods specifically for small satellites were presented and discussed, as well as emerging technologies designed for use in small satellites. The case study also demonstrated the use of passive thermal control methods to manipulate the resulting temperatures of a satellite so that they remain in the necessary range for a successful mission. By presenting this information in an organized and comprehensive manner, this thesis study benefits those who are new to satellite thermal control system design.

APPENDIX A.
THERMAL MODELING, ANALYSIS, AND DESIGN PROCESS

Overview of the Thermal Modeling, Analysis, and Design Process

1. Collect Necessary Information. Before starting the process of constructing a thermal model and running an analysis, it is necessary to collect the necessary input information. All input information should be organized into documentation so that it can be used for future reference. Effective organization of this documentation can be very beneficial to the thermal engineer throughout the modeling, analysis, and design process. Documentation should be kept up-to-date and should include references to where the information originally came from.

A. Mission Profile. The mission profile consists of information about the mission orbit type, orbit parameters, and the mission duration. For Thermal Desktop, the simplest orbit type options include a basic circular orbit or a Keplerian orbit. For a basic circular orbit, the altitude in kilometers as well as the beta angle will be needed. For a Keplerian orbit, the orbit inclination, right ascension of the ascending node, argument of periapsis, minimum and maximum altitude in kilometers, and eccentricity will be needed. In Thermal Desktop the user can set up multiple heating rate cases with different parameters to represent different mission modes.

B. Satellite Orientation. The orientation (attitude) of the satellite will be necessary to determine the incident radiation on the satellite surfaces from the heating environment. In Thermal Desktop the user can specify the pointing direction of the satellite with respect to the Earth based on the chosen reference frame of the model. The user can also specify the direction of the velocity vector of the satellite, and additional satellite rotations if necessary. In Thermal Desktop satellite orientations can be set up for different heating rate cases representing different mission modes.

C. Heating Environment. The satellite heating environment must be defined in order to determine the heating fluxes experienced by the satellite. This environment includes the solar flux, albedo flux, and internal satellite heat generation. In Thermal Desktop the user can select the solar flux constant and albedo constant. Thermal Desktop also provides the user with the option to use solar flux versus time, albedo versus time, and albedo versus latitude or longitude.

a. Solar Constant. Due to the Earth's elliptical orbit around the Sun, the solar flux varies based on the time of year. The solar constant is highest when the Earth is closest to the Sun during the northern hemisphere's winter, and lowest when the Earth is farthest from the Sun during the northern hemisphere's summer. For thermal extrema cases, it is recommended that the user select the highest solar constant for the hot case and the lowest solar constant for the cold case. The average solar constant value is often used in industry for non-extrema cases.

Solar Constant Values [25]

Case	Solar Constant [W/m ²]
Hot	1419
Average	1368
Cold	1317

b. Albedo Factor. The amount of albedo radiation incident upon a satellite is a function of spacecraft orientation and orbit as well as the reflectance of the albedo factor. The albedo factor depends upon the surface properties of the Earth. Clouds, water, ice, land, and forests have different reflectance values and result in different albedo factors. For extrema cases, it is recommended to use the most realistically extreme values for the factor. Non-extrema cases may use an average albedo factor.

Albedo Factor Values [1]

Case	Albedo Factor
Hot	0.56
Average	0.37
Cold	0.18

c. Internal Satellite Heat Generation. The internal heat generation of a satellite will depend upon energy dissipation from the satellite components. For satellites without moving parts, the internal heat generation depends only upon the electrical-power

draw of the components. Different mission modes will likely have different power requirements and internal heat generation. In Thermal Desktop, the user can alter the values of the applied heat loads in the Case Set Manager for the different mission modes.

D. Satellite Component Temperature Requirements. Each component in a satellite has an operational temperature range that the component must remain within in order to operate properly during the mission. Components also have a survival or storage temperature range that they must remain within while not operating in order to avoid damage. These temperature ranges must be determined and included in documentation so that the resulting temperatures of the components from analyses can be compared with the operational and survival temperature ranges. If a component exceeds its necessary temperature range during an analysis, this signals to the thermal engineer areas of the satellite that will require additional thermal control.

E. Satellite Geometries and Material Properties. Geometries of satellite components such as structural panels, solar panels, component boxes, electrical components, and propellant tanks will be necessary in order to construct a detailed thermal model of a satellite. Properties including material densities, specific heat, thermal conductivity will be needed as well as surface absorptivity and emissivity. Simplified models will require effective properties to be calculated using the equations presented in Section 3.3.3.

2. Construct Thermal Model. In order to run a thermal analysis, the thermal model must first be constructed. The process of creating an accurate and representative thermal model can begin with a simplified thermal model. A simple first-order model uses a simplified geometric shape such as a cube, sphere, cylinder, or several flat surfaces that represent the satellite shape. It is suggested that multiple iterations of the thermal model be constructed, starting with the simplest model. Each subsequent model can incrementally incorporate surfaces, complexity, and nodal resolution. The purpose of this gradual process is to ensure accuracy of the model before it becomes more complex, and ensure that there are no error messages in the software.

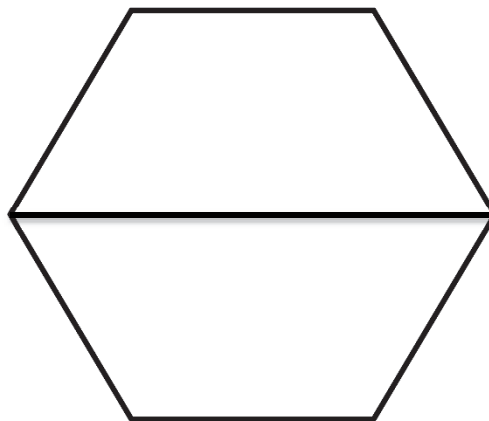
A. First-Order Model. A first order model can be as simple as representing the exterior surfaces of the satellite with thin shell surfaces. Thermal Desktop allows the user to easily create simple objects such as solid or hollow spheres, rectangular prisms, cones,

and circular or elliptical cylinders. In order to create a single node model, the user should represent each side of the surface with a single node. The nodes can then be merged by navigating through the “Thermal” menu to “FD/FEM Network” and selecting “Merge Coincident Nodes.”

B. Multi-Node Models. More complex model iterations can be created by more explicitly modeling satellite panels, components, and boxes. Panels can be created using Thermal Desktop Rectangles. Rectangular boxes can be created by navigating through the “Thermal” menu to “Surfaces/Solids” and selecting “Box.” Boxes can also be constructed by the user with individual Thermal Desktop rectangles. Thermal Desktop Polygons can be used to create non-rectangular shapes.

In order to create a polygon with a greater number of nodes than the Thermal Desktop Polygon, the user must create the polygon using AutoCAD lines. The shape should be drawn in sections containing only four lines. For example, to draw a hexagon the user must draw the shape in two halves, as shown in the figure. To set the desired nodal resolution, “SURFTAB1” and “SURFTAB2” should be set by typing the command in AutoCAD and following the prompts. The user should then type “EDGESURF” and click around one of the four-sided shapes. This should be done for each four-sided section. The user must then navigate through the “Thermal” menu to “FD/FEM Network” and select “Convert AutoCAD Surface to Nodes/Elements.”

Hexagonal Shape Composed of Two Sections



Components can be modeled using many of the Thermal Desktop objects such as the Thermal Desktop Rectangle, Brick, and Cylinder. The simplest way to model a component is through the use of one of these objects, with each object having a single arithmetic node. If it is desired to examine the temperature gradient across the object, multiple diffusion nodes will be necessary. More complex components can be modeled using multiple objects to model the interior design of the component, if it is deemed necessary.

3. Perform Thermal Analysis. The performance of the thermal analysis involves computing heat fluxes incident on the satellite, heat fluxes absorbed by satellite surfaces and components, and the radiation dissipation capabilities of the satellite surfaces and components. Typically, computer software is used for these computations. Thermal Desktop performs these computations based on the information input by the user into the thermal model, the Orbit Manager, and the Case Set Manager.

The information regarding the mission orbit will be entered into the Orbit Manager. Multiple different heating rate cases can be created to represent hot and cold cases as well as different mission mode satellite orientations. The user can also select the positions of the satellite in an orbit by setting number of increments around each orbit. Solar constant and albedo values are also set in the Orbit Manager.

The Case Set Manager is used to set up analysis cases and solution types. For example, for the case study presented in this thesis study both steady state and transient solutions were calculated. For the transient solution, it was selected to calculate the steady state temperatures before the transient analysis began. The transient case was started at zero seconds and ended after four orbit periods, which was entered as the expression “hrPeriod*4.” The Radiation Tasks selected for the case study were the Heating Rates for the thermal extrema case orbit calculated using the Monte Carlo method with 5000 rays per node, the Radks for the Base analysis group calculated using the Monte Carlo method with 5000 rays per node, and the View Factors for the Base analysis group with 5000 rays per node. The selected outputs for the case study included the temperatures and the incident heat. For many of the cases symbols were driven from Excel, which was selected in the Symbols tab of the editing window in the Case Set Manager.

Once an analysis has been run, the user can select the objects whose temperature results the user need to examine in the Model Browser and then select “XY Plot.” A window opens displaying a plot of the object temperatures versus time. The data can be exported by navigating through the File menu to “Export Tabular Data.” In order to view the results of different analyses run, the user can select open the Post Processing Manager, select the necessary case, and then select “Set Current.”

4. Analyze Results. The results of each thermal analysis should be examined, and the resulting temperatures compared with the temperature requirements of the satellite components. The temperature results of all cases should be examined, and the adequacy of the thermal design evaluated. Areas of the satellite where components do not remain within their necessary temperature ranges will require additional thermal management. Possible thermal control methods that can be utilized are listed in Section 4.

5. Redesign. The redesign process can involve altering surface finishes, altering the path of conduction, including thermal control hardware, and moving components and component boxes in the satellite. The model will need to be updated to reflect the redesign, though the preceding model files should be kept for reference. The analysis will need to be run again, and the results analyzed again. Additional redesign may be necessary. The feasibility of any changes to the design will need to be analyzed to ensure that their use does not negatively impact other subsystems. Design changes and thermal control methods must be vetted on a system and subsystem level before being implemented for the final satellite design.

6. Testing. A thermal balance test performed in a thermal vacuum chamber is used to verify a thermal model before flight. By this point, it is expected that any discrepancies between the model results and the test results will be minor. The results of the thermal balance test are used to correlate the model results to the test results by updating the model as appropriate. Intermediary and system level tests can also be performed before this point to confirm hardware properties and performance.

APPENDIX B.
PROPERTIES OF COMMON SURFACE COATINGS AND FINISHES

Optical Properties of Common Surface Coatings and Finishes [14]

Material	Absorptivity	Emissivity
<u>Optical Solar Reflectors</u>		
Teflon, Aluminized, 0.5 mm	0.14	0.4
Teflon, Aluminized, 1 mm	0.14	0.6
Teflon, silvered, 2 mm	0.08	0.68
Teflon, silvered, 10 mm	0.09	0.88
<u>Black Coating</u>		
Chemglaze Z306 Black Paint	0.96	0.91
Black Z306 polyurethane paint, 3 mm	0.95	0.87
Ebanol C Black	0.97	0.73
Rough black matte, black paint	0.9	0.9
<u>Films and Tapes</u>		
Kapton, aluminized, 0.25 mm	0.31	0.45
Kapton, black (carbon loaded), 1 mm	0.92	0.88
Tape, 235-3M, black	0.95	0.9
Tape, aluminum	0.1	0.04
<u>White Coatings</u>		
Chemglaze A276 white paint	0.24	0.9
Hughson A-276 white paint	0.26	0.88
Magnesium oxide white paint	0.09	0.9
Polyurethane white paint	0.27	0.84
<u>Other Paints</u>		
Aluminum Paint	0.3	0.31
Chromacoat aluminum paint	0.28	0.05
Silicone aluminum paint	0.29	0.3
<u>Metals</u>		
Aluminum, buffed	0.16	0.03
Aluminum, polished	0.15	0.05
Beryllium copper	0.31	0.03
Copper, buffed	0.3	0.03
Copper foil tape, tarnished	0.55	0.04
Gold, electroplated	0.23	0.03
Silver, polished, unoxidized	0.04	0.02
Stainless steel	0.47	0.14
Titanium	0.4	0.55
<u>Anodized Aluminum</u>		
Black anodize	0.65	0.82
Chromic anodize	0.44	0.56
Clear anodize	0.27	0.76
Plain anodize	0.26	0.04

APPENDIX C.
GEOMETRIES, MATERIAL PROPERTIES OF PANELS, BOXES, AND
COMPONENTS, AND CONDUCTANCE USED IN
THERMAL MODEL CONSTRUCTION

Geometries of Satellite Panel Components

Part	Quantity	Material	Length [m]	Width [m]	Thickness [m]	Mass [kg]	Calculated Density [kg/m ³]
Isogrid Panel 1	1	6061-T6 Anodized Aluminum	0.38	0.216	0.01	0.72046	2710.984333
Isogrid Panel 2	1	6061-T6 Anodized Aluminum	0.38	0.216	0.01	0.69328	2710.989754
Isogrid Panel 3	1	6061-T6 Anodized Aluminum	0.38	0.216	0.01	0.69328	2710.989754
Isogrid Panel 4	1	6061-T6 Anodized Aluminum	0.38	0.216	0.01	0.72046	2710.984027
Isogrid Panel 5	1	6061-T6 Anodized Aluminum	0.38	0.216	0.01	0.69565	2711.004539
Isogrid Panel 6	1	6061-T6 Anodized Aluminum	0.38	0.216	0.01	0.69564	2710.965568
Isogrid Panel 7 (Bottom Panel)	1	7075-T73511 Aluminum	0.475	0.475	0.02524	5.54085	2710.995666
Isogrid Panel 8 (Top Panel)	1	6061-T6 Anodized Aluminum	0.459093	0.418012	0.0115	2.52131	2799.597338
Top Solar Panel PCB Portion 1	1	PCB 4.6% Cu	0.293	0.226	0.0016	0.465932921	2259.77
Top Solar Panel PCB Portion 2	1	PCB 4.6% Cu	0.293	0.226	0.0016	0.458772921	2259.77
Top Solar Panel PCB Portion 3	1	PCB 4.6% Cu	0.293	0.226	0.0016	0.458392921	2259.77
Top Solar Panel PCB Portion 4	1	PCB 4.6% Cu	0.293	0.226	0.0016	0.458392921	2259.77
Top Solar Panel PCB Portion 5	1	PCB 4.6% Cu	0.293	0.226	0.0016	0.460472921	2259.77
Top Solar Panel PCB Portion 6	1	PCB 4.6% Cu	0.293	0.226	0.0016	0.458392921	2259.77
Bottom Solar Panel PCB Portion	6	PCB 4.6% Cu	0.14	0.226	0.0016	0.198997275	2259.77
Top Honeycomb Panel Portion 1	1	5052 Alum. Skin/7075 Alum. Core	0.293	0.226	0.004762	0.028791279	91.3052
Top Honeycomb Panel Portion 2	1	5052 Alum. Skin/7075 Alum. Core	0.293	0.226	0.004762	0.028791279	91.3052
Top Honeycomb Panel Portion 3	1	5052 Alum. Skin/7075 Alum. Core	0.293	0.226	0.004762	0.028791279	91.3052
Top Honeycomb Panel Portion 4	1	5052 Alum. Skin/7075 Alum. Core	0.293	0.226	0.004762	0.028791279	91.3052
Top Honeycomb Panel Portion 5	1	5052 Alum. Skin/7075 Alum. Core	0.293	0.226	0.004762	0.028791279	91.3052
Top Honeycomb Panel Portion 6	1	5052 Alum. Skin/7075 Alum. Core	0.293	0.226	0.004762	0.028791279	91.3052
Bottom Honeycomb Panel Portion	6	5052 Alum. Skin/7075 Alum. Core	0.14	0.226	0.004762	0.013756925	91.3052
Solar Cells	126	Germanium	0.0691	0.0396	0.0055	0.0021798	144.8374018

Geometries of Boxes and Electrical Components

Component	Model	Quantity	Material	Length [m]	Width [m]	Height [m]	Radius [m]	Thickness [m]	Mass [kg]	Calculated Density [kg/m ³]
T/Ni Separation Device		3	6061-T6 Anodized Aluminum	0.0414	-	-	0.0165	-	0.1	2824.11188
MCU Digital	T/Ni;ERM E500	1	PCB 4.6% Cu	0.012	0.012	0.0012	-	-	0.005	28935.18519
Isolation Valves	ATMEGA644 Microcontroller	3	Stainless Steel 316	0.03	-	-	0.00315	-	0.0076	8126.833409
Thrustor Valves	Lee Company IEPA2411241H Solenoid Valve	12	Stainless Steel 316	0.03	-	-	0.00315	-	0.0076	8126.833409
Propellant Tank	Lee Company IEPA2411241H Solenoid Valve	1	Stainless Steel 316L	0.34	-	-	0.057	-	1.5108	435.3399019
Pressure Transducer	Marotta BS25-001	2	Stainless Steel 17-4 PH	0.06858	-	-	0.0165	-	0.0739	1259.880043
Comm Radio	Honeywell A-205a	1	Black Anodized Aluminum Shield	0.065	0.04	0.0065	-	-	0.0245	1449.704142
GPS Receiver	GomSpace AX100	1	PCB 4.6% Cu	0.071	0.046	0.011	-	-	0.024	668.0398597
GPS Antenna	NovAtel OEM-615	1	Fiberglass Polyimide	-	-	-	0.044	0.01847	0.191	1700.243981
Flight Computer R-Pi	Novatel 3GOXX16A4-XTR-1-1-Cert	1	PCB 4.6% Cu	0.0676	0.031	-	-	0.0026	0.006	1101.208393
IMU	Raspberry Pi CM3 Lite	1	PCB 4.6% Cu	0.024	0.01	0.01	-	-	0.01	4166.666667
Sun Sensor Cameras	Epson M-G364PD	2	PCB 4.6% Cu	0.0409	0.031	0.01922	-	-	0.01	410.3567814
Sun Sensor Boards	CubeSense module	2	PCB 4.6% Cu	0.096	0.09	-	-	0.01	0.039	451.3888889
MCU Analog	CubeSense module	1	PCB 4.6% Cu	0.012	0.012	0.0012	-	-	0.005	28935.18519
Magnetometer	ATMEGA644 Microcontroller	1	5052-H32 Aluminum	0.00826	0.00351	0.00323	-	-	0.1	1067850.152
Magnetic Torque Coil (Top Panel)	Billingsky TFM 100G2	1	6061-T6 Anodized Aluminum	0.22	0.1	0.0187	-	-	0.397	964.9975693
Magnetic Torque Coil (Panel 5)	MWS 28 Gauge Wire	1	6061-T6 Anodized Aluminum	0.17	0.154	0.038	-	-	0.409	411.1213864
Magnetic Torque Coil (Panel 6)	MWS 28 Gauge Wire	1	6061-T6 Anodized Aluminum	0.17	0.154	0.038	-	-	0.409	411.1213864
Camera	MWS 28 Gauge Wire	2	PCB 4.6% Cu	0.044	0.041	0.0255	-	-	0.037	804.312856
Payload R-Pi	Point Grey Chameleon 1.3 MP	1	PCB 4.6% Cu	0.0676	0.031	-	-	0.0026	0.006	1101.208393
EPS Board	Raspberry Pi CM3 Lite	1	PCB 4.6% Cu	0.28	0.254	-	-	0.0016	0.257	2259.77
Lithium-Ion Batteries	Custom 4 Layer from Kimball Power Electronics	32	PCB 4.6% Cu	0.065	-	-	0.009	-	0.0405	2448.537586
Camera Baffles	Sony 18650HC Li-Ion Cells	2	6061-T6 Anodized Aluminum	0.044	-	-	0.0315	0.006	0.071076	518.2022829
Camera Boxes	-	2	6061-T6 Anodized Aluminum	0.054	0.054	0.035	-	0.004	0.090903	890.6819518
EPS Box	-	1	6061-T6 Anodized Aluminum	0.3	0.28	0.0508	-	0.004	2.283589	2710
MR SAT Box	-	1	6061-T6 Anodized Aluminum	0.3	0.28	0.0508	-	0.004	2.283589	2710
Battery Boxes	-	4	6061-T6 Anodized Aluminum	0.15	0.08	0.0335	-	0.004	0.3829048	2710

Material Properties of Panels, Boxes, and Electrical Components

Material	Absorptivity (α)	Emissivity (ϵ)	Conductivity [W/mK]	Specific Heat [J/kg/K]
Printed Circuit Board - 4.6% Cu by Volume ¹⁴	0.81	0.9	18.04	1544.11
Solar Cell - Germanium ¹⁵	0.92	0.85	60.6	324
Fiberglass Polyimide ¹⁶	0.75	0.89	0.26	1080
Stainless Steel 316 ¹⁷	0.47	0.14	163	420
Stainless Steel 316L ¹⁶	0.47	0.14	163	420
Stainless Steel 17-4 PH ¹⁶	0.47	0.14	180	384
Black Anodized Aluminum ¹⁶	0.65	0.82	121.2	768
7075-T73511 Aluminum ¹⁶	0.27	0.76	121.2	801
7075 Aluminum ¹⁶	0.16	0.3	121.2	801
6061-T6 Anodized Aluminum ¹⁸	0.14	0.76	237	921.096
5052 Aluminum ¹⁶	0.16	0.3	138.5	768
5052-H32 Aluminum ¹⁶	0.65	0.82	138.5	768
Top Panel Portion 5052 Alum. Honeycomb Core ¹⁹	0.16	0.3	172.4718947	768
Bottom Panel Portion 5052 Alum. Honeycomb Core ¹⁸	0.16	0.3	82.40977903	768

¹⁴ Optical Properties from [38]; Thermophysical Properties from [39]

¹⁵ Optical Properties from [40]; Thermophysical Properties from [14]

¹⁶ Optical Properties from [14]; Thermophysical Properties from [41]

¹⁷ Properties from [14]

¹⁸ Properties from [42], [43]

¹⁹ Conductivity and Specific Heat calculated using method presented in Appendix B of [14] for honeycomb core through thickness material properties.

Conductance of Bolted Contacts

Location	Bolt Type	Number of Bolts	Surface Type	Conductance per bolt [W/K]	Calculated Conductance Value [W/K]
Side Panel to Bottom Panel	10-32	7	Large Thin	0.527	3.689
Side Panel to Top Panel	10-32	7	Large Thin	0.527	3.689
Battery Box to Bottom Panel	10-32	4	Large Thin	0.527	2.108
EPS Box to Battery Boxes	10-32	2	Large Thin	0.527	1.054
MR SAT Box to EPS Box	10-32	6	Large Thin	0.527	3.162
Pressure Transducer to Prop Tank	10-32	1	Small Stiff	1.32	1.32
Iso Valve to Prop Tank	10-32	1	Small Stiff	1.32	1.32
Torque Coil to Isogrid Panel	10-32	4	Large Thin	0.527	2.108
Magnetometer to Side Panel	10-32	2	Large Thin	0.527	1.054
TiNi to Top Panel	8-32	4	Large Thin	0.264	1.056
Camera to Camera Box	10-32	2	Small Stiff	1.32	2.64
Camera Box to Top Panel	10-32	4	Large Thin	0.527	2.108
Camera Baffle to Camera Box	10-32	4	Small Stiff	1.32	5.28
GPS Antenna to Solar Panel PCB	10-32	4	Large Thin	0.527	2.108
Sun Sensor Camera to Solar Panel PCB	2-56	4	Large Thin	0.105	0.42
EPS Board to EPS Box	4-40	4	Small Stiff	0.26	1.04
IMU to MR SAT Box	4-40	4	Large Thin	0.132	0.528
Flight Raspberry Pi to MR SAT Box	4-40	4	Small Stiff	0.26	1.04
Payload Raspberry Pi to MR SAT Box	4-40	4	Small Stiff	0.26	1.04
MCU Digital to MR SAT Box	4-40	4	Small Stiff	0.26	1.04
MCU Analog to MR SAT Box	4-40	4	Small Stiff	0.26	1.04
Sun Sensor Boards to MR SAT Box	4-40	4	Small Stiff	0.26	1.04
Comm Radio to MR SAT Box	4-40	4	Small Stiff	0.26	1.04
GPS Receiver to MR SAT Box	4-40	4	Small Stiff	0.26	1.04

Conductance of Adhesive Contacts

Location	Type of Adhesive	Adhesive Conductivity [W/mK]	Contact Area [m ²]	Adhesive Thickness [m]	Calculated Conductance Value [W/K]
Honeycomb to PCB (Top Portion)	Epotek H74	1.3	0.066218	0.000004	21520.85
Honeycomb to PCB (Bottom Portion)	Epotek H74	1.3	0.03164	0.000004	10283
Thruster to Isogrid Panel	Epotek H74	1.3	0.000594	0.000004	193.05
Propulsion Tank to MR SAT Box	Epotek H74	1.3	0.121768	0.000004	39574.6
Batteries to Battery Box	Epotek H74	1.3	0.003676	0.000004	1194.7

APPENDIX D.
SINGLE NODE ANALYSIS – MODEL REVISION A
AND EIGHT NODE ANALYSIS – MODEL REVISION B
INPUT PARAMETERS

Lumped Panel Geometries and Material Properties

Lumped Panel Assembly ²⁰	Total Thickness [m]	Total Mass [kg]	Calculated Density [kg/m ³]	Effective Absorptivity (α_e)	Effective Emissivity (ϵ_e)	Effective Conductivity [W/mK]	Effective Specific Heat [J/kgK]
Panel 1	0.0071	1.4737142	1223.630906	0.871256617	0.872156083	12.20234245	1179.229031
Panel 2	0.0071	1.4393742	1205.15109	0.871256617	0.872156083	12.20234245	1182.288353
Panel 3	0.0071	1.4389942	1204.832926	0.871256617	0.872156083	12.20234245	1182.192805
Panel 4	0.0071	1.4661742	1217.370383	0.871256617	0.872156083	12.20234245	1177.352581
Panel 5	0.0071	1.4434442	1207.676239	0.871256617	0.872156083	12.20234245	1182.285631
Panel 6	0.0071	1.4413542	1205.927614	0.871256617	0.872156083	12.20234245	1181.765299
Panel 7 (Bottom Panel) ²¹	5.54085	5.54085	2710.995666	0.27	0.76	121.2	801
Panel 8 (Top Panel) ²¹	2.52131	2.52131	2799.597338	0.14	0.76	237	921.096

²⁰ Each lumped panel assembly includes an isogrid aluminum panel, top and bottom portions of the honeycomb aluminum panel, top and bottom portions of the solar panel PCB, and solar cells.

²¹ Panels 7 and 8 do not require lumped parameters, as they consist only of the aluminum isogrid Panel 7 and 8, respectively. The properties presented in this table for Panels 7 and 8 are identical to the properties for Panel 7 and 8 in Appendix B.

APPENDIX E.
MULTI NODE ANALYSIS – MODEL REVISION C AND D
EXPLICITLY MODELED PANELS
INPUT PARAMETERS

Lumped Solar Panel Geometries and Material Properties

Assembly	Total Thickness [m]	Total Mass [kg]	Calculated Density [kg/m ³]	Effective Absorptivity (Top/Out)	Effective Emissivity (Top/Out)	Effective Conductance [W/mK]	Effective Specific Heat [J/kgK]
Upper Solar Panel 1	0.0071	0.496450121	1567.827068	0.895514708	0.900527935	13.90162767	1469.108828
Upper Solar Panel 2	0.0071	0.489290121	1545.215246	0.895514708	0.900527935	13.90162767	1468.011302
Upper Solar Panel 3	0.0071	0.488910121	1544.015177	0.895514708	0.900527935	13.90162767	1467.952156
Upper Solar Panel 4	0.0071	0.488910121	1544.015177	0.895514708	0.900527935	13.90162767	1467.952156
Upper Solar Panel 5	0.0071	0.490990121	1550.583975	0.895514708	0.900527935	13.90162767	1468.274786
Upper Solar Panel 6	0.0071	0.488910121	1544.015177	0.895514708	0.900527935	13.90162767	1467.952156
Bottom Solar Panel Portion	0.0071	0.214255875	1373.665271	0.967590627	0.976225327	13.90162767	1457.217771

APPENDIX F.
MULTI NODE ANALYSIS – HEAT LOADS
FOR MODEL REVISIONS C AND D

Component Heat Load Information

Component	Quantity	Panel Location of Component	Panel Side	Mission Mode 1 Individual Component Heat Loads [W]	Safe Mode Individual Component Heat Loads [W]
TiNi Separation Device	3	8	Bottom/In	0	0
MCU Digital	1	7	Bottom/In	0.25	0
Isolation Valves	3	7	Bottom/In	0.636666667	0
Thruster Valves	12	1,4,7,8	Bottom/In	0.635	0
Pressure Transducer	2	7	Bottom/In	0.06	0
Comm Radio	1	7	Bottom/In	0.05	0.4
GPS Receiver	1	7	Bottom/In	0.33	0.33
GPS Antenna	1	Solar Panel 2	Top/Out	0.6	0.6
Flight Computer R-Pi	1	7	Bottom/In	2.9	2.9
IMU	1	7	Bottom/In	0.1	0.1
Sun Sensor Cameras	2	Solar Panel 3,6	Top/Out	0.105	0.105
Sun Sensor Boards	2	7	Bottom/In	0.105	0.105
MCU Analog	1	7	Bottom/In	0.23	0.23
Magnetometer	1	2	Bottom/In	0.3	0.3
Magnetic Torque Coil (Top Panel)	1	8	Bottom/In	0	0
Magnetic Torque Coil (Panel 5)	1	5	Bottom/In	0	0
Magnetic Torque Coil (Panel 6)	1	6	Bottom/In	0	0
Camera	2	8	Top/Out	1.32	0
Payload R-Pi	1	7	Bottom/In	2.9	0
EPS Board	1	7	Bottom/In	1	1
Lithium-Ion Batteries	32	7	Bottom/In	0.033390625	0.0098125

APPENDIX G.
MULTI NODE ANALYSIS – MODEL REVISION D
STEADY STATE ANALYSIS RESULTS

Model Revision D – Hot Case Steady State Analysis for Panels

Panel Number	Maximum Panel Temperature [°C]		
	Solar Panel (PCB and Solar Cells)	Honeycomb Panel	Isogrid Panel
1	40.61	40.60	9.59
2	1.90	1.91	3.19
3	-3.79	-3.72	-0.54
4	-0.38	-0.35	0.93
5	6.48	6.48	4.57
6	42.64	42.64	10.33
7	-	-	4.65
8	-	-	5.91

Model Revision D – Cold Case Steady State Analysis for Panels

Panel Number	Minimum Panel Temperature [°C]		
	Solar Panel (PCB and Solar Cells)	Honeycomb Panel	Isogrid Panel
1	-21.50	-21.50	-21.84
2	-18.53	-18.57	-20.83
3	-21.38	-21.39	-21.76
4	-26.18	-26.18	-22.63
5	-21.01	-21.02	-22.16
6	-26.51	-26.51	-22.59
7	-	-	-22.06
8	-	-	-22.62

Model Revision D - Steady State Analysis Results for Batteries

Component	Hot Case Temp [°C]	Cold Case [°C]
Box 1 - Battery 1	2.3644	-21.4729
Box 1 - Battery 2	2.3679	-21.4712
Box 1 - Battery 3	2.3694	-21.4712
Box 1 - Battery 4	2.3669	-21.4715
Box 1 - Battery 5	2.3685	-21.4716
Box 1 - Battery 6	2.3623	-21.4729
Box 1 - Battery 7	2.3644	-21.4729
Box 1 - Battery 8	2.3623	-21.4729
Box 2 - Battery 1	3.1384	-21.3526
Box 2 - Battery 2	3.1407	-21.3518
Box 2 - Battery 3	3.1429	-21.3518
Box 2 - Battery 4	3.1399	-21.3520
Box 2 - Battery 5	3.1421	-21.3520
Box 2 - Battery 6	3.1358	-21.3530
Box 2 - Battery 7	3.1384	-21.3526
Box 2 - Battery 8	3.1357	-21.3530
Box 3 - Battery 1	4.2914	-21.1996
Box 3 - Battery 2	4.3116	-21.2049
Box 3 - Battery 3	4.3148	-21.2052
Box 3 - Battery 4	4.3116	-21.2049
Box 3 - Battery 5	4.3148	-21.2052
Box 3 - Battery 6	4.2880	-21.1994
Box 3 - Battery 7	4.2914	-21.1996
Box 3 - Battery 8	4.2880	-21.1994
Box 4 - Battery 1	3.5591	-21.2155
Box 4 - Battery 2	3.5613	-21.2138
Box 4 - Battery 3	3.5631	-21.2140
Box 4 - Battery 4	3.5605	-21.2141
Box 4 - Battery 5	3.5624	-21.2143
Box 4 - Battery 6	3.5570	-21.2156
Box 4 - Battery 7	3.5591	-21.2155
Box 4 - Battery 8	3.5570	-21.2156

Model Revision D – Steady State Analysis Results for Components

Component	Hot Case Temp [°C]	Cold Case [°C]
TiNi 1	3.6428	-22.2845
TiNi 2	1.0420	-22.3236
TiNi 3	2.2344	-22.5941
MCU Digital	7.7109	-17.8458
Isovalve 1	7.9744	-17.8972
Isovalve 2	7.9747	-17.8971
Isovalve 3	7.9748	-17.8972
Thruster 1	6.9003	-21.6303
Thruster 2	8.8201	-21.3146
Thruster 3	7.3535	-21.6806
Thruster 4	9.5806	-21.5602
Thruster 5	0.1154	-22.5632
Thruster 6	-0.2911	-22.5211
Thruster 7	0.7649	-22.3067
Thruster 8	0.0855	-22.5509
Thruster 9	2.4791	-21.9911
Thruster 10	3.4196	-21.6206
Thruster 11	1.6336	-22.5578
Thruster 12	3.5873	-21.7766
Pressure Transducer 1	7.5165	-17.9056
Pressure Transducer 2	7.5222	-17.9052
Comm Radio	7.5176	-17.4635
GPS Receiver	7.7635	-17.5459
GPS Antenna	-1.7652	-9.2202
Flight Raspberry Pi	10.1900	-15.1088
IMU	7.6569	-17.6585
Sun Sensor Camera 1	-21.2684	-17.4305
Sun Sensor Camera 2	40.0789	-24.8270
Sun Sensor Board 1	7.7772	-17.3380
Sun Sensor Board 2	7.5253	-17.7821
MCU Analog	7.6918	-17.6248
Magnetometer	2.0414	-20.0721
Torque Coil - Top Panel	2.4361	-22.3414
Torque Coil - Panel 5	3.6295	-21.8182
Torque Coil - Panel 6	8.4083	-22.3285
Camera 1	2.0818	-23.0480
Camera 2	3.3388	-22.3606
EPS Board	6.0222	-18.9450
Payload Raspberry Pi	10.1932	-15.1073

APPENDIX H.
MODEL REVISION E INPUT INFORMATION

Component Design Changes

	Original Material			New Top/Out Material			New Bottom/In Material		
	Material	Absorptivity	Emissivity	Material	Absorptivity	Emissivity	Material	Absorptivity	Emissivity
Camera Boxes	6061-T6 Anodized Aluminum	0.14	0.76	Plain Anodize	0.26	0.04	Plain Anodize	0.26	0.04
Thrusters and Iso Valves	Stainless Steel 316	0.47	0.14	Copper Foil Tape, tarnished	0.55	0.04	-	-	-
Sun Sensor Boards	Printed Circuit Board - 4.6% Cu by Volume	0.81	0.9	Kapton, black (carbon loaded), 1 mm	0.92	0.88	Kapton, black (carbon loaded), 1 mm	0.92	0.88
Sun Sensor Cameras	Printed Circuit Board - 4.6% Cu by Volume	0.81	0.9	Kapton, black (carbon loaded), 1 mm	0.92	0.88	-	-	-
Sun Sensor Box Panel 3	-	-	-	Plain Anodize	0.26	0.04	Plain Anodize	0.26	0.04
Sun Sensor Box Panel 6	-	-	-	Black Anodize	0.88	0.88	Green Anodize	0.66	0.88
Honeycomb Panels	5052 Aluminum	0.16	0.3	Plain Anodize	0.26	0.04	Plain Anodize	0.26	0.04
Solar Panel PCBs	Printed Circuit Board - 4.6% Cu by Volume	0.81	0.9	Ebanol C Black Paint	0.97	0.73	Tape, 235-3M, black	0.95	0.9
Isogrid Panels	6061-T6 Anodized Aluminum	0.14	0.76	Plain Anodize	0.26	0.04	Plain Anodize	0.26	0.04
Battery Boxes	6061-T6 Anodized Aluminum	0.14	0.76	Plain Anodize	0.26	0.04	Plain Anodize	0.26	0.04
Component Boxes	6061-T6 Anodized Aluminum	0.14	0.76	Plain Anodize	0.26	0.04	Plain Anodize	0.26	0.04

Conductance of Bolted Contacts for New Components

Bolted Contact					
Location	Bolt Type	Number of Bolts	Surface Type	Conductance per bolt [W/K]	Calculated Conductance Value [W/K]
Camera Box to Top Panel	10-32	4	Large Thin	0.527	2.108

Dimensions of New Components

Component	Quantity	Material	Length [m]	Width [m]	Height [m]	Thickness [m]	Density [kg/m ³]
Sun Sensor Camera Boxes	2	6061-T6 Anodized Aluminum	0.031	0.01922	0.0409	0.004	2710

BIBLIOGRAPHY

- [1] R.D. Karam, *Satellite Thermal Control for Systems Engineers*. Reston, VA: American Institute of Aeronautics and Astronautics, Inc., 1998.
- [2] A.S. Gohardani, "Small Satellites: Observations and Considerations," presented at 2018 AIAA Aerospace Sciences Meeting, AIAA SciTech Forum, Kissimmee, FL, 2018. [Online], Available: <https://arc-aiaa-org.libproxy.mst.edu/doi/pdf/10.2514/6.2018-1937>. [Accessed Feb. 7, 2018].
- [3] A. Bonnema and J. Rotteveel, "Are We There Yet? Looking Back at a Decade Of Disruption of the Space Market Using Cubesats," In Proc. AIAA/USU Conference on Small Satellites, SSC16-III-2, Logan, UT, 2016. [Online], Available: <https://digitalcommons.usu.edu/smallsat/2016/S3BigPicture/2/>. [Accessed Feb. 7, 2018].
- [4] R. Fleeter, "Small Sats," in *Space Mission Engineering: The New SMAD*, J. R. Wertz, D. F. Everett, and J. J. Puschell, Eds. Hawthorne, CA: Microcosm Press, 2011, pp-791-802.
- [5] National Aeronautics and Space Administration, "What are SmallSats and CubeSats?" 2015. [Online]. Available: <https://www.nasa.gov/content/what-are-small-sats-and-cubesats>. [Accessed: Feb. 7, 2018].
- [6] IDA Science and Technology Policy Institute, "Global Trends in Small Satellites," *Institute for Defense Analyses*, 2017. [Online]. Available: <https://www.ida.org/>. [Accessed: Feb. 11, 2018].
- [7] The White House: President Barack Obama, "Investing Big in Small Satellites," *Obama White House Archives*, 2016. [Online]. Available: <https://obamawhitehouse.archives.gov/blog/2016/12/22/investing-big-small-satellites>. [Accessed March 2018].
- [8] Bliley Technologies, "20 Popular Cube Satellite Companies in Today's Market," 2017. [Online]. <http://blog.bliley.com/top-20-best-cubesat-satellite-manufacturers>. [Accessed March 2018].
- [9] The National Academies of Sciences Engineering Medicine, "DOD Perspective on CubeSats," 2015. [Online]. https://sites.nationalacademies.org/cs/groups/ssbsite/documents/webpage/ssb_166652.pdf. [Accessed March 2018].

- [10] National Aeronautics and Space Administration, “Small Spacecraft Technology State of the Art,” Mission Design Division, Ames Research Center, Moffett Field, California, NASA/TP-2015-216648/REV1, Dec. 2015.
- [11] R. Creel, “LUROVA – From Render Engine to Thermal Model,” presented at the Thermal and Fluids Analysis Workshop, Glenn Research Center, Cleveland, OH, 2014. [Online]. Available: <https://tfaws.nasa.gov/files/TFAWS-2014-PT-05-Paper.pdf>. [Accessed Feb. 12, 2018].
- [12] R. K. MacGregor, “Spacecraft Thermal Design Verification through Modeling,” in *Fundamentals of Spacecraft Thermal Design*, J. W. Lucas, Ed. Reston, VA: American Institute of Aeronautics and Astronautics, Inc., 1972, pp 361-382.
- [13] National Aeronautics and Space Administration, “Guidelines for Thermal Analysis of Spacecraft Hardware,” Goddard Space Flight Center, Greenbelt, MD, Guideline. GD-AP-2302.
- [14] D. G. Gilmore, Ed., *Spacecraft Thermal Control Handbook Volume I: Fundamental Technologies*. El Segundo, CA: The Aerospace Press, Reston, VA: American Institute of Aeronautics and Astronautics, Inc., 2002.
- [15] J. A. Richmond, “Adaptive Thermal Modeling Architecture for Small Satellite Applications,” M.S. thesis, Massachusetts Institute of Technology, Cambridge, MA, 2010.
- [16] C. B. VanOutryve, “A thermal analysis and design tool for small spacecraft,” M.S. thesis, San Jose State University, San Jose, CA, 2008.
- [17] Y. A. Cengel, *Heat Transfer A Practical Approach*. Boston, MA: McGraw-Hill, Inc., 1998.
- [18] J. F. Oberright, “Spacecraft Thermal Control,” in *Space Mission Engineering: The New SMAD*, J. R. Wertz, D. F. Everett, and J. J. Puschell, Eds. Hawthorne, CA: Microcosm Press, 2011, pp-685-700.
- [19] J. Han, *Analytical Heat Transfer*. Boca Raton, FL: CRC Press, 2012.
- [20] J. R. Howell, “A Catalog of Radiation Heat Transfer Configuration Factors,” [Online]. Available: <http://www.thermalradiation.net/tablecon.html>. [Accessed 2016].

- [21] I. Martinez, "Radiative View Factors," [Online]. Available: <http://webserver.dmt.upm.es/~isidoro/tc3/Radiation%20View%20factors.pdf>. [Accessed 2016].
- [22] P. Fortescue, G. Swinerd, and J. Stark, *Spacecraft Systems Engineering*. Chichester, West Sussex: Wiley, 1998, 2011.
- [23] H. D. Curtis, *Orbital Mechanics for Engineering Students*. Burlington, MA: Butterworth-Heinemann, 2009.
- [24] D. W. Hengeveld, M. M. Mathison, J. E. Braun, E. A. Groll, and A. D. Williams, "Review of Modern Spacecraft Thermal Control Technologies," *HVAC&R Research*, vol. 16, no. 2, pp. 189-220, 2010.
- [25] W. K. Tobiska, "The Space Environment," in *Space Mission Engineering: The New SMAD*, J. R. Wertz, D. F. Everett, and J. J. Puschell, Eds. Hawthorne, CA: Microcosm Press, 2011, pp-127-148.
- [26] C&R Technologies, "Products". [Online]. Available: <https://www.crtech.com/products>. [Accessed: Feb. 27, 2018].
- [27] Department of Defense, *Product Verification Requirements for Launch, Upper Stage, and Space Vehicles*. MIL-STD-1540D. 1999.
- [28] Department of Defense, *Test Requirements for Launch, Upper-Stage, and Space Vehicles Vol I: Baseline*. MIL-HDBK-340A. 1999.
- [29] National Aeronautics and Space Administration, "Technology Readiness Level," 2012. [Online]. Available: https://www.nasa.gov/directorates/heo/scan/engineering/technology/txt_accordion1.html. [Accessed Feb. 27, 2018].
- [30] Dunmore Aerospace, "Polyimide Tape," 2018. [Online]. Available: <https://www.dunmore.com/products/polyimide-tape.html>. [Accessed Feb. 28, 2018].
- [31] Department of Defense, *Anodic Coatings for Aluminum and Aluminum Alloys*, MIL-A-8625F Amendment 1. 2003.
- [32] Department of Defense, *Chemical Conversion Coatings on Aluminum and Aluminum Alloys*, MIL-DTL-5541F. 1990.

- [33] Thermotive LLC, “Products.” [Online] <http://thermotive.com/thermalstraps.html>. [Accessed March 2018].
- [34] Carbice Corporation, “Carbice Tape.” [Online]. <http://www.carbice.com/>. [Accessed March 2018].
- [35] Missouri S&T Satellite Research Team, “Who We Are,” *mst.edu/~mrsat*, 2017. [Online]. Available: <http://web.mst.edu/~mrsat/about/>. [Accessed: March 2, 2018].
- [36] S. V. Bapat, “Thermal Analysis of the MR SAT Spacecraft,” M. S. thesis, University of Missouri-Rolla, Rolla, MO, 2004.
- [37] T. D. Panczak, S. G. Ring, M. J. Welch, D. J. Johnson, B. A. Cullimore, and D. P. Bell, *Thermal Desktop User’s Manual Version 6.0*, C&R Technologies, 2017.
- [38] M. M. Finckenor and R.F. Coker, “Optical Properties of Nanosatellite Hardware,” National Aeronautics and Space Administration Marshall Space Flight Center, Greenbelt, MD. NASA/TM-2014-218195, June 2014.
- [39] Boedeker Plastics Inc, “Plastic Sheet, Rod, Tube & Machined Parts,” [Online]. Available: <http://boedeker.com/>. [Accessed February 2018].
- [40] Spectrolab, “26.8% Improved Triple Junction (ITJ) Solar Cells,” datasheet.
- [41] Professional Plastics, “Thermal Properties of Plastic Materials,” [Online]. Available: <https://www.professionalplastics.com/professionalplastics/ThermalPropertiesofPlasticMaterials.pdf>. [Accessed February 2018].
- [42] Solar-AC, “Absorptivity & Emissivity table,” [Online]. Available: <http://www.solarmirror.com/fom/fom-serve/cache/43.html>. [Accessed May 2016].
- [43] Infrared Services Inc, “Emissivity Values for Common Materials,” [Online]. Available: <http://www.infrared-thermography.com/material.htm>. [Accessed May 2016].

VITA

Katelyn Elizabeth Boushon was born in Lake County, Illinois. She began her aerospace engineering studies at Missouri University of Science and Technology in the fall of 2010. As an undergraduate student, Katelyn worked on the Missouri S&T Satellite Research Team as a member of the outreach, integration, and structures subsystems. She was also involved in several organizations including the Society of Women Engineers, Zeta Tau Alpha national women's fraternity, and the Missouri Miner Newspaper. In the summer semesters Katelyn participated in internship programs with Spirit AeroSystems in Wichita, Kansas and the Air Force Research Laboratory in Albuquerque, New Mexico. Katelyn graduated with her Bachelor of Science degree in Aerospace Engineering in the spring of 2015. In the fall of 2015, Katelyn entered the graduate aerospace engineering program at Missouri S&T. She began working on thermal analysis for the Missouri S&T Satellite Research Team as a research assistant under Dr. Hank Pernicka in the spring of 2016. She received her MS degree in Aerospace Engineering from Missouri University of Science and Technology in May of 2018.

